

**APERTURE-TOLERANT, CHEMICAL-BASED METHODS TO REDUCE
CHANNELING**

Annual Scientific/Technical Progress Report
Reporting Period: October 1, 2004 through September 30, 2005

And

Semi-Annual Scientific/Technical Progress Report
Reporting Period: April 1, 2005 through September 30, 2005

Principal Author: Randall S. Seright
(505) 835-5571

Report Date: October 2005

DOE Award Number: DE-FC26-04NT15519

Name and Address of Submitting Organization:
New Mexico Petroleum Recovery Research Center
New Mexico Institute of Mining and Technology
Socorro, New Mexico 87801

NM PRRC Contributors: Richard Schrader, Kathryn Wavrik,
Ying Wang, Erica Ocampo, Fred Frazier, Dongmei Wang

PRRC Report 05-08

DISCLAIMER

This report was prepared as an account of work sponsored by an agency of the United States Government. Neither the United States Government nor any agency thereof, nor any of their employees, makes any warranty, expressed or implied, or assumes any legal liability or responsibility for the accuracy, completeness, or usefulness of any information, apparatus, product, or process disclosed, or represents that its use would not infringe privately owned rights. Reference herein to any specific commercial product, process, or service by trade name, trademark, manufacturer, or otherwise does not necessarily constitute or imply its endorsement, recommendation, or favoring by the United States Government or any agency thereof. The views and opinions of authors expressed herein do not necessarily state or reflect those of the United States Government or any agency thereof.

ABSTRACT

This technical progress report describes work performed from October 1, 2004, through September 30, 2005, for the project, “Aperture-Tolerant, Chemical-Based Methods to Reduce Channeling.” This report considered several scenarios where a fracture (or fractures) allowed direct channeling between an injection well and a production well. We examined the effects of plug size and location on production rate, sweep efficiency, and pattern pressure gradients. The scenarios considered included (1) vertical wells where channeling was dominated by a single vertical fracture, (2) an injector and a producer that had either parallel fractures or parallel horizontal wells and that were directly connected by a single vertical fracture, (3) fractures that offset or parallel the main fracture that directly connected two wells, (4) a fracture or fractures that crossed the main direct fracture, and (5) more complex naturally fractured systems.

We investigated two potential uses of low-concentration gels to improve conformance in reservoirs. In both cases, we worked with gels where the gelation reactions were nearly complete. In the first concept, we considered whether low-concentration Cr(III)-acetate-HPAM gels could effectively propagate into and plug narrow fractures. In fractures with widths around 0.1 mm, gels containing 0.2% or 0.25% HPAM propagated well and effectively healed the fracture. But, the gels were ineffective at healing fractures with widths of 0.5 mm or greater. In the second concept, we investigated if low-concentration gels could flow effectively through 1.5- to 10-darcy porous media, where no fractures were present. We tried to force formed gels (with 0.15%, 0.2%, and 0.25% HPAM) through 1.5- to 10-darcy porous media (not fractured). In all cases, severe face-plugging occurred, and the effective viscosities were low (i.e., similar to or less than the viscosity of uncrosslinked polymer solutions) for interior sections of the cores.

Although some polymers and gels reduce permeability to water more than to oil, several factors currently limit widespread field applications of this property. We are investigating pore-filling gels to overcome these limitations. For porous media at residual oil saturation with initial permeability to water (k_w) ranging from 120 to 6,500 md, a Cr(III)-acetate-HPAM gel reduced k_w to 240 μd ($\pm 84 \mu\text{d}$). For porous media with initial k_w values ranging from 100 to 8,100 md (no residual oil), the gel (with 0.5% HPAM) reduced k_w to 24 μd ($\pm 20 \mu\text{d}$). Compared with “weak” gels and adsorbing polymers, pore-filling gels can provide greater reliability and behavior that is insensitive to the initial rock permeability. With sufficient oil throughput, pore-filling gels can be dehydrated—thus increasing permeability to oil. We found three cases where gels provided water residual resistance factors greater than 2,100 and ultimate oil residual resistance factors of 2 or less—providing hope that our current approach will identify a gel that can successfully and reliably treat either fractured or unfractured production wells without zone isolation.

We investigated the ability of concentrated gels to rehydrate (swell) during water flow after gel placement in fractures. Three gels were examined that contained the same HPAM concentration, but that used different crosslinkers, including Cr(III) acetate, resorcinol formaldehyde, and polyethyleneimine. For all three gels, little or no gel rehydration occurred when flooding with large volumes of brine. Flooding with distilled water caused immediate swelling and restriction of the wormholes and diversion of water flow away from the fractures and into the porous rock. Switching back to brine injection caused immediate gel dehydration.

TABLE OF CONTENTS

DISCLAIMER	ii
ABSTRACT.....	iii
LIST OF FIGURES	vii
LIST OF TABLES.....	x
ACKNOWLEDGMENTS	xi
EXECUTIVE SUMMARY	xii
1. INTRODUCTION	1
Objectives	1
Report Content.....	1
2. OPTIMUM AREAL PLACEMENT LOCATIONS FOR GEL PLUGS IN FRACTURES	2
Scenario 1: Direct Fracture Channel between Two Vertical Wells.....	2
A 25-ft Long Gel Plug Substantially Reduced Productivity in Moderate to Wide Fractures.	4
Gel Plugs Were Not Needed in Narrow Fractures ($w_f \leq 0.25$ mm if $k_{matrix} = 100$ md)	5
Gel Plugs Filling > 10% of the Fracture Were Needed to Significantly Improve Sweep	8
Plugs up to 80% of Fracture Length Improved Matrix Pressure Gradients.....	8
Effect of Plug Size for Gel Positioned in the Center of the Fracture.....	11
For Plugs Centered in the Fracture, Sweep Improvement Was Not Sensitive to Plug Size if the Plugs Were Longer than 20% of the Fracture Length	11
Off-Centered Plugs Didn't Affect Rates Much if the Plugs Were Not Close to a Well.....	14
Sweep Decreased as Plugs Moved Off-Center	15
Centered Plugs Maintained the Highest Pattern Pressure Gradients	15
Translating Results to Cases with Other Rock Permeabilities.....	16
Summary for Scenario 1	17
Scenario 2: Direct Fracture Channel between Two Parallel Fractures or Horizontal Wells	18
Pressure Gradients and Sweep Were Good with Parallel Fractures or Horizontal Wells	20
In Moderate to Wide Fractures, Small Plugs Greatly Reduced Production Rates.....	20
For Narrow Fractures, Gel Plugs Were Not Needed	21
Small Gel Plugs Were Often Adequate for Treating Fractures in Horizontal Wells.....	22
Summary for Scenario 2	25
Scenario 3: Offset Fracture Parallel to the Main Direct Fracture	25
Parallel Offset Fractures Had Little Effect on Rate but Can Greatly Harm Sweep.....	27
Plugging the Main Direct Fracture Did Not Aid Sweep Beyond the Offset Fracture	27
Effect of Position of the Offset Fracture.....	27
Effect of Fracture Width.....	27
Effective Gel Placement in the Offset Fracture is Unlikely for Scenario 3.....	30
Summary for Scenario 3	30
Scenario 4: Fractures Crossing the Main Direct Fracture.....	31
Sweep Improved as the Crossing Fracture Moved Away from the Pattern Center	34
Plugging the Direct Fracture Reduced Channeling but May Not Improve Matrix Sweep... ..	34
A Centered Partial Plug in the Main Fracture Improved Sweep and Pattern Pressures	35
The Most Effective Plugs Blocked the Entrances to the y-Direction Fractures	36
Summary for Scenario 4	39

Scenario 5: Both Cross-Direction and Offset Fractures	39
With Only One Cross-Direction Fracture, Sweep for the Outer Pattern Remained Poor.....	39
Parallel Cross-Direction Fractures Provided Good Pattern Pressure Gradients	41
Plugging the Direct Fracture Reduced Rates but Did Not Improve Pattern Pressures.....	43
Centered Partial Plugs Reduced Rate and Improved Sweep for the Inner Pattern	43
For Parallel Cross-Direction Fractures, Pattern Sweep Remained Good	45
Any Fracture Pathways that Remain Unplugged Can Allow Severe Channeling	46
Summary for Scenario 5	48
Scenario 6: More Complex Naturally Fractured Systems	48
Summary for Scenario 6	52
Conclusions.....	52
Future Work.....	53
3. INVESTIGATION OF GELS WITH LOW POLYMER CONCENTRATIONS.....	54
Low-Concentration Gels in Narrow Fractures.....	54
Behavior during Gel Injection	56
Behavior during Brine Injection after Gel Placement.....	58
Low-Concentration Gels in Very Permeable Porous Media.....	59
Conclusions.....	64
4. OPTIMIZING DISPROPORTIONATE PERMEABILITY REDUCTION	66
Challenges for Applications of Disproportionate Permeability Reduction	66
Variable Performance	66
F_{rro} Must Be < 2 for Radial Flow	66
Permeability Dependence of F_{rr}	67
Overcoming the Obstacles	68
Variability	68
Linear versus Radial Flow	69
Permeability Dependence	70
Permeability to Water after Gel Placement	70
k_w versus Initial Core Permeability and Core Material.....	70
k_w with/without S_{or}	71
k_w versus Polymer Content.....	72
Stability of k_w	73
Are F_{rrw} Values High Enough?.....	73
Permeability to Oil after Gel Placement	75
Concepts from Previous Work.....	75
Experimental Results during Oil Injection	76
Are F_{rro} Values Low Enough?	81
How Fast Will Oil Zones Clean Up?	82
Second Water Flow after Oil Flow	83
Summary	85
5. REHYDRATION OF GEL IN FRACTURES	87
Review of Gel Extrusion Behavior	87
Do Gels Rehydrate during Brine Flow After Gel Placement?.....	87
New Experiments.....	87
Injecting Large Volumes of Brine Did Not Rehydrate the Gel	89
Injecting Less Saline $CaCl_2$ Brine Rehydrated the Gel Slowly	91

Higher Rates and Pressure Gradients Widened Wormholes.....	92
Injecting Distilled Water Rehydrated Gel Rapidly. Brine Rapidly Dehydrated Gel.....	93
Cr(III)-Acetate-HPAM Gel Using HPAM with 30% Degree of Hydrolysis.....	97
To What Degree Must Flow in a Fracture Be Restricted?.....	102
Laboratory Flow Capacities.....	103
Flow Capacities in Field Applications.....	103
Summary.....	104
NOMENCLATURE	105
REFERENCES	106
APPENDIX A: Technology Transfer.....	109
Presentations	109
Web Site.....	109
Papers and Publications	110

LIST OF FIGURES

Fig. 1—Scenario 1: Areal view of fracture connecting an injection well and a production well...	2
Fig. 2—Pressure distribution when 1-mm fracture was fully open.....	3
Fig. 3—Pressure distribution with no fracture.....	4
Fig. 4—Production rate versus gel plug size and fracture width. Scenario 1.....	5
Fig. 5—Sweep efficiency in pattern with $w_f = 0.25$ mm.	6
Fig. 6—Sweep efficiency in pattern with $w_f = 0.5$ mm.	6
Fig. 7—Sweep efficiency in pattern with $w_f = 1$ mm.	7
Fig. 8—Sweep efficiency in pattern with $w_f = 2$ mm.	7
Fig. 9—Pattern pressures when 100-ft plug extended from producer into 0.25-mm fracture.....	8
Fig. 10—Percent of pattern experiencing high pressure gradients. Scenario 1.....	9
Fig. 11—Pattern pressures when 100-ft plug extended from producer into 1-mm fracture.....	9
Fig. 12—Pattern pressures when 500-ft plug extended from producer into 1-mm fracture.....	10
Fig. 13—Pattern pressures when 800-ft plug extended from producer into 1-mm fracture.....	10
Fig. 14—Effect of centered plug size on production rate.....	11
Fig. 15—Effect of centered plug size on sweep efficiency.	12
Fig. 16—Effect of centered plug size on pressure gradients.	12
Fig. 17—Pressure distribution with a 10-ft plug centered in a 1-mm fracture.....	13
Fig. 18—Pressure distribution with a 100-ft plug centered in a 1-mm fracture.....	13
Fig. 19—Pressure distribution with a 800-ft plug centered in a 1-mm fracture.....	14
Fig. 20—Effect of plug position on production rate.....	14
Fig. 21—Effect of plug position on sweep efficiency.....	15
Fig. 22—Effect of plug position on pressure gradients.....	15
Fig. 23—Pressures for a 100-ft gel plug positioned 250 ft from producer in a 1-mm fracture....	16
Fig. 24—Curves for translating results to reservoirs with different rock permeabilities.	17
Fig. 25—Scenario 2: Areal view of a fracture connecting parallel fractures or horizontal wells.	18
Fig. 26—Pattern pressures with a direct open fracture: 1-mm parallel fractures case.....	19
Fig. 27—Pattern pressures for parallel 1-mm fractures case, no connecting fracture.....	19
Fig. 28—Production rate versus gel plug size and fracture width. Scenario 2.....	20
Fig. 29—Pattern pressures when all three 0.25-mm fractures are fully open.....	21
Fig. 30—Pattern pressures when all three 0.5-mm fractures are fully open.....	22
Fig. 31—Percent of pattern experiencing high pressure gradients. Scenario 2.....	23
Fig. 32—Pattern pressures for 100-ft plug in 0.5-mm fracture. Scenario 2.....	23
Fig. 33—Pattern pressures for 100-ft plug in 1-mm fracture. Scenario 2.....	24
Fig. 34—Pattern pressures for 100-ft plug in 2-mm fracture. Scenario 2.....	24
Fig. 35—Scenario 3: Areal view of an offset fracture parallel to the main direct fracture.....	25
Fig. 36—Two views of pressures for Scenario 3: Open 1-mm fractures at $y=0$ ft and $y=250$ ft..	26
Fig. 37—Two views of pattern pressures when the main direct fracture was plugged.....	28
Fig. 38—Pattern pressures when the offset x-direction fracture was at $y=125$ ft.....	29
Fig. 39—Pattern pressures when the offset x-direction fracture was at $y=25$ ft.....	29
Fig. 40—Average pressures in the outer half of the pattern versus width of the offset fracture..	30
Fig. 41—Gel caused substantial damage to the matrix in reaching the offset fracture.....	31
Fig. 42—Scenario 4: Areal view of a fracture crossing the main direct fracture.....	32
Fig. 43—Pattern pressures when a fracture at $x=500$ ft crossed the main direct fracture.....	32

Fig. 44—Pattern pressures when a fracture at $x=250$ ft crossed the main direct fracture.	33
Fig. 45—Pattern pressures when a fracture at $x=750$ ft crossed the main direct fracture.	33
Fig. 46—Pattern pressures when a fracture at $x=0$ ft crosses the main direct fracture.....	34
Fig. 47—Pattern pressures after complete plugging of the main fracture in Fig. 42.....	35
Fig. 48—Pattern pressures for a fracture at $x=500$ ft and a half-plugged main fracture.	36
Fig. 49—Pattern pressures for a 500-ft plug centered in the main fracture.....	37
Fig. 50—Pattern pressures for a 100-ft plug centered in the main fracture.....	37
Fig. 51—Pattern pressures for a 100-ft plug centered at 445 ft in the main fracture.	38
Fig. 52—Pattern pressures for a 100-ft plug centered at 555 ft in the main fracture.	38
Fig. 53—Scenario 5: Both cross-direction and offset fractures.....	39
Fig. 54—Pattern pressures for fractures at $x=500$ ft, $y=0$ ft, and $y=250$ ft.	40
Fig. 55—Pattern pressures for fractures at $x=250$ ft, $y=0$ ft, and $y=250$ ft.	40
Fig. 56—Pattern pressures for fractures at $x=0$ ft, $y=0$ ft, and $y=250$ ft.	41
Fig. 57—Pattern pressures for fractures at $x=0$ ft, $x=1,000$ ft, $y=0$ ft, and $y=250$ ft.....	42
Fig. 58—Pattern pressures for fractures at $x=0$ ft, $x=500$ ft, $x=1,000$ ft, $y=0$ ft, and $y=250$ ft.	42
Fig. 59—Pattern pressures for fractures at $x=0$ ft, $x=500$ ft, $y=0$ ft, and $y=250$ ft.....	43
Fig. 60—Complete plugging of the main direct fracture in Figs. 53 and 54.....	44
Fig. 61—Plugging from 450 to 550 ft in the main direct fracture in Figs. 53 and 54.	44
Fig. 62—Plugging from 250 to 750 ft in the main direct fracture in Figs. 53 and 54.	45
Fig. 63—Complete plugging of the main direct fracture in Fig. 58.	46
Fig. 64—Plugging from 450 to 550 ft in the main direct fracture in Fig. 58.	47
Fig. 65—Plugging from 250 to 750 ft in the main direct fracture in Fig. 58.	47
Fig. 66—Plugging from 900 to 1,000 ft in the main direct fracture in Fig. 58.	48
Fig. 67—Scenario 6: Simplified areal view of a naturally fractured pattern.....	49
Fig. 68—Severity of channeling through the most direct fracture.	50
Fig. 69—Effect of plugging the most direct fracture.....	50
Fig. 70—Effect of plugging the most direct fracture (varied spacing for x -direction fractures)..	51
Fig. 71—Effect of plugging the most direct fracture (varied spacing for y -direction fractures)..	51
Fig. 72—Viscosity versus shear rate for HPAM solutions (no crosslinker).....	55
Fig. 73—Pressure gradients along closed fractures during gel injection.....	56
Fig. 74—Pressure gradients along 0.5-mm-wide fractures during gel injection.	57
Fig. 75—Pressure gradients along 1-mm-wide fractures during gel injection.	57
Fig. 76—Pressure gradients during gel injection: 0.08-mm fracture, 0.25% HPAM gel.....	58
Fig. 77—Pressure gradients during gel injection: 0.5-mm fracture, 0.25% HPAM gel.....	58
Fig. 78—Effective viscosities during gel injection: 0.15% HPAM gel.....	60
Fig. 79—Effective viscosities during gel injection: 0.2% HPAM gel.....	60
Fig. 80—Effective viscosities during gel injection: 0.25% HPAM gel.....	60
Fig. 81—Effective viscosities in the second sections during gel injection.....	61
Fig. 82—Pressure gradients during gel injection into 1,570-md fused silica.	62
Fig. 83—Effective viscosities (resistance factors) in the first section during gel injection.	62
Fig. 84—Residual resistance factors during brine injection.....	63
Fig. 85—Pressure gradients in the first section during brine flow at various rates.	64
Fig. 86—Losses of zone flow capacity for radial flow.....	67
Fig. 87—Permeability dependence of water residual resistance factors (F_{rw}).	68
Fig. 88—Gel restricting water entry into a fracture.....	69
Fig. 89—Permeabilities to oil and water after gel placement in Berea.	70

Fig. 90— k_w after gel placement versus time.....	74
Fig. 91—Oil forming wormholes through gel.....	75
Fig. 92— k_o versus pore volume for Entry 1 in Tables 3 and 4.....	77
Fig. 93— k_o versus pore volume for Entry 4 in Tables 3 and 4.....	77
Fig. 94— k_o versus pore volume for Entry 5 in Tables 3 and 4.....	77
Fig. 95— k_o versus pore volume for Entry 6 in Tables 3 and 4.....	78
Fig. 96— k_o versus pore volume for Entry 7 in Tables 3 and 4.....	78
Fig. 97— k_o versus pore volume for Entry 8 in Tables 3 and 4.....	78
Fig. 98— k_o versus pore volume for Entry 9 in Tables 3 and 4.....	79
Fig. 99— k_o versus pore volume for Entry 10 in Tables 3 and 4.....	79
Fig. 100— k_o versus pore volume for Entry 11 in Tables 3 and 4.....	79
Fig. 101— k_o versus pore volume for Entry 13 in Tables 3 and 4.....	80
Fig. 102— k_o versus pore volume for Entry 14 in Tables 3 and 4.....	80
Fig. 103— k_o versus pore volume for Entry 15 in Tables 3 and 4.....	80
Fig. 104— k_o versus pore volume for Entry 16 in Tables 3 and 4.....	81
Fig. 105— k_o versus pore volume for Entry 17 in Tables 3 and 4.....	81
Fig. 106—Clean up times for the case where $k_w = 0.24$ md.....	83
Fig. 107—Apparent gel swelling and shrinking in a polyethylene core.....	85
Fig. 108—Top schematic view of a fractured core.....	88
Fig. 109—Pressure gradients during first brine flow after gel placement.....	89
Fig. 110—Pressure gradients during >200 fracture volumes of brine after gel placement.....	90
Fig. 111—Percent of brine flowing through the matrix after gel placement.....	90
Fig. 112—Pressure gradients during flow of brine with 0.1% CaCl_2	91
Fig. 113—Percent of flow through matrix for brine with 0.1% CaCl_2	92
Fig. 114—Higher rates and pressure gradients shift flow away from the matrix.....	93
Fig. 115—Distilled water shifted flow to matrix for the Cr(III)-acetate-HPAM gel.....	94
Fig. 116—Distilled water increased dp/dl for the Cr(III)-acetate-HPAM gel.....	94
Fig. 117—Distilled water shifted flow to matrix for the resorcinol-formaldehyde-HPAM gel... ..	95
Fig. 118—Distilled water increased dp/dl for the resorcinol-formaldehyde-HPAM gel.....	95
Fig. 119—Distilled water shifted flow to matrix for the polyethyleneimine-HPAM gel.....	96
Fig. 120—Distilled water increased dp/dl for the polyethyleneimine-HPAM gel.....	96
Fig. 121—Breaching pressure gradient versus HPAM degree of hydrolysis.....	97
Fig. 122—Stabilized pressure gradients versus degree of hydrolysis: 1% NaCl, 0.1% CaCl_2	98
Fig. 123—Percent of flow through matrix versus degree of hydrolysis: 1% NaCl, 0.1% CaCl_2	98
Fig. 124—Pressure gradients versus degree of hydrolysis: 0.1% CaCl_2	99
Fig. 125—Percent of flow through matrix versus degree of hydrolysis: 0.1% CaCl_2	100
Fig. 126—Effect of rate on gel with SNF 3830 HPAM.....	101
Fig. 127—Pressure gradients for SNF 3830: effect of salinity.....	101
Fig. 128—Percent of flow through matrix for SNF 3830: effect of salinity.....	102
Fig. 129—Flow capacity of fracture relative to matrix: vertical well, vertical fracture.....	104

LIST OF TABLES

Table 1—Use of low-concentration gels in tight fractures	55
Table 2—Adsorbed polymers and “weak” gels can harm flow profiles	68
Table 3— k_w during brine flow after gel placement	71
Table 4—Ultimate k_o and F_{rro} during oil flow after gel placement	76
Table 5—Ultimate k_w and F_{rrw} during the second water flow after gel placement	84

ACKNOWLEDGMENTS

Financial support for this work is gratefully acknowledged from the United States Department of Energy (NETL/National Petroleum Technology Office), the State of New Mexico, ConocoPhillips, Marathon, and ExxonMobil. I greatly appreciate the efforts of those individuals who contributed to this project. Richard Schrader and Kate Wavrik performed the experimental work with help from Ying Wang, Erica Ocampo, and Fred Frazier. Bob Sydansk was consistently a great sounding board for ideas. I especially appreciate the thorough review of this manuscript by Julie Ruff and Annette Carroll.

EXECUTIVE SUMMARY

This technical progress report describes work performed from October 1, 2004, through September 30, 2005, for the project, “Aperture-Tolerant, Chemical-Based Methods to Reduce Channeling.”

Optimum Areal Placement Locations for Gel Plugs in Fractures. We considered several scenarios where a fracture (or fractures) allowed direct channeling between an injection well and a production well. We examined the effects of plug size and location on production rate, sweep efficiency, and pattern pressure gradients. Depending on the flow capacity of the fracture(s) relative to that of the reservoir rock, gel plugs may or may not be needed. For example, for fracture widths of 0.25 mm or less, channeling should not be a problem in 100-md rock. However, channeling can be a problem for fracture widths greater than 0.5 mm in this rock. A method was provided to apply these guidelines to rock with other permeabilities.

For vertical wells where channeling was dominated by a single vertical fracture, a small near-wellbore plug (e.g., 25 ft long) dramatically reduced pattern flow rates (i.e., water channeling), but did not improve pattern pressure gradients in a manner that enhanced oil displacement from deep within the reservoir. Significant improvements in oil displacement required plugging of at least 10% (and preferably more than 20%) of the length of the offending fracture, and ideally, this plug should be placed near the center of the fracture.

A second scenario considered an injector and a producer that had either parallel fractures or parallel horizontal wells and that were directly connected by a single vertical fracture. Pattern pressure gradients and sweep were very desirable for this scenario—with or without gel plugs. Small near-wellbore plugs were often sufficient to greatly reduce channeling.

A third scenario considered fractures that offset or parallel the main fracture that directly connected two wells. For vertical wells, these offset fractures had a negative impact on pattern sweep and pressure gradients that was difficult to overcome. These offset fractures presented less of a problem for cases similar to Scenario 2 (e.g., parallel horizontal wells).

In the fourth scenario, a fracture or fractures crossed the main direct fracture. Sweep efficiency and average pressure gradients increased in the pattern as the cross-direction fractures moved closer to the wells. However, the number and position of these cross-direction fractures had only a minor effect on pattern production rates. Complete plugging of the main direct fracture reduced channeling but may not improve matrix sweep and pressure gradients. A centered partial plug in the main fracture improved pattern sweep and pressure gradients. The most effective plugs blocked the entrances to the cross-direction fractures.

Much additional work remains regarding the optimum size and placement of gel plugs in naturally fractured reservoirs. Also, the work described in this report did not consider fractures that cut through multiple zones (i.e., at least one water zone and one hydrocarbon zone). In other words, the work in this report assumed that it was desirable to completely stop flow through the most direct and conductive fracture. Future work should consider fractures that allow flow of both water and hydrocarbon. Even for those cases where the plug is desired to completely block

flow, issues remain on how to prevent gravity segregation within a given fracture from compromising the effectiveness of a gel plug.

Investigation of Gels with Low Polymer Concentrations. We investigated two potential uses of low-concentration gels to improve conformance in reservoirs. In both cases, we worked with one-day-old Cr(III)-acetate-HPAM gels where the gelation reactions were nearly complete. (In other words, we were NOT working with fluid gelant solutions.) In the first concept, we considered whether low-concentration Cr(III)-acetate-HPAM gels could effectively propagate into and plug narrow fractures. In the second concept, we investigated whether low-concentration gels could flow effectively through 1.5- to 10- darcy porous media, where no fractures were present.

In fractures with widths around 0.1 mm, gels containing 0.15%, 0.2% or 0.25% HPAM propagated effectively, exhibiting effective viscosities that were similar to the viscosity of polymer solutions without crosslinker (i.e., 3-7 cp). In contrast, our previous work revealed that Cr(III)-acetate-HPAM gels with 0.5% HPAM would not enter these narrow fractures unless extremely high pressure gradients were applied. The gels containing 0.2% or 0.25% HPAM effectively healed these narrow fractures, forcing all post-gel-treatment brine to flow through the Berea sandstone matrix rather than the narrow fractures. In contrast, the gel with 0.15% HPAM was ineffective at healing the fracture. Also, all three gels were ineffective at healing fractures that were 0.5 mm or 1 mm in width. Consequently, these compositions do not fulfill our requirements for aperture-tolerant plugging materials.

For the second approach, we tried to force one-day-old gels (again with 0.15%, 0.2%, and 0.25% HPAM) through 1.5- to 10-darcy porous media (not fractured). In all three cases, severe face-plugging occurred, and the effective viscosities were low (e.g., similar to or less than the viscosity of uncrosslinked polymer solutions) for interior sections of the cores. We suspect that these gels can be made to flow through porous media if the permeability and/or the pressure gradient are large enough. However, the permeability that allows gel flow (as opposed to gelant flow) is greater than 10 darcys for pressure gradients that are typically encountered in field applications.

Optimizing Disproportionate Permeability Reduction. Although some polymers and gels reduce permeability to water more than to oil, several factors currently limit widespread field applications of this property. First, adsorbed polymers, “weak” gels, and suspensions of gel particles show large variations in performance. Second, in unfractured wells (i.e., radial flow into porous sand or rock), the oil residual resistance factor, F_{rro} , (permeability reduction factor) must be reliably less than 2. Third, adsorbed polymers, “weak” gels, and particle suspensions reduce permeability by greater factors in low-permeability rock than in high-permeability rock. We are investigating pore-filling gels to overcome these limitations, beginning with Cr(III)-acetate-HPAM gels. For porous media at residual oil saturation with initial permeability to water (k_w) ranging from 120 to 6,500 md, a Cr(III)-acetate-HPAM gel (with 0.5% HPAM) consistently reduced k_w to 240 μ d (± 84 μ d). For porous media with initial k_w values ranging from 100 to 8,100 md (no residual oil), the gel (with 0.5% HPAM) reduced k_w to 24 μ d (± 20 μ d). Thus, pore-filling gels can provide greater reliability and behavior that is insensitive to the initial rock permeability.

With sufficient oil throughput, pore-filling gels can be dehydrated—thus increasing permeability to oil. We found three cases where gels provided water residual resistance factors greater than 2,100 and ultimate F_{rro} values of 2 or less. As noted above, F_{rro} must be less than 2 for radial flow treatments where hydrocarbon zones are not protected during gel placement. So, our recent results provide hope that our current approach will identify a gel that can successfully and reliably treat either fractured or unfractured production wells without zone isolation.

Rehydration of Gels in Fractures. Gels dehydrate when extruding through fractures. This concentrated gel is quite immobile and can effectively reduce the flow capacity of fractures. When brine or oil flow is resumed after gel placement, small wormhole paths open through the gel in the fractures when a critical pressure gradient is reached. In many cases (e.g., fractures or fracture-like features in very permeable sand or rock), these wormhole pathways do not restore fracture conductivity enough to be of concern. However, for other cases (e.g., wide fractures in moderate to low permeability rock), plugging of these wormholes may be desirable to divert flow through the porous rock and eliminate channeling through the fractures. We investigated the ability of concentrated gels to rehydrate (swell) during water flow after gel placement. Three gels were examined that contained the same HPAM concentration, but that used different crosslinkers, including Cr(III) acetate, resorcinol formaldehyde, and polyethyleneimine. For all three gels, no gel rehydration or restriction of the wormholes occurred when flooding with large volumes of brine with the same composition as that used to prepare the gels (1% NaCl, 0.1% CaCl₂). Very gradual rehydration and restriction of the wormholes occurred when flooding with large volumes of brine containing 0.1% CaCl₂. Flooding with distilled water caused immediate swelling and restriction of the wormholes and diversion of water flow away from the fractures and into the porous rock. Switching back to brine injection (1% NaCl, 0.1% CaCl₂, or 0.1% CaCl₂) caused immediate gel dehydration and re-opening of the wormholes. Of course, injection of distilled water is impractical in most cases. Nevertheless, these results provide hope that a swelling mechanism may be exploitable in future developments.

Technology Transfer. Technology transfer efforts for the project are listed in Appendix A. In addition to presenting many workshops, papers, and talks, we maintain a website that is a valuable resource for all who apply water shutoff treatments.

1. INTRODUCTION

Fractures, vugs, karst, and similar void channels often cause excess water production and poor sweep efficiency in reservoirs. In both hydraulically and naturally fractured reservoirs, void channels often allow injected fluids to flow directly between injection and production wells. This problem is especially important for enhanced oil recovery projects, where high-value fluids are injected. In production wells, void channels often extend into an aquifer—thus accentuating water production. In many cases, gels have effectively mitigated channeling through fractures, fracture-like features, and voids. Gels have reduced channeling through fractures in waterfloods and gas floods. Gels have also reduced water production in wells where fractures, fracture-like features, and voids connect to an underlying aquifer. Although many gel treatments have been quite successful, many important questions exist concerning how best to design and implement them. Current methods are very sensitive to the aperture of the fracture or void. Unfortunately, these apertures are usually not known in field applications. Thus, a particular need exists for treatments that are not sensitive to the aperture of the fracture or void.

Objectives

The objective of this project is to develop aperture-tolerant, chemical-based methods to reduce channeling through voids (e.g., fractures, vugs, karst) during hydrocarbon production. The project has two tasks. The objective of the first task is to develop materials that can be effectively placed and will consistently minimize flow through voids with a wide range of apertures. The objective of the second task is to develop methods to minimize water entry into voids from the surrounding rock. This task requires chemicals (i.e., gels, polymers) that predictably and controllably reduce the permeability to water much more than that to hydrocarbon.

Report Content

This report describes work performed during the first year of the project. Chapter 2 describes a theoretical study of the optimum areal placement locations for gel plugs in fractures. Chapter 3 investigates the use of gels with low polymer concentrations to plug very narrow fractures or extremely permeable porous media. Chapter 4 presents a new approach to reliably maximize disproportionate permeability reduction—i.e., providing predictably high reductions in permeability to water while causing reliably low reductions in permeability to oil. Chapter 5 examines gel swelling (rehydration) as a means to reduce the flow capacity of fractures. Finally, technology transfer activities are described in Appendix A.

2. OPTIMUM AREAL PLACEMENT LOCATIONS FOR GEL PLUGS IN FRACTURES

When fractures allow severe channeling through reservoirs, where are the optimum locations for placement of a blocking agent? In this report, we considered several scenarios where a fracture allowed direct channeling between an injection well and a production well. In these scenarios, we assumed (1) the pattern area was 1,000 by 1,000 ft, (2) the matrix permeability was uniformly 100 md, (3) a pressure drop (Δp) of 1,000 psi was applied between the two wells, (4) displacements were unit mobility (i.e., the injected fluid had the same mobility as the displaced fluid), (5) gravity and capillary effects were negligible, and (6) fluids were incompressible. We focused on the importance of areal locations of gel plugs in reservoirs with fractures. The optimum vertical placement for gel/gelant in fractures is a crucial issue that was considered to some extent earlier^{1,2} and will receive extensive additional attention in our future work.

Scenario 1: Direct Fracture Channel between Two Vertical Wells

First, consider two vertical wells that were directly connected by a fracture (Fig. 1).

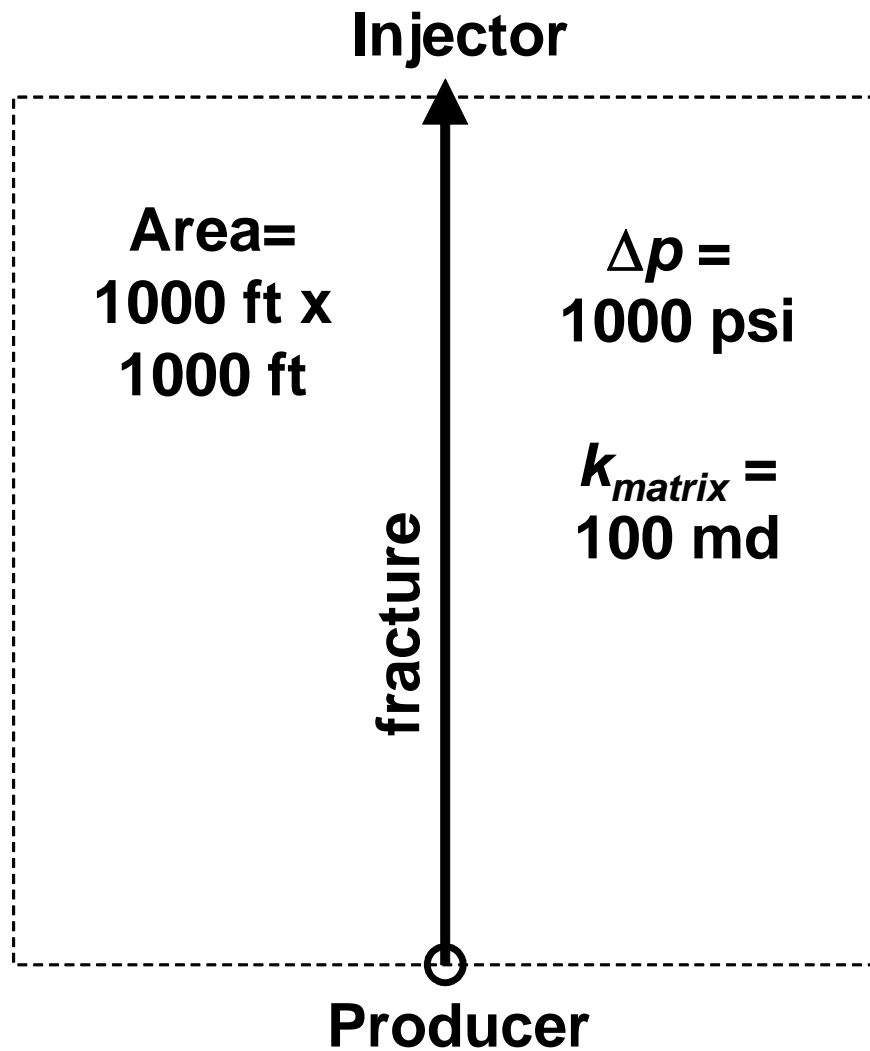


Fig. 1—Scenario 1: Areal view of fracture connecting an injection well and a production well.

For a fracture width of 1 mm, the pressure distribution is shown in Fig. 2. Because the pressure distribution was symmetrical about the fracture, only one-half of the pattern from Fig. 1 is illustrated. (The fracture is located on the front face of Fig. 2 and subsequent similar figures.) Fig. 3 shows the pressure distribution for the same half-pattern when no fracture connected the wells. For the open-fracture case, the flow rate through the half-pattern was 21 times greater than for the no-fracture case. On the positive side, the fracture allowed the pattern to experience much higher injectivity and productivity indexes than the no-fracture case. However, on the negative side, most of the injected fluid simply channeled through the fracture. Also on the positive side, higher pressure gradients were distributed more deeply through the pattern for the open-fracture case than for the no-fracture case (compare Figs. 2 and 3). For the open-fracture case, 75% of the pattern experienced a pressure gradient over 0.5 psi/ft, while for the no-fracture case, only 26% of the pattern experienced a pressure gradient over 0.5 psi/ft. Of course, higher pressure gradients aid in driving oil from deep within the pattern. However, from a practical view, a 1,000-psi pressure difference may be difficult to maintain across the pattern when the fracture is fully open. If high flow rates overwhelm the pumps used, a lower pressure drop may result—leading to lower pressure gradients throughout the pattern than are indicated in Fig. 2. Incidentally, it may help to view the pressure distributions in this report as “waterfalls” or inclined surfaces that direct the drainage of fluid from the pattern. Near-horizontal surfaces indicate poor drainage, while steep surfaces indicate rapid drainage.

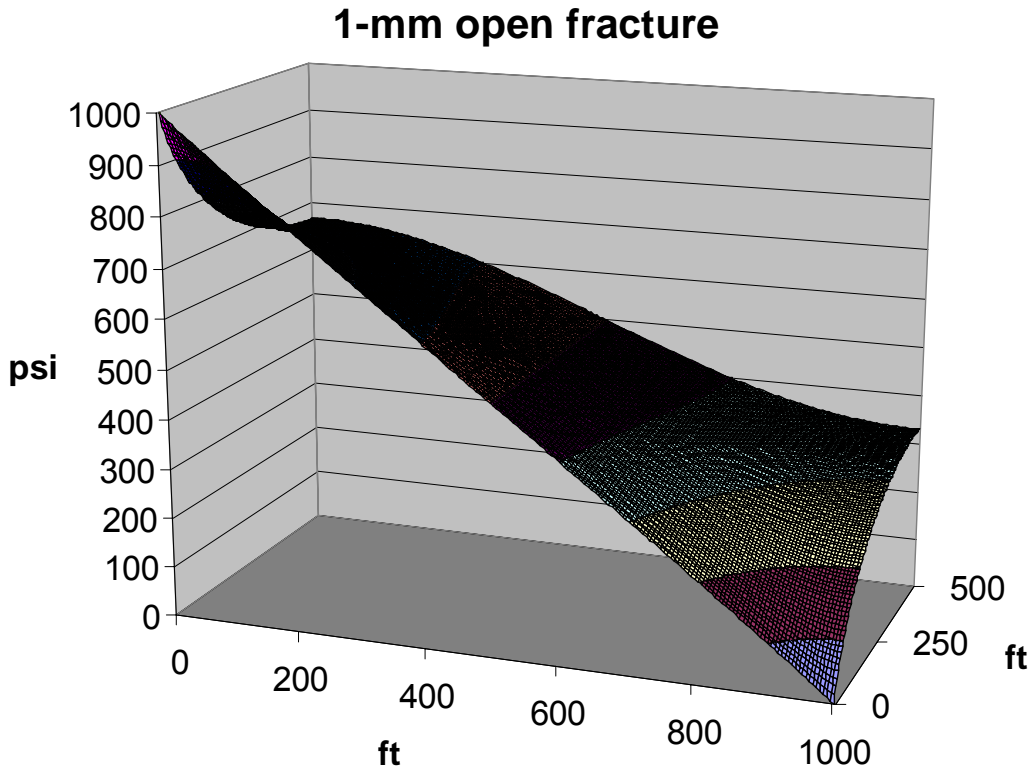


Fig. 2—Pressure distribution when 1-mm fracture was fully open.

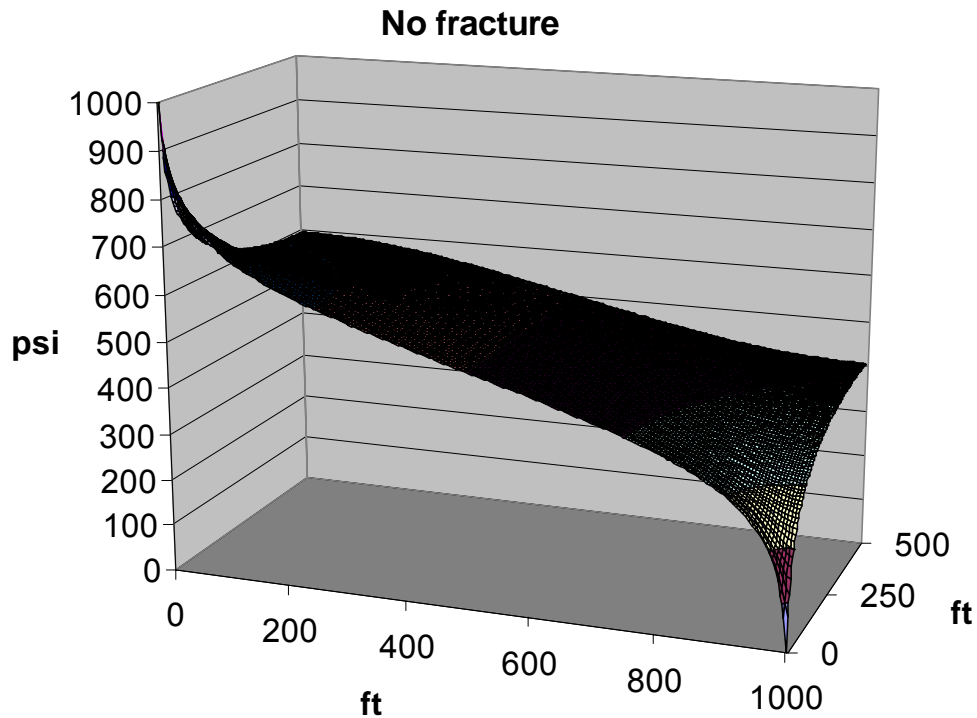


Fig. 3—Pressure distribution with no fracture.

A 25-ft Long Gel Plug Substantially Reduced Productivity in Moderate to Wide Fractures.

If a blocking agent (e.g., a gel) is used, how do the production rate, sweep efficiency, and pressure gradients in the pattern vary as a function of the position of blocking agent within the fracture? Fig. 4 plots the production rate (relative to that for an open fracture) as a function of the distance that a gel plug extends from the production well into the fracture. In these cases, the gel plug was assumed to completely stop flow within the gel-contacted portion of the fracture, but the gel did not reside in the porous rock. Four different fracture widths (w_f) were examined, ranging from 0.25 to 2 mm. For fractures with widths of 0.5 mm or greater, large reductions in production rate were achieved by gel penetrating only 25 ft from the production well. Further gel penetration into the fracture (up to 900 ft from the producer) had little additional impact on the rate.

As expected, the impact of partially plugging a fracture was most dramatic for the widest fractures. Interestingly, partial plugging of fractures had little impact on production rate for fractures with widths of 0.25 mm or less (solid circles in Fig. 4).

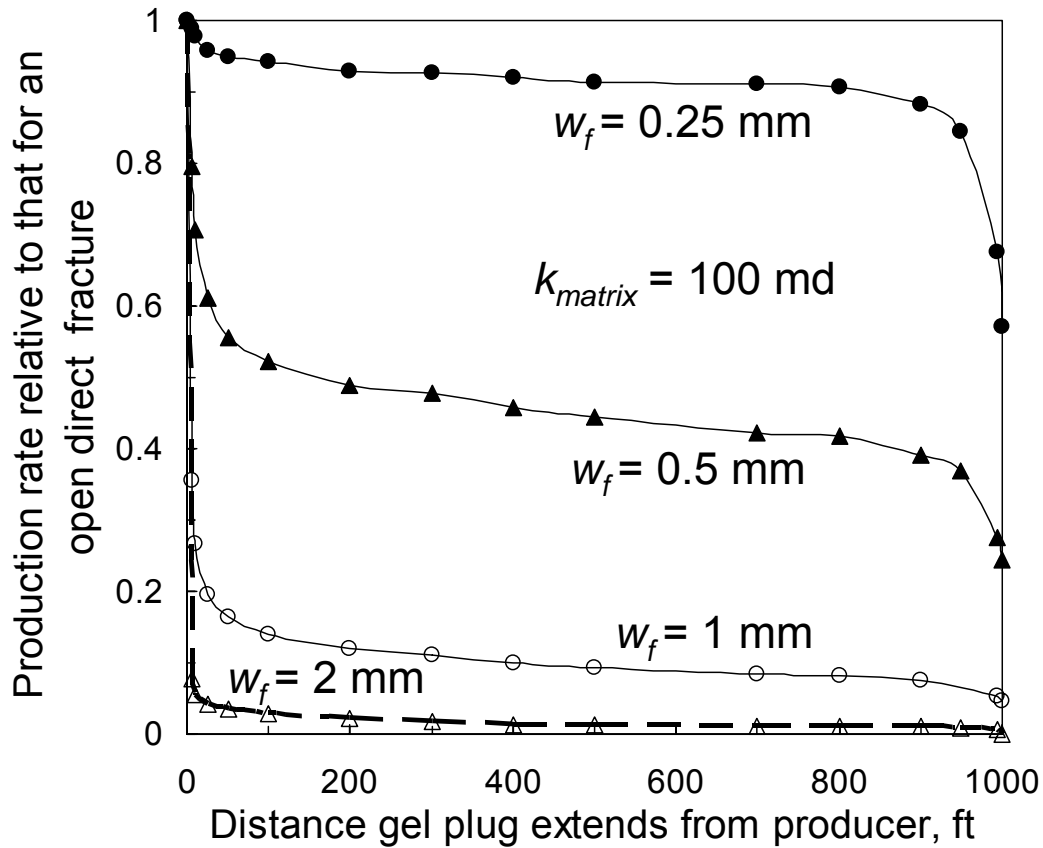


Fig. 4—Production rate versus gel plug size and fracture width. Scenario 1.

Gel Plugs Were Not Needed in Narrow Fractures ($w_f \leq 0.25$ mm if $k_{matrix} = 100$ md). How is sweep efficiency affected by fracture width and size of the gel plug? This question is addressed in Figs. 5-8. These figures plot the fraction of the injected fluid that sweeps into various portions of the pattern as a function of distance that the gel plug extends from the producer. For example, in Fig. 5 when gel extended 10 ft into the 0.25-mm fracture, 67% of the injected fluid was forced to flow at least 25 ft away from the direct fracture (i.e., the outer 95% of the pattern); 64% of the injected fluid was forced to flow at least 50 ft away from the direct fracture (i.e., the outer 90% of the pattern); 55% of the injected fluid was forced to flow at least 100 ft away from the direct fracture (i.e., the outer 80% of the pattern); and 32% of the injected fluid was forced to flow at least 250 ft away from the direct fracture (i.e., the outer 50% of the pattern). For comparison, the ideal sweep would force 50% of the fluid to flow through the outer 50% of the pattern.

Fig. 5 shows that sweep efficiency was not particularly sensitive to distance of gel penetration into the 0.25-mm fracture. Combined with the behavior noted in Fig. 4, we confirm that an individual fracture with $w_f \leq 0.25$ mm had a relatively small influence on flow capacity and sweep efficiency in 100-md rock. Fig. 9 shows pattern pressures when a 100-ft plug extended into a 0.25-mm wide fracture. Note the similarity of this figure with the no-fracture case illustrated in Fig. 3. Consequently, a gel treatment was of little value for this particular case.

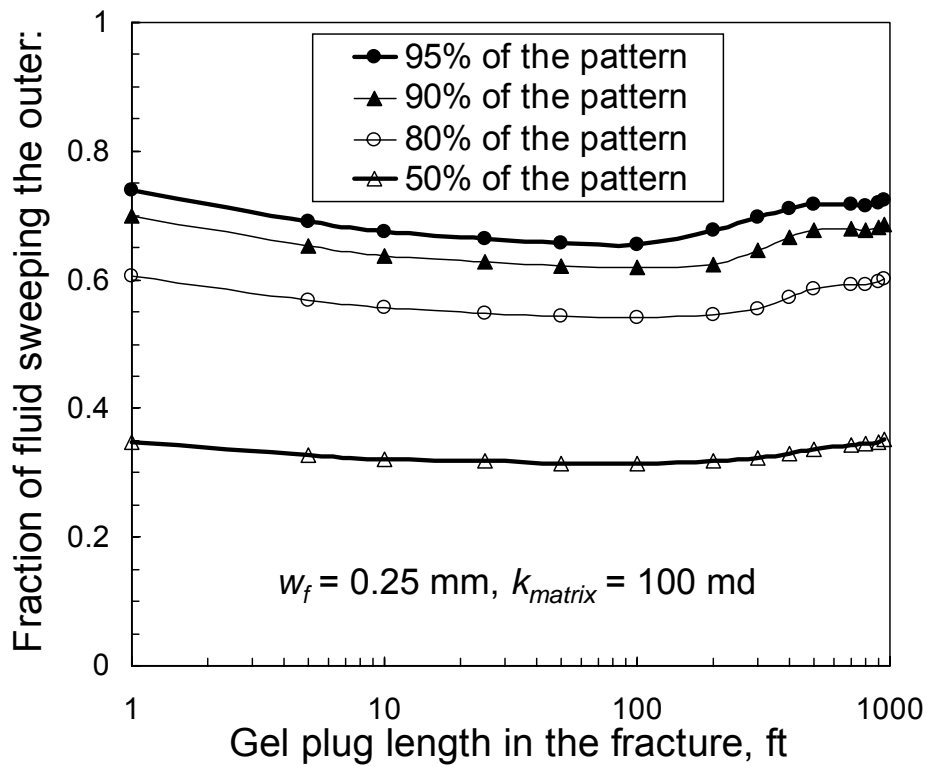


Fig. 5—Sweep efficiency in pattern with $w_f = 0.25 \text{ mm}$.

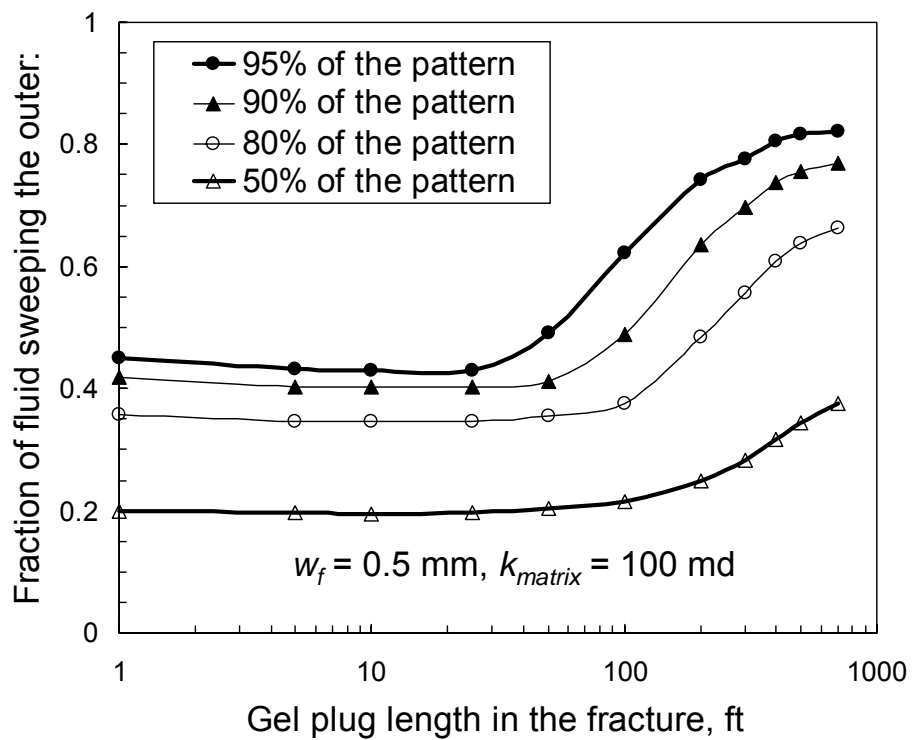


Fig. 6—Sweep efficiency in pattern with $w_f = 0.5 \text{ mm}$.

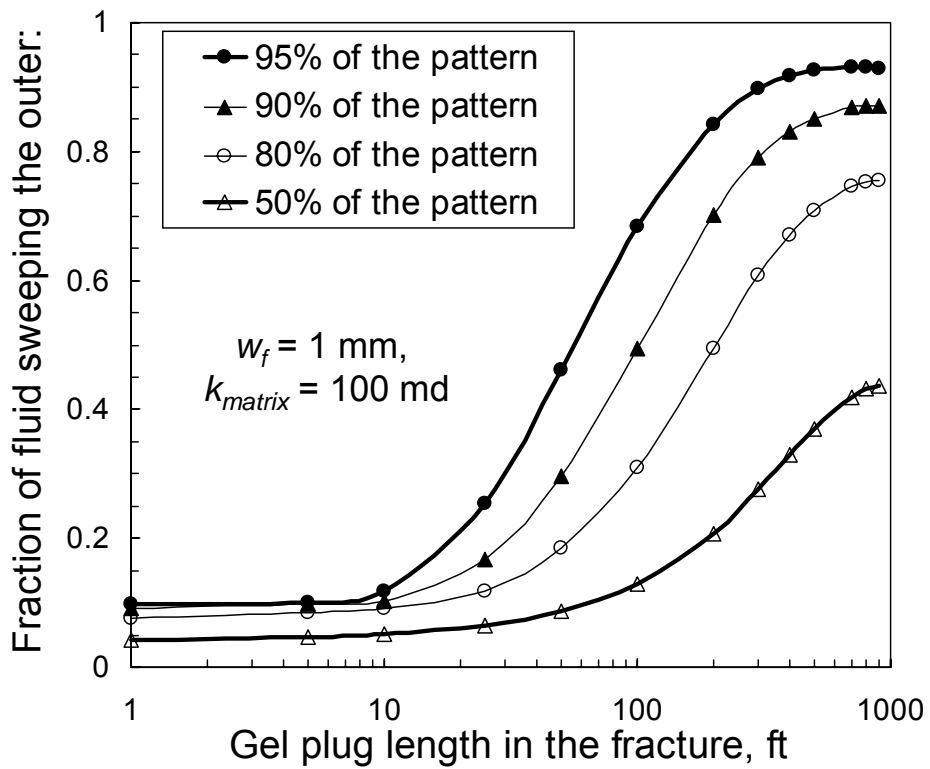


Fig. 7—Sweep efficiency in pattern with $w_f = 1 \text{ mm}$.

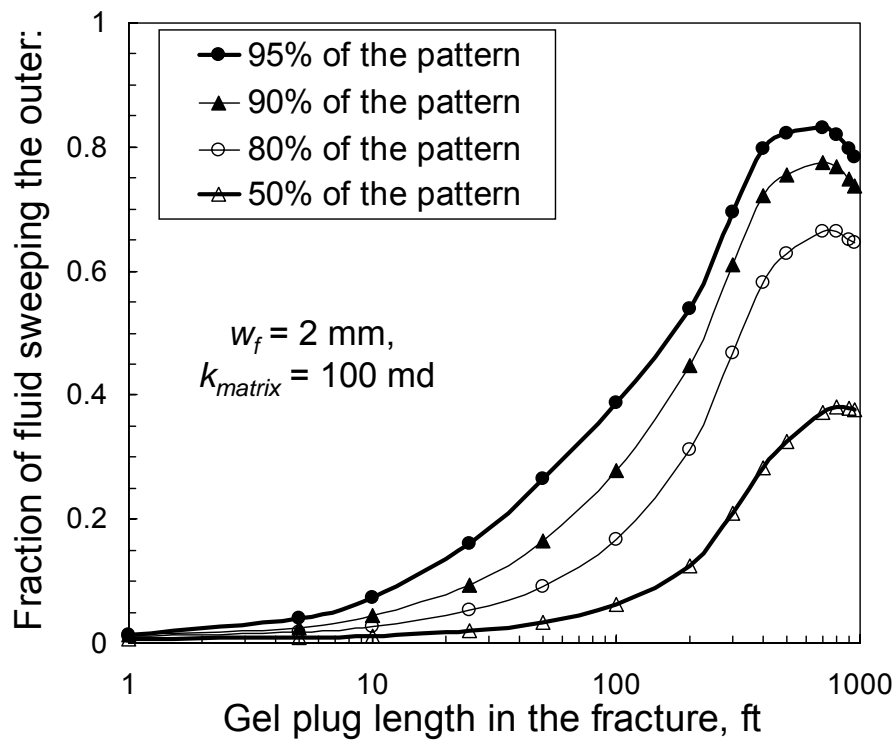


Fig. 8—Sweep efficiency in pattern with $w_f = 2 \text{ mm}$.

100-ft plug extending from producer into a 0.25-mm fracture

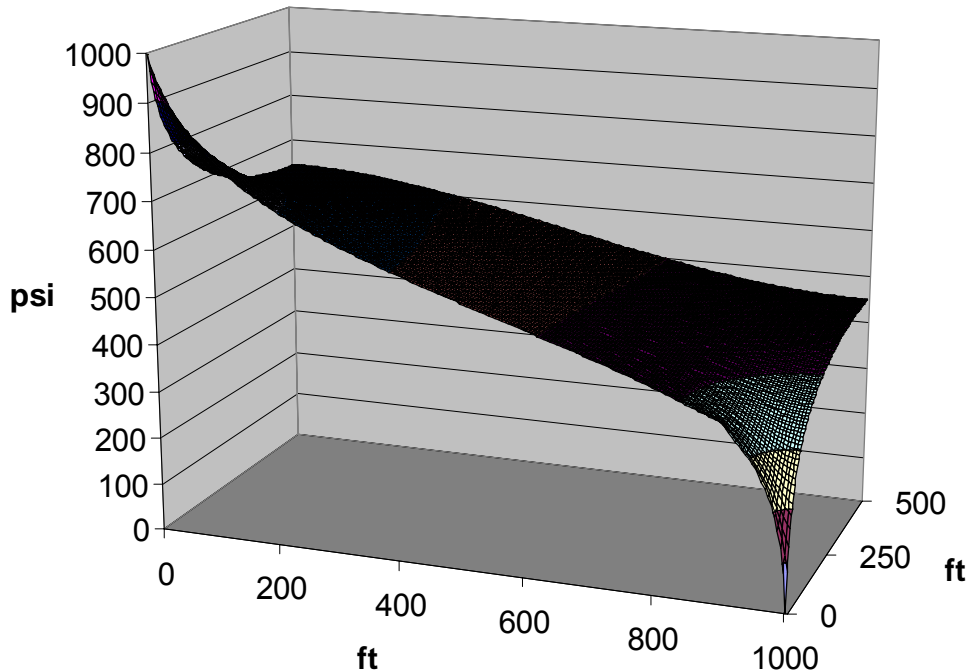


Fig. 9—Pattern pressures when 100-ft plug extended from producer into 0.25-mm fracture.

Gel Plugs Filling > 10% of the Fracture Were Needed to Significantly Improve Sweep. For fractures with widths of 0.5 mm or greater, the distance of gel penetration into the fracture more strongly affected sweep efficiency (Figs. 6-8). These figures suggest that the gel plug should penetrate at least 100 ft from the production well (i.e., fill at least 10% of the fracture) in order to significantly improve sweep efficiency. The figures also indicate that substantial improvements in sweep efficiency can be realized by filling up to half of the fracture with gel.

Plugs up to 80% of Fracture Length Improved Matrix Pressure Gradients. Fig. 10 shows the percent of the pattern that experienced pressure gradients over 0.5 psi/ft as a function of fracture width and distance of gel penetration from the producer. Consistent with our earlier observations, little benefit was realized for a gel treatment in fractures with $w_f \leq 0.25$ mm. For wider fractures, a large fraction of the pattern area appeared to experience high pressure gradients when the fracture was completely open. However, as mentioned earlier, pump limitations may make it impractical to maintain a high pressure difference between the wells when the fracture is completely open. For cases where at least the near-wellbore portion of the fracture was plugged, the fraction of the pattern area with pressure gradients above 0.5 psi/ft increased with increased gel plug size for plugs extending up to 800 ft from the producer. As mentioned, higher pressure gradients (especially in remote portions of the pattern) provide increased ability to drive oil to the producer. Figs. 11-13 show pattern pressures for several plug sizes (extending from 100 ft to 800 ft from the producer) in a 1-mm wide fracture. These figures aid in understanding the improved pattern drainage when using larger plugs.

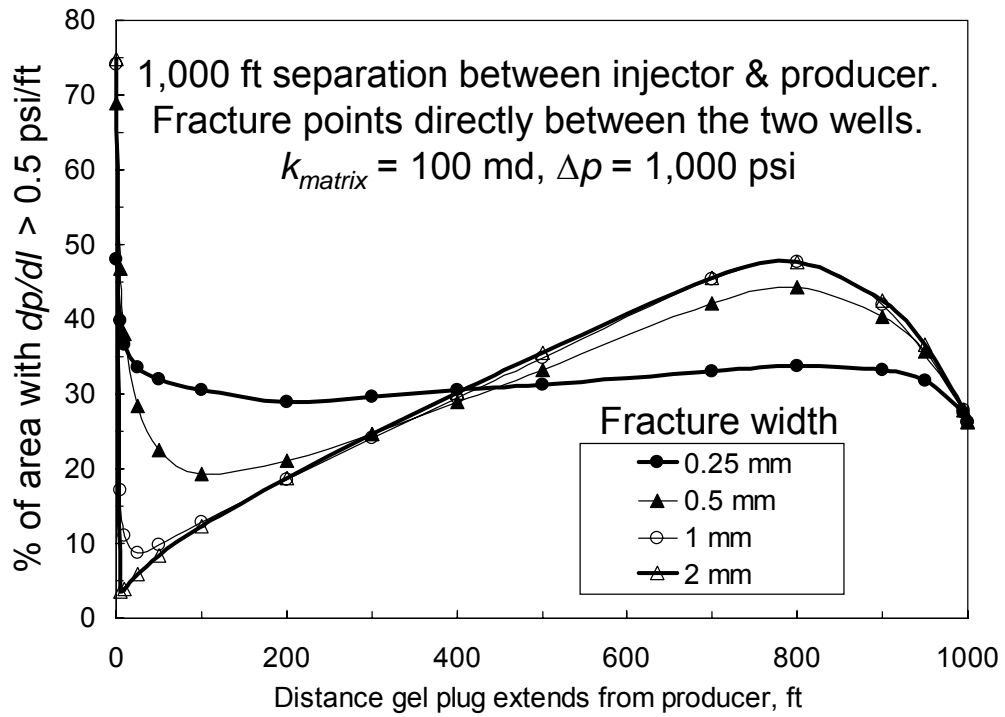


Fig. 10—Percent of pattern experiencing high pressure gradients. Scenario 1.

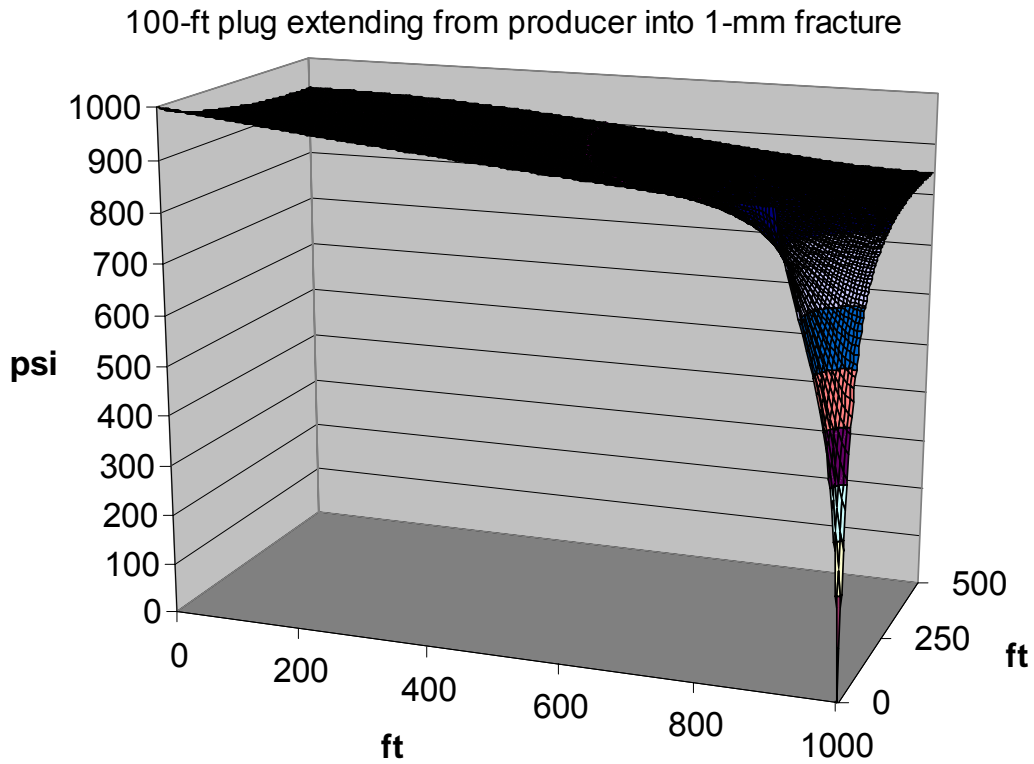


Fig. 11—Pattern pressures when 100-ft plug extended from producer into 1-mm fracture.

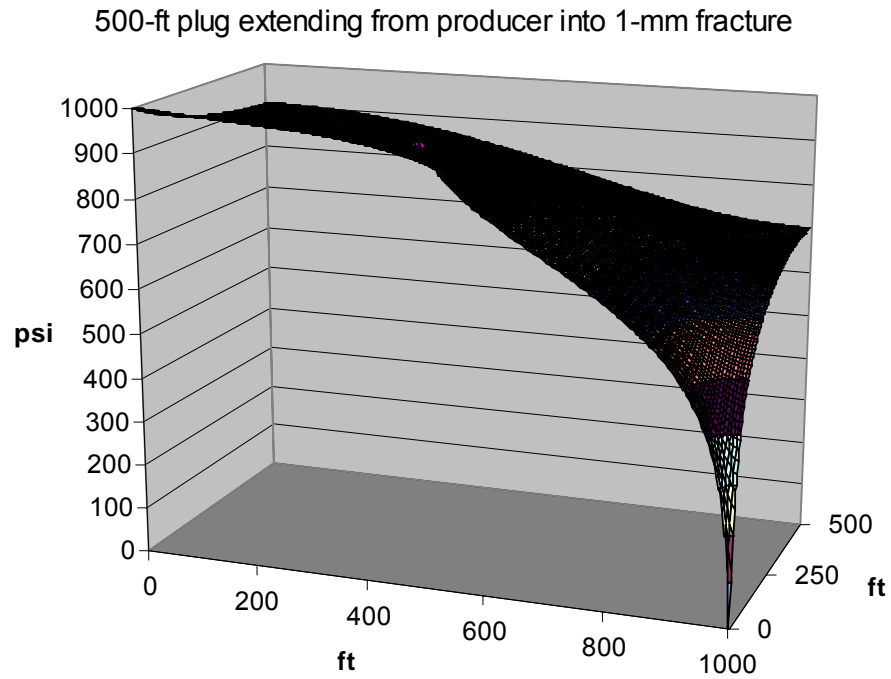


Fig. 12—Pattern pressures when 500-ft plug extended from producer into 1-mm fracture.

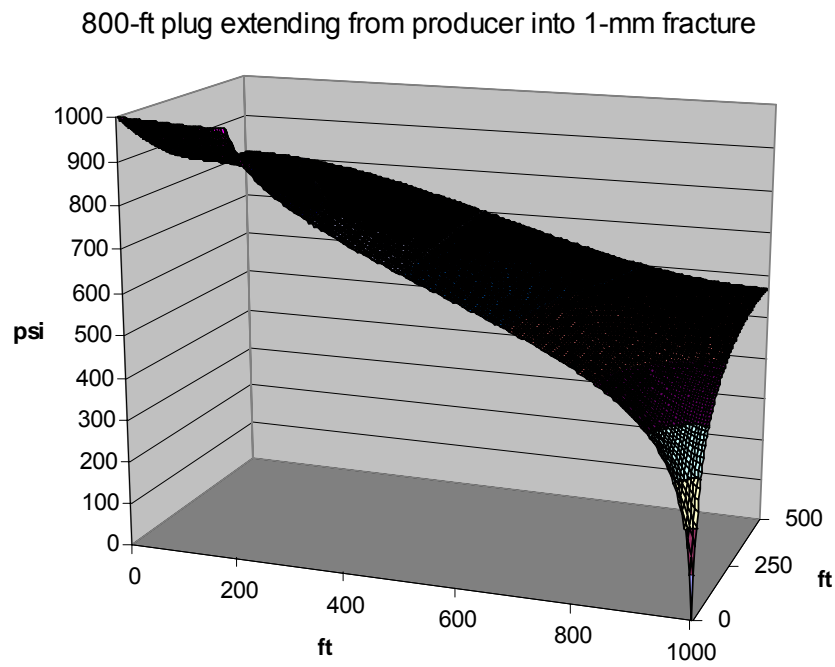


Fig. 13— Pattern pressures when 800-ft plug extended from producer into 1-mm fracture.

Effect of Plug Size for Gel Positioned in the Center of the Fracture. If a gel plug is centered halfway between the two wells in the fracture, how will production rate and sweep efficiency be affected by the length of the gel plug? For four fracture widths, Fig. 14 plots the production rate as a function of the length of the centered gel plug. As expected, the shortest gel plug provided the highest production rate. For the case of a 1-mm wide fracture, a 10-ft long plug centered halfway in the fracture (i.e., between 495 and 505 ft from the producer) allowed a production rate that was 46% of the rate associated with an open fracture. A 1,000-ft long plug that filled the entire fracture led to a production rate that was only 5% of the rate associated with an open 1-mm wide fracture.

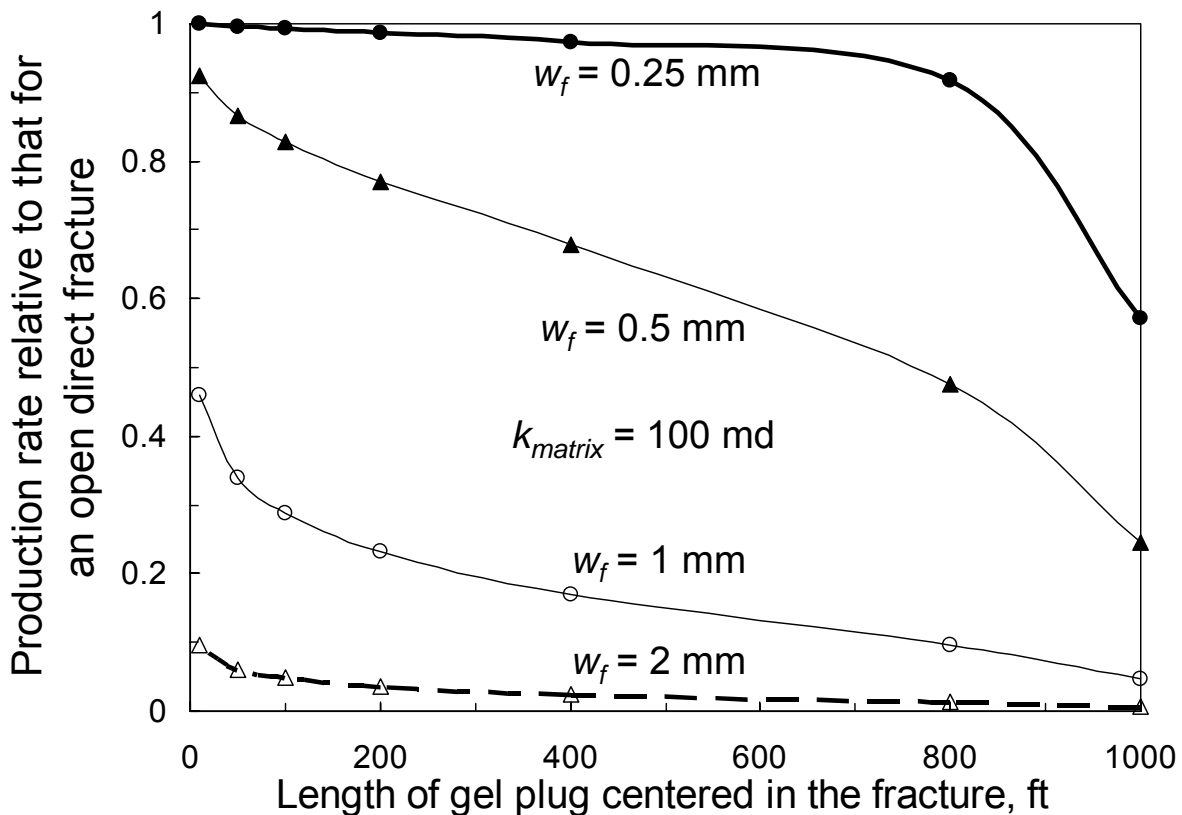


Fig. 14—Effect of centered plug size on production rate.

For Plugs Centered in the Fracture, Sweep Improvement Was Not Sensitive to Plug Size if the Plugs Were Longer than 20% of the Fracture Length. Fig. 15 illustrates the sweep efficiency as a function of the length of the centered gel plug. Sweep efficiency increased sharply with increased plug size for plugs up to 100 ft in length. Above 200 ft, sweep efficiency was fairly insensitive to plug length.

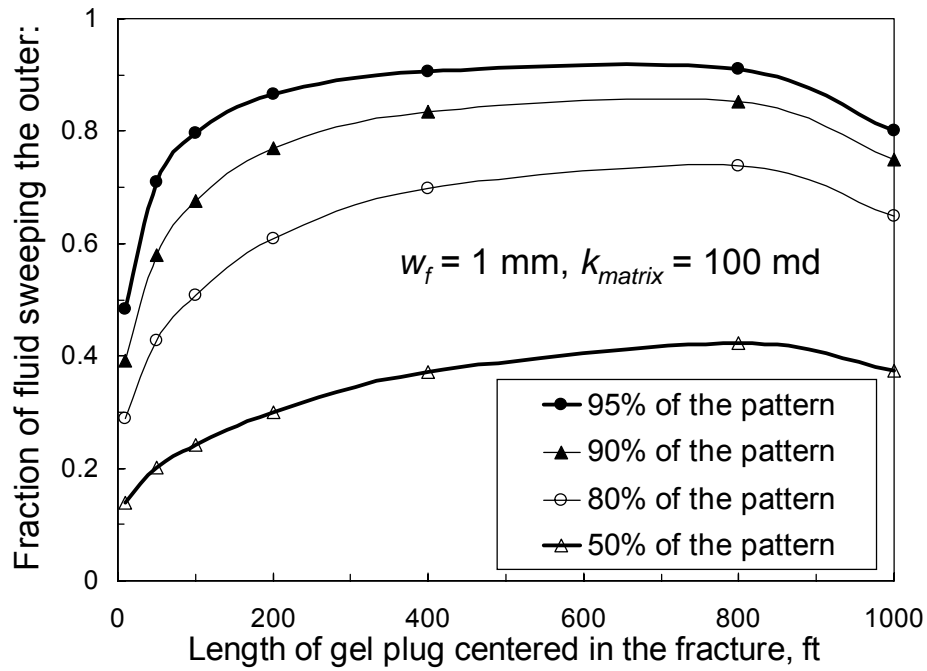


Fig. 15—Effect of centered plug size on sweep efficiency.

Fig. 16 shows how the length of the centered gel plug affected pressure gradients in the pattern. For a wide range of plug sizes (10 to 800 ft for the wider fractures), pressure gradients above 0.5 psi/ft were maintained in over 70% of the pattern.

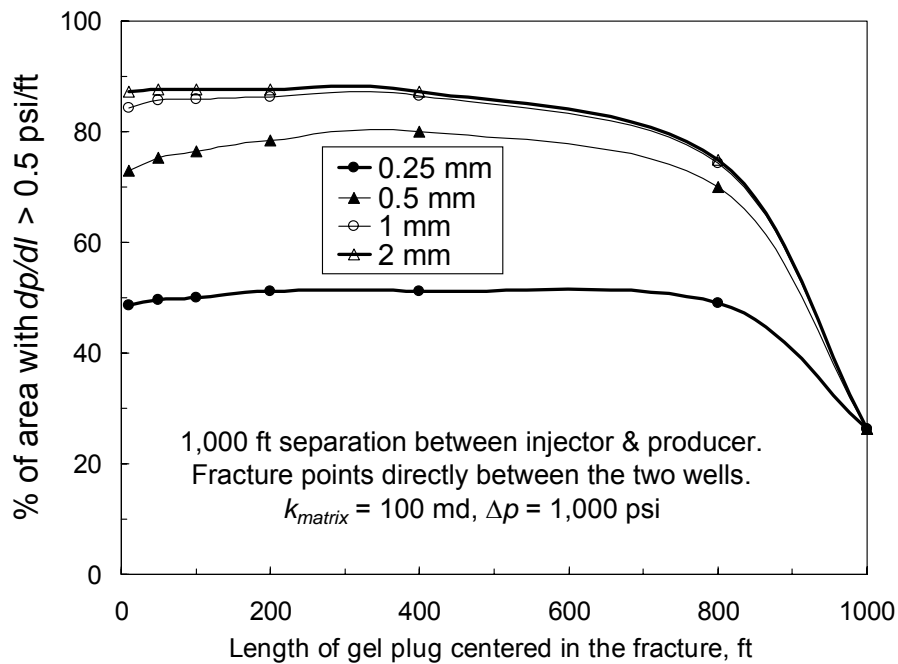


Fig. 16—Effect of centered plug size on pressure gradients.

Figs. 17-19 illustrate pressure distributions in the pattern for three plug sizes ranging from 10 to 800 ft. These figures illustrate how pressure gradients and drainage varied within the pattern when the gel plugs were centered in 1-mm wide fractures.

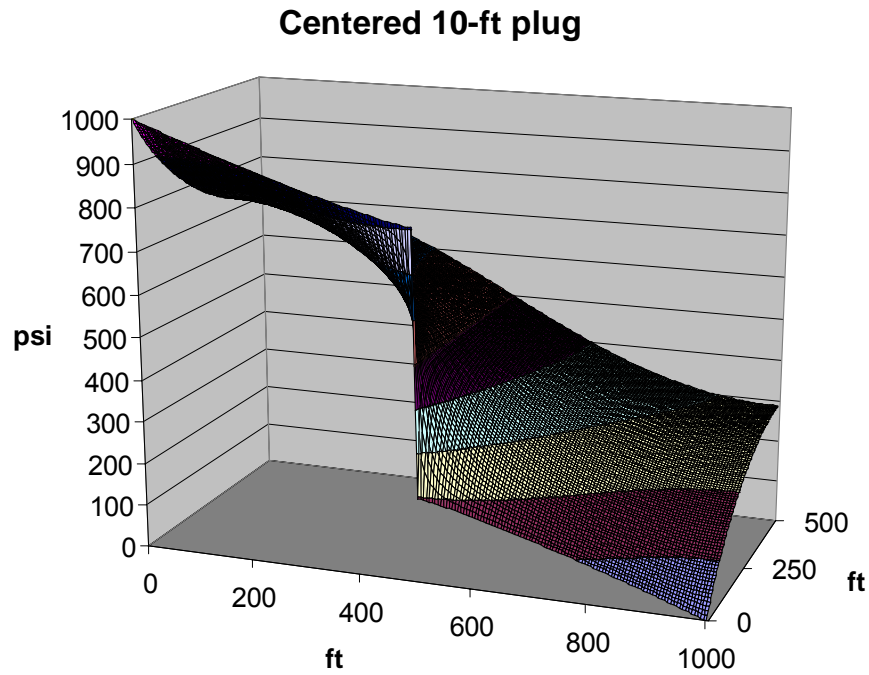


Fig. 17—Pressure distribution with a 10-ft plug centered in a 1-mm fracture.

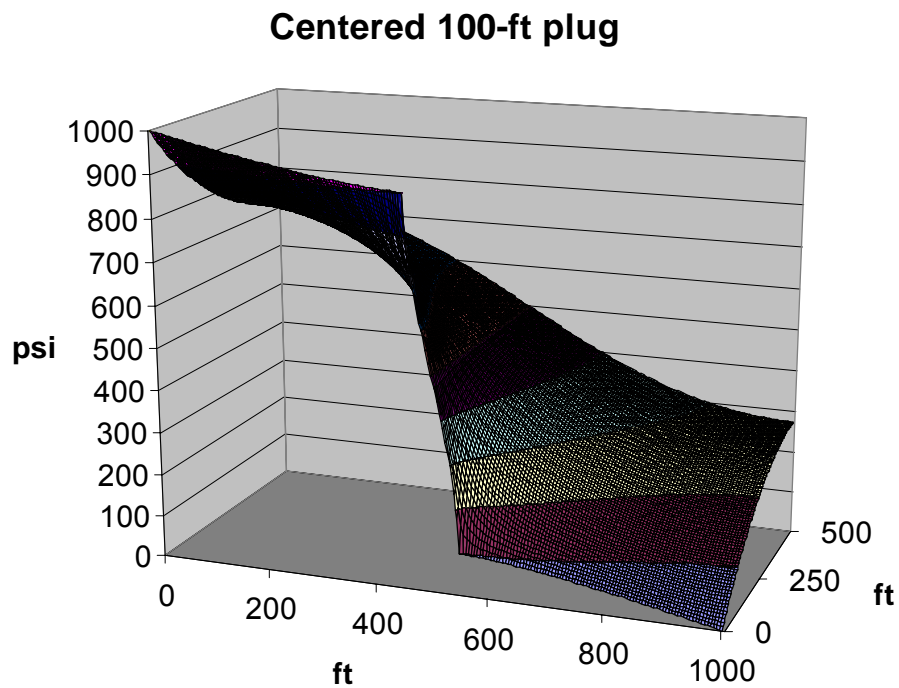


Fig. 18—Pressure distribution with a 100-ft plug centered in a 1-mm fracture.

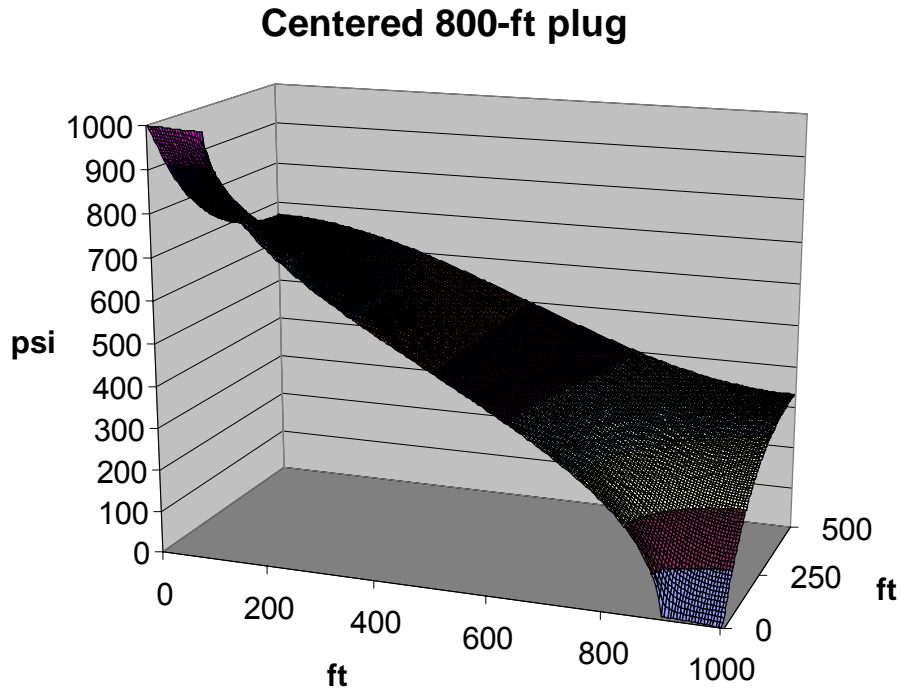


Fig. 19—Pressure distribution with a 800-ft plug centered in a 1-mm fracture.

Off-Centered Plugs Didn't Affect Rates Much if the Plugs Were Not Close to a Well. The previous section suggested that the gel plug should be at least 100 ft long to provide a high sweep efficiency. If the gel plug is fixed at 100 ft in length, how much does it matter where the plug is positioned in the fracture? Fig. 20 shows how production rate varied with plug position. The x-axis plots the position of the center of each 100-ft long gel plug. This figure shows that the production rate was insensitive to plug positions that were centered between 150 and 850 ft in the fracture.

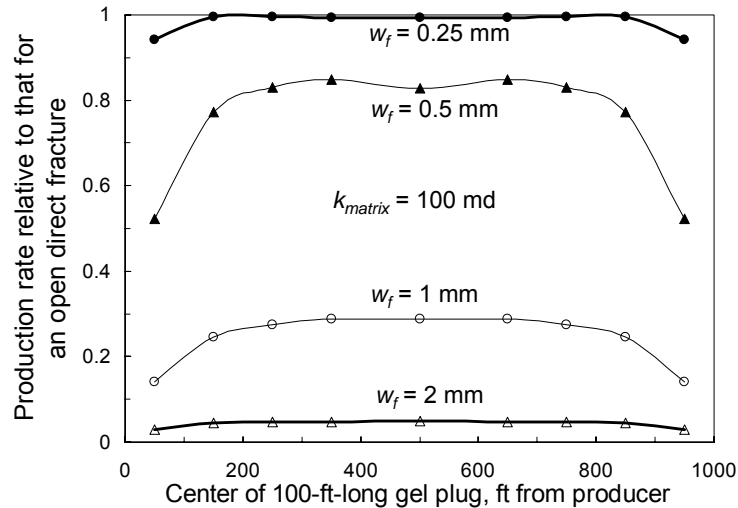


Fig. 20—Effect of plug position on production rate.

Sweep Decreased as Plugs Moved Off-Center. Fig. 21 demonstrates how sweep efficiency varied with plug position. Sweep efficiency declined as the plug moved farther off center. However, the decline was not generally dramatic if the plug was not in the vicinity of a well.

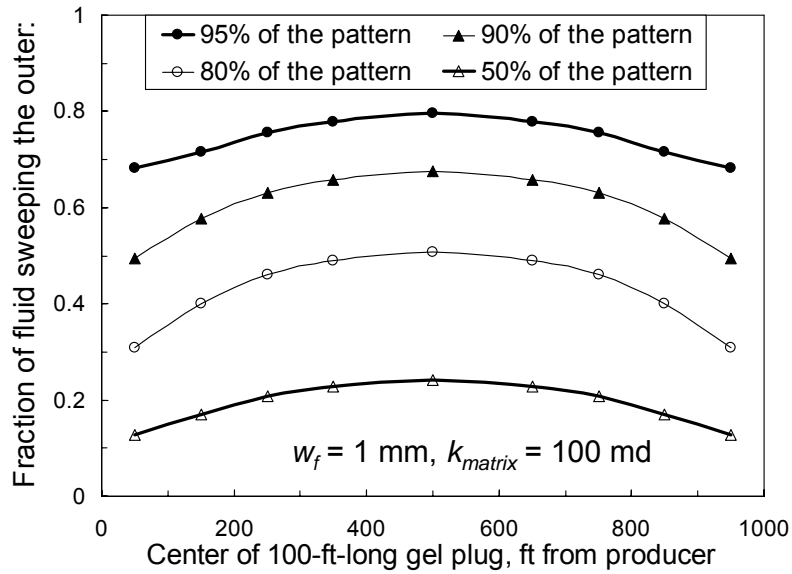


Fig. 21—Effect of plug position on sweep efficiency.

Centered Plugs Maintained the Highest Pattern Pressure Gradients. Fig. 22 illustrates the percent of the pattern area that experienced pressure gradients above 0.5 psi/ft as a function of plug position. Especially for the wider fractures, the maximum values were noted when the plug was positioned near the center of the fracture.

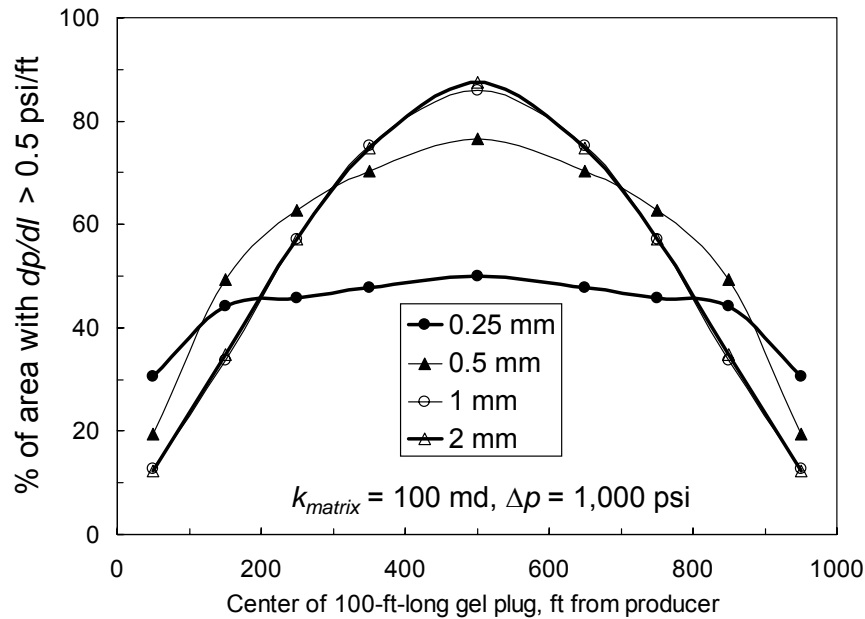


Fig. 22—Effect of plug position on pressure gradients.

Figs. 11, 18, and 23 illustrate the distribution of pressures in the pattern for three positions of 100-ft plugs in a 1-mm fracture. When the plug was close to the production well, the pressure gradients were very low except within a 100-ft radius of the producer (Fig. 11). When the plug was centered at 250 ft from the producer, the pressure gradients were noticeably higher throughout the pattern (Fig. 23). High pressure gradients were most widespread through the pattern when the plug was centered in the middle of the fracture (Fig. 18).

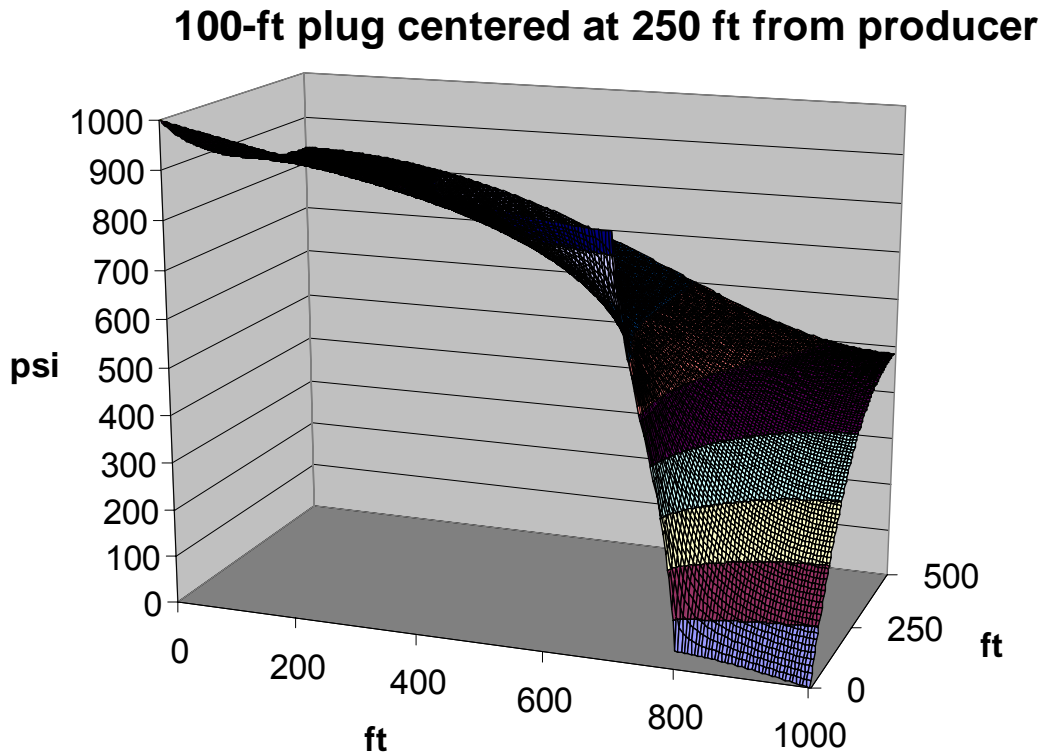


Fig. 23—Pressures for a 100-ft gel plug positioned 250 ft from producer in a 1-mm fracture.

Translating Results to Cases with Other Rock Permeabilities. For the work presented to this point, the rock permeability was assumed to be 100 md. How will the results change if a different permeability is applied? Our results can be scaled to other permeabilities if the ratio of fracture flow capacity ($k_f w_f h_f$) to matrix flow capacity ($k_{matrix} w_{matrix} h_{matrix}$) is fixed. Here, we assumed that the heights of the fracture and the matrix were the same. We also recognized the relation between fracture width (in mm) and fracture conductivity ($k_f w_f$, in darcy-ft)^{3,4}:

$$w_f = 0.153 (k_f w_f)^{1/3} \dots\dots\dots(1)$$

Given the reference permeability (i.e., 0.1 darcys), a reference fracture width ($w_{f\ ref}$, e.g., 1 mm), and the new rock permeability (k_{new}), a fracture width ($w_{f\ new}$) can be calculated that will allow the figures in this report to be used.

$$w_{f_{new}} = w_{f_{ref}} (k_{new} / 0.1)^{1/3} \dots\dots\dots(2)$$

Alternatively, Fig. 24 can be used to make these determinations. For example, if the effective permeability of the reservoir rock was really 10 md (0.01 darcys), then the behavior of the curves for $w_f = 1$ mm used in this report would apply to fracture widths of 0.46 mm in the new reservoir rock [$0.46 = 1 (0.01/0.1)^{1/3}$]. Similarly, the curves for 2-mm, 0.5-mm, and 0.25-mm fractures in this report would apply to fracture widths of 0.93 mm, 0.23 mm, and 0.12 mm, respectively.

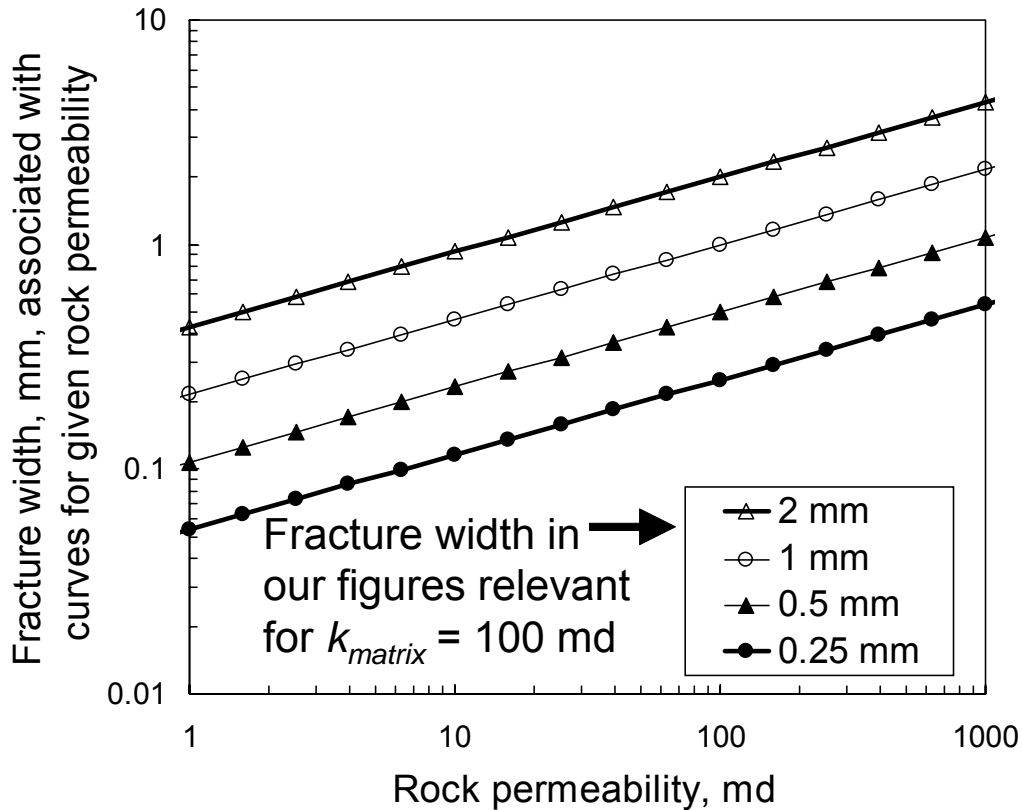


Fig. 24—Curves for translating results to reservoirs with different rock permeabilities.

For reservoir rock of 1 md, the curves for 2-mm, 1-mm, 0.5-mm, and 0.25-mm fractures in this report would apply to fracture widths of 0.43 mm, 0.22 mm, 0.11 mm, and 0.05 mm, respectively. Since we rarely think of economic oil reservoirs or pay zones with permeabilities less than 1 md, our results suggest that fractures narrower than 0.05 mm would rarely be targets for gel treatments. (Narrow fractures in tight gas sands might provide an exception.)

Summary for Scenario 1. For a reservoir pattern (1,000 x 1,000 ft) with two vertical wells (one injector and one producer) that were directly connected by a single vertical fracture, we examined the effects of plug size and location on production rate, sweep efficiency, and pattern pressure gradients. A gel plug that extended 25 ft from the production well substantially reduced productivity in moderate to wide fractures (e.g., $w_f \geq 0.5$ mm if $k_{matrix} = 100$ md). Gel plugs were not needed in narrow fractures (e.g., $w_f \leq 0.25$ mm if $k_{matrix} = 100$ md). To significantly improve sweep efficiency in moderate to wide fractures, gel plugs were needed that filled more than 10%

of the fracture. For plugs that extended from the production well, plug lengths up to 80% of the fracture length improved matrix pressure gradients. For plugs centered in the fracture, sweep improvement was not sensitive to plug size if the plugs were longer than 20% of the fracture length. Off-centered plugs didn't affect rates very much if the plugs were not close to a well. Sweep decreased as plugs became farther off-center. Centered plugs maintained the highest pattern pressure gradients (i.e., higher than off-centered plugs).

Scenario 2: Direct Fracture Channel between Two Parallel Fractures or Horizontal Wells

For the second scenario, we considered a similar pattern, except the injection well also intersected a vertical fracture that paralleled an equivalent fracture in the production well (Fig. 25). For patterns where the distance between the wells was large relative to the formation height, this scenario was equivalent to two parallel horizontal wells that were directly connected by a vertical fracture.

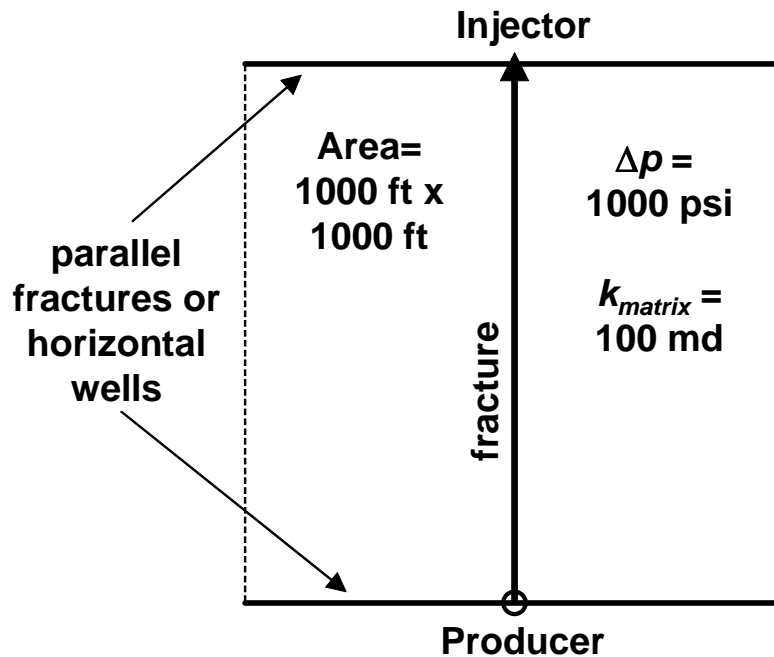


Fig. 25—Scenario 2: Areal view of a fracture connecting parallel fractures or horizontal wells.

For a case where the fracture width was 1 mm (for all three fractures), the pressure distribution is shown in Fig. 26. As with the previous scenario, only one-half of the pattern from Fig. 25 is illustrated because the pressure distribution was symmetrical about the direct connecting fracture. (The direct fracture that connects the wells was located on the front face of Fig. 26 and subsequent similar figures.) Fig. 27 shows the pressure distribution for the same half-pattern when no fracture connected the wells. For the open-fracture case, the flow rate through the half-pattern was seven times greater than for the no-direct-fracture case and twenty-three times greater than the case with no fractures or horizontal wells (i.e., the case of vertical wells with no fractures, as in Fig. 3).

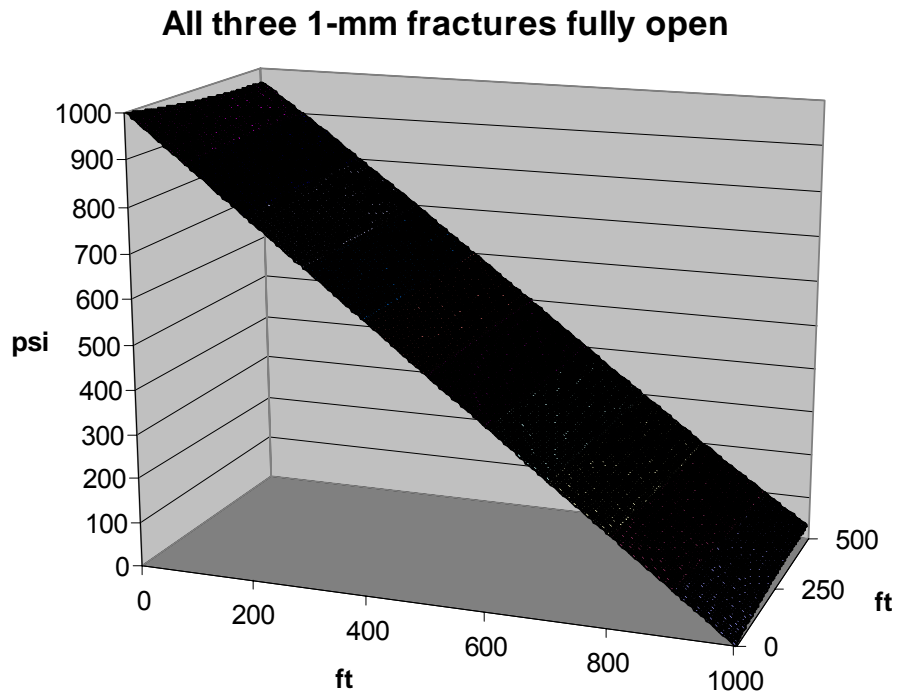


Fig. 26—Pattern pressures with a direct open fracture: 1-mm parallel fractures case.

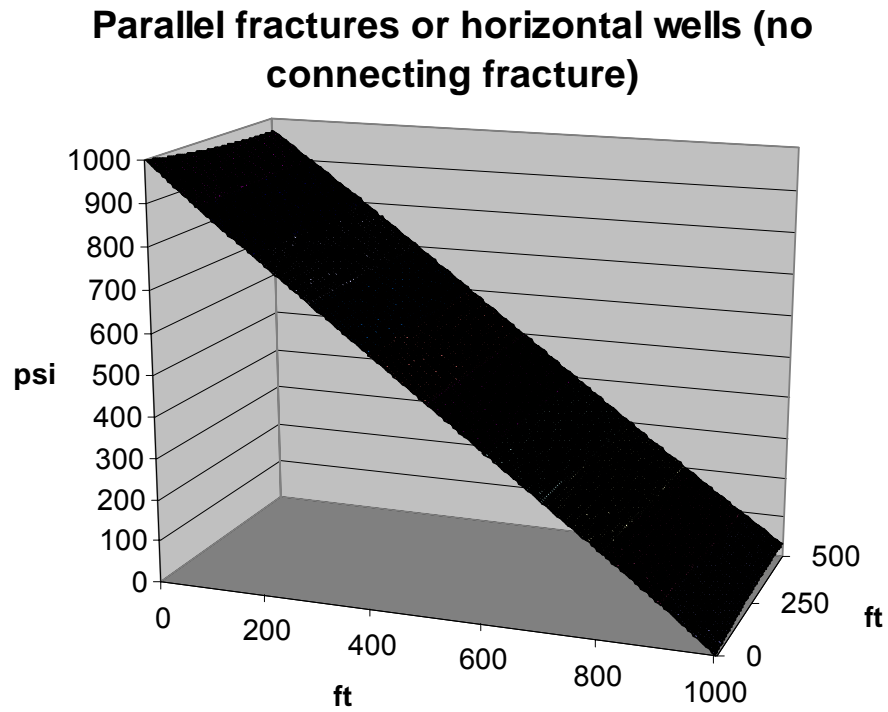


Fig. 27—Pattern pressures for parallel 1-mm fractures case, no connecting fracture.

Pressure Gradients and Sweep Were Good with Parallel Fractures or Horizontal Wells. A comparison of Figs. 26 and 27 revealed the same pressure gradients and sweep for the two cases. The pressure gradients were near 1 psi/ft throughout the pattern—the most desirable situation that can be achieved. However, as mentioned for the previous scenario, a 1,000-psi pressure difference may be difficult to maintain across the pattern when the fracture is fully open. If high flow rates overwhelm the pumps used, a lower pressure drop may result—leading to lower pressure gradients throughout the pattern than are indicated in Fig. 26.

In Moderate to Wide Fractures, Small Plugs Greatly Reduced Production Rates. Fig. 28 plots the production rate (relative to that for an open fracture) as a function of the distance that a gel plug extended from the production well into the fracture that directly connected the wells. (The parallel fractures or horizontal wells were assumed to remain completely open.) As in the previous section, the gel plug was assumed to completely stop flow within the gel-contacted portion of the fracture, but the gel did not reside in the porous rock. Again, four different fracture widths were examined, ranging from 0.25 to 2 mm. For any given fracture width, the plugs had a somewhat smaller impact on rates in Fig. 28 than in Fig. 4. However, overall, Fig. 28 had much in common with Fig. 4. For the widest fractures, large reductions in production rate were achieved by gel penetrating only 25 ft from the production well. Further gel penetration into the direct fracture (up to 900 ft from the producer) had a reduced impact on the rate. Also as was noted in Fig. 4, partial plugging of the direct fracture had little impact on production rate for fractures with widths of 0.25 mm or less.

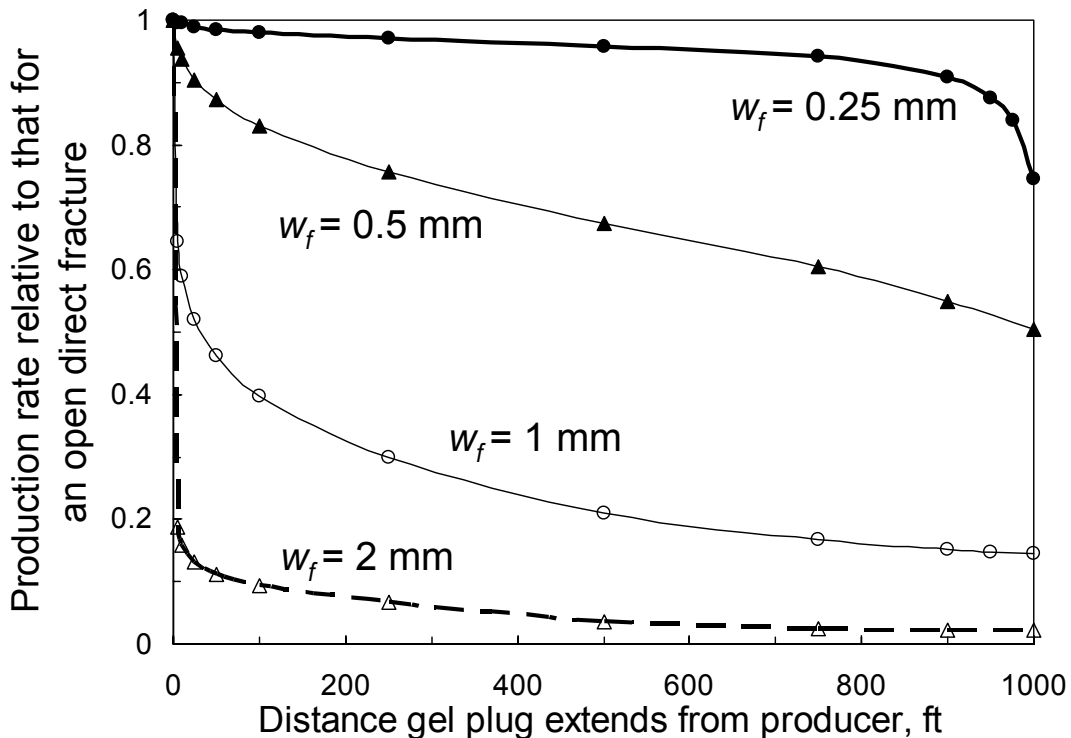


Fig. 28—Production rate versus gel plug size and fracture width. Scenario 2.

For Narrow Fractures, Gel Plugs Were Not Needed. The diminished effect of gel plugs for the narrower fractures can be understood by comparing Figs. 26, 29, and 30. When the two parallel fractures and the direct fracture had widths of 0.25 mm (Fig. 29), the flow capacity of the fracture system was less than that of the porous rock. Consequently, the pattern pressures had similarities with those for the case where no fractures were present (compare Figs. 3 and 29). As the flow capacity of the parallel fractures (or “horizontal wells”) increased, fluid flow was distributed more uniformly through the pattern (compare Figs. 26, 29, and 30). If the parallel fractures associated with Figs. 29 and 30 were significantly more conductive (as they would be for the case of parallel horizontal wells), the pattern pressures would resemble those shown in Fig. 26.

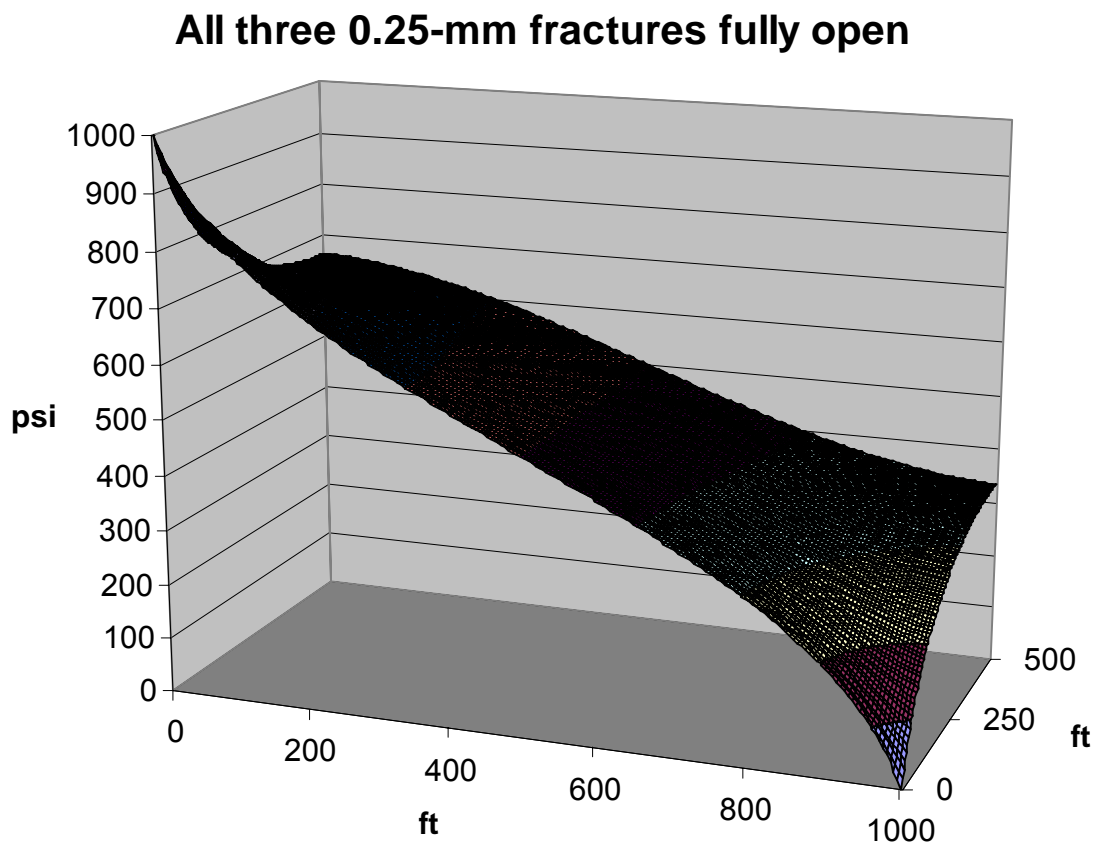


Fig. 29—Pattern pressures when all three 0.25-mm fractures are fully open.

All three 0.5-mm fractures fully open

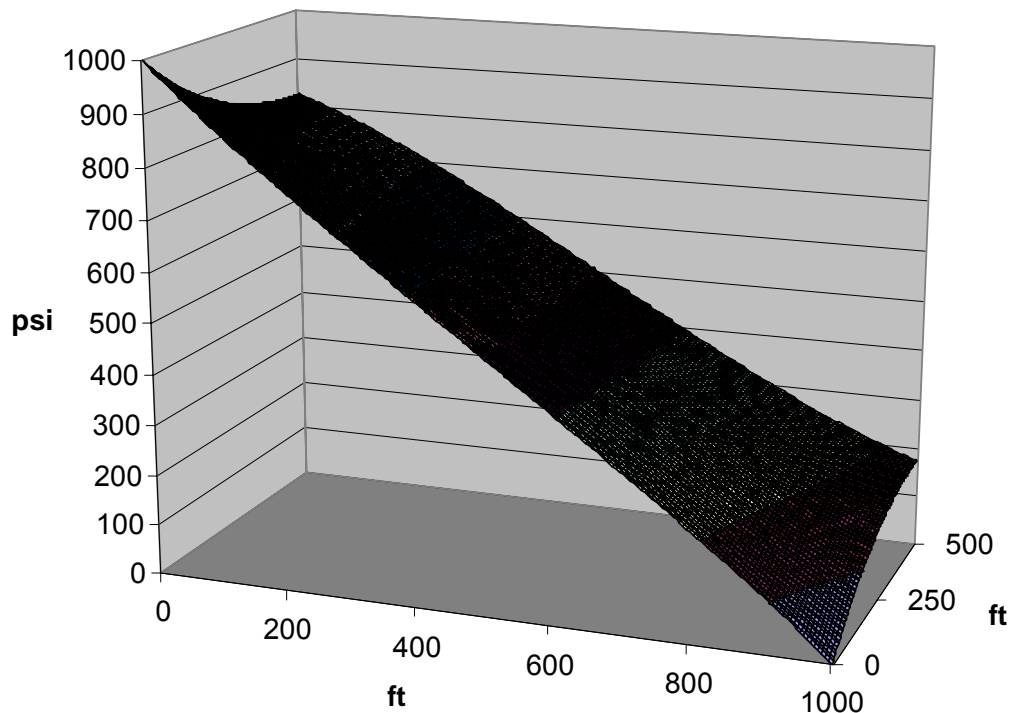


Fig. 30—Pattern pressures when all three 0.5-mm fractures are fully open.

Small Gel Plugs Were Often Adequate for Treating Fractures in Horizontal Wells. Fig. 31 shows the percent of the pattern that experienced pressure gradients over 0.5 psi/ft as a function of fracture width and distance of gel penetration from the producer. Consistent with our earlier observations, little benefit was realized for a gel treatment in fractures with $w_f \leq 0.25$ mm. For wider fractures, a large fraction of the pattern area appeared to experience high pressure gradients when the fracture was completely open. However, as mentioned earlier, pump limitations may make it impractical to maintain a high pressure difference between the wells when the fracture is completely open. For cases where at least the near-wellbore portion of the fracture was plugged, the fraction of the pattern area with pressure gradients above 0.5 psi/ft increased with increased gel plug size. This finding was consistent with that noted for Scenario 1, where no parallel fractures or horizontal wells were present (Fig. 10). However, for all plug lengths, a much greater percentage of the pattern experienced high pressure gradients than those in Scenario 1 (compare Figs. 10 and 31). Consequently, small gel plugs were much more effective for Scenario 2 (Fig. 25, with parallel fractures or horizontal wells) than for Scenario 1 (Fig. 1). This finding was consistent with that reported in Refs. 5-7. Figs. 32-34 aid in understanding how gel plugs affect pattern pressures for different fracture widths. Note in these figures that for the wider fractures, pressure gradients tended to be lowest near the injection well. Since the near-wellbore region was most likely to have been swept previously, this situation was not necessarily detrimental.

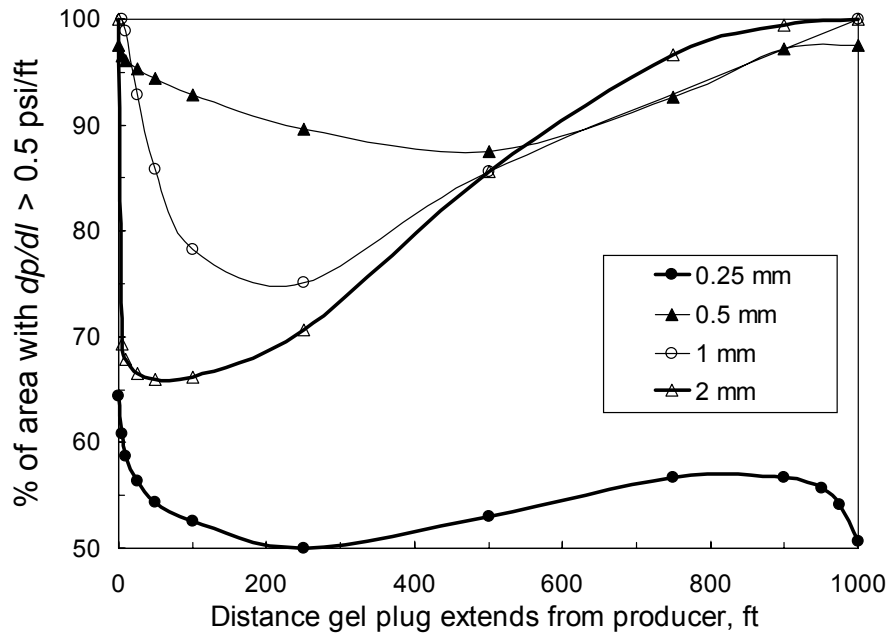


Fig. 31—Percent of pattern experiencing high pressure gradients. Scenario 2.

100-ft plug extending from producer into 0.5-mm fracture

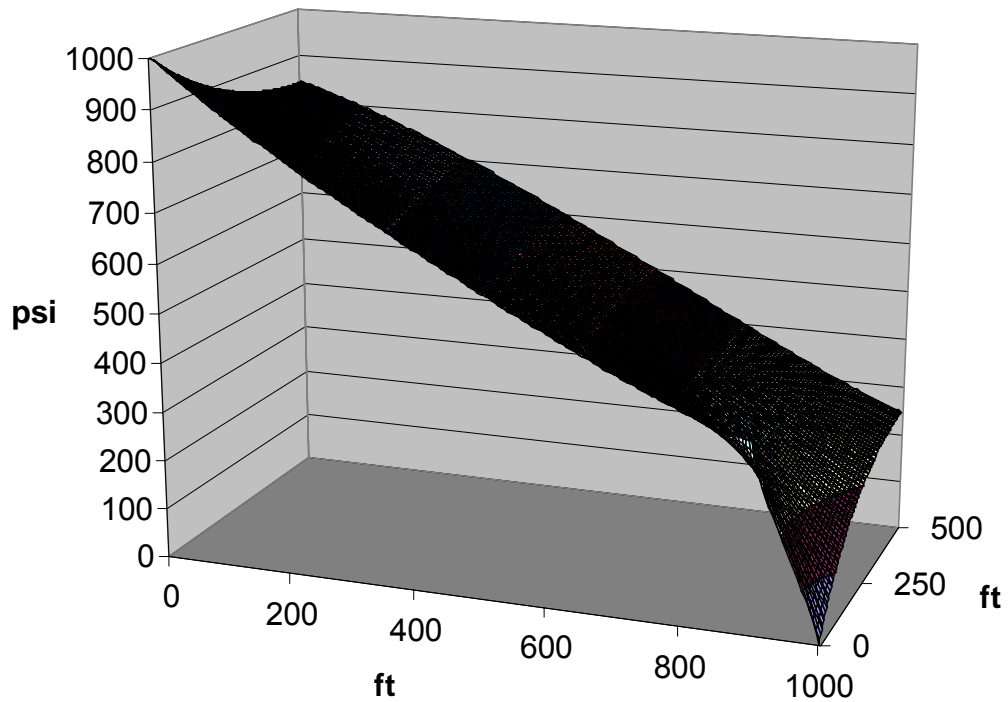


Fig. 32—Pattern pressures for 100-ft plug in 0.5-mm fracture. Scenario 2.

100-ft plug extending from producer into 1-mm fracture

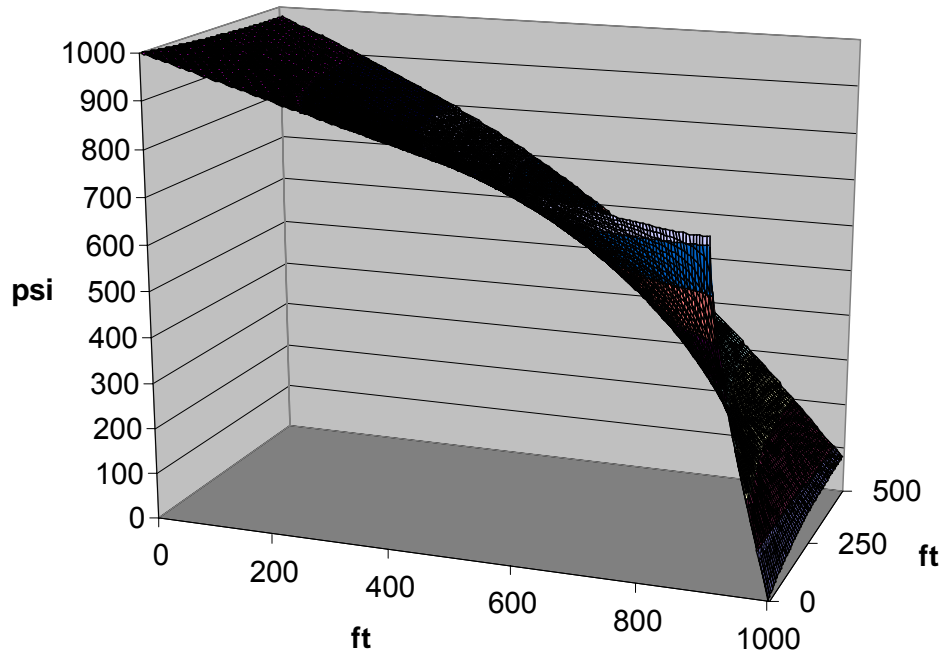


Fig. 33—Pattern pressures for 100-ft plug in 1-mm fracture. Scenario 2.

100-ft plug extending from producer into 2-mm fracture

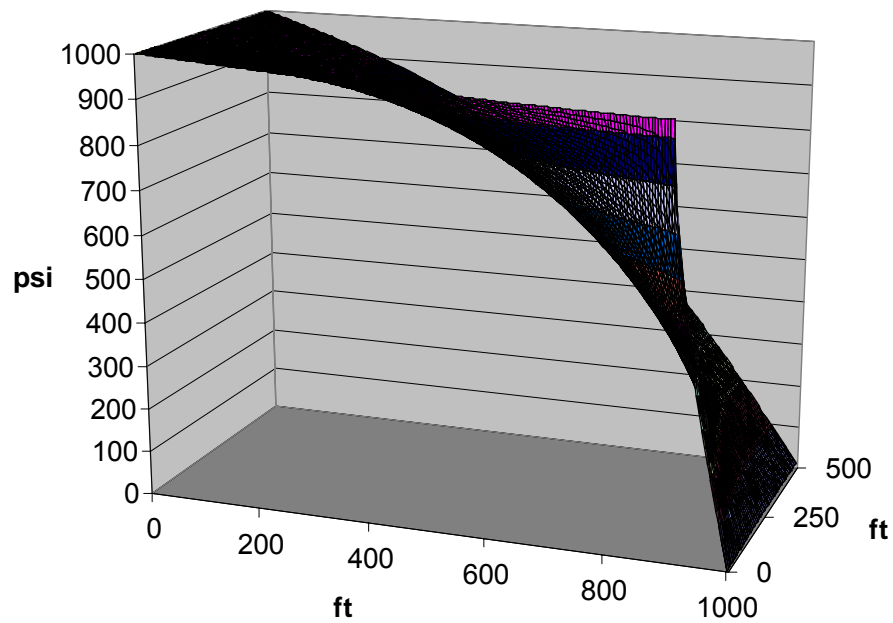


Fig. 34—Pattern pressures for 100-ft plug in 2-mm fracture. Scenario 2.

Summary for Scenario 2. For a reservoir pattern (1,000 x 1,000 ft) with two wells (one injector and one producer) that had either parallel fractures or parallel horizontal wells and that were directly connected by a single vertical fracture, we examined the effects of plug size and location on production rate, sweep efficiency, and pattern pressure gradients. Pattern pressure gradients and sweep were very desirable for parallel fractures or horizontal wells. In moderate to wide fractures, small plugs greatly reduced production rates. For narrow fractures, gel plugs were not needed. Small gel plugs (e.g., 25 ft long in the fracture) were often adequate for treating fractures in horizontal wells.

Scenario 3: Offset Fracture Parallel to the Main Direct Fracture

For the first two scenarios considered in this report, only one fracture was responsible for severe channeling between an injector-producer pair. In the third scenario (Fig. 35), a vertical fracture connected a pair of vertical wells (as in Scenario 1). However, in addition, a parallel fracture existed some distance away from the fracture that directly connected the two wells.

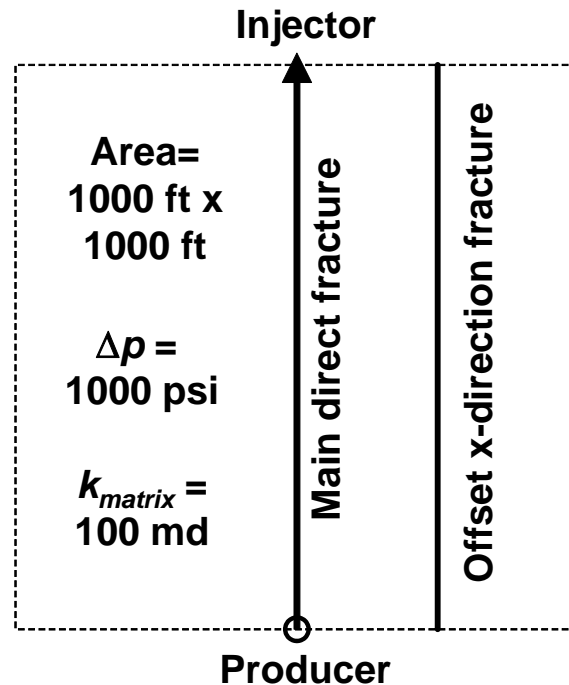
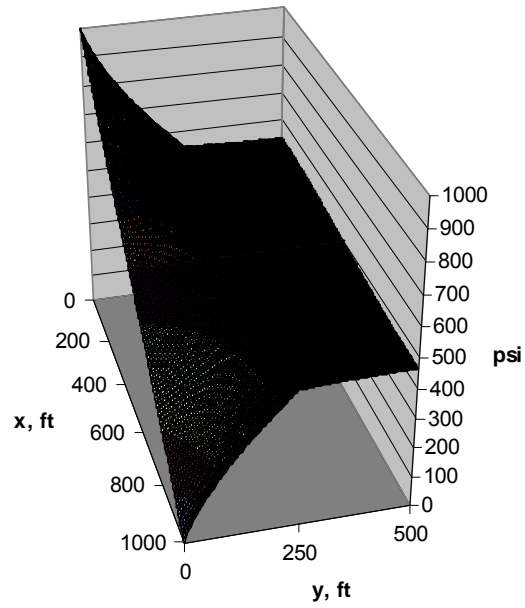


Fig. 35—Scenario 3: Areal view of an offset fracture parallel to the main direct fracture.

The case where the offset fracture was located 250 ft from the main direct fracture is considered in Fig. 36. For this and subsequent figures, we adopt a coordinate system where the injector is located at the origin ($x=0, y=0$), and the x -axis points toward the production well. The main direct fracture that connected the two wells followed the x -axis. For the case considered here, the offset fracture paralleled the main direct fracture and was located 250 ft away—at $y=250$ ft. Fig. 36 shows two views of the pattern pressures for this case, where both fractures were open and had widths of 1 mm.

x-direction fractures at y=0 ft & 250 ft



x-direction fractures at y=0 ft & 250 ft

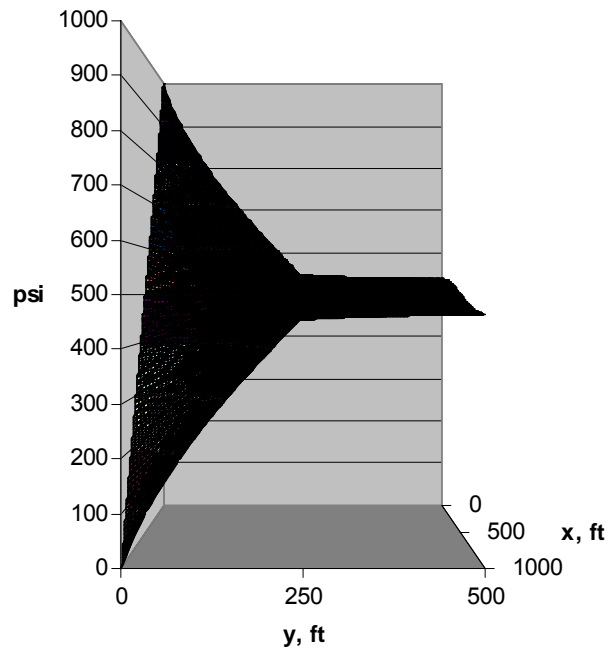


Fig. 36—Two views of pressures for Scenario 3: Open 1-mm fractures at y=0 ft and y=250 ft.

Parallel Offset Fractures Had Little Effect on Rate but Can Greatly Harm Sweep. For this case, the well production rate was only 4% greater than that for the case where only the main direct fracture connected the two wells (Fig. 26) and was 22.1 times greater than that for a pattern with no fractures (Fig. 3). For the half of the pattern that was closest to the direct fracture (i.e., on the x -axis), the pressure gradients and sweep efficiency were quite high (see Fig. 36). In contrast, the outer half of the pattern was poorly swept, and the pressure gradients were low (averaging only 0.078 psi/ft).

Plugging the Main Direct Fracture Did Not Aid Sweep Beyond the Offset Fracture. If the main direct fracture was completely plugged while the offset fracture remained open, Fig. 37 shows two views of the resulting pattern pressures. Here, the well production rate was only 5% of that for the case shown in Fig. 36 and was 17% greater than that for a pattern with no fractures. Pressures in the inner half of the pattern resembled those for normal radial flow (Fig. 3). However, pressure gradients and sweep efficiency in the outer half of the pattern remained low—pressure gradients averaged only 0.036 psi/ft in the outer half of the pattern. Consequently, a gel treatment that partially or completely plugged the main direct fracture in Scenario 3 only benefited fluid displacement for the inner half of the pattern.

Effect of Position of the Offset Fracture. Can sweep in the outer half of the pattern be improved if the offset fracture is located closer to the main direct fracture? Figs. 38 and 39 show the pattern pressures when the offset fracture was located at $y=125$ ft and $y=25$ ft, respectively. A comparison of Figs. 36, 38, and 39 revealed that sweep of the outer portion of the pattern improved as the offset fracture approached the main direct fracture. Average pressure gradients in the outer half of the pattern also increased—e.g., 0.078 psi/ft for $y=250$ ft, 0.109 psi/ft for $y=125$ ft, and 0.226 psi/ft for $y=25$ ft. However, in all cases, the sweep and pressure gradients in the outer parts of the pattern were much less desirable than in the inner portions of the pattern.

As mentioned above (comparing Figs. 36 and 37), completely plugging the main direct fracture did not improve pressure gradients or sweep in the outer part of the pattern. This finding also held when the offset fractures were located at $y=125$ ft and $y=25$ ft. With an open direct 1-mm fracture between the two wells, pressure gradients in the outer half of the pattern averaged 0.078 psi/ft, 0.109 psi/ft, and 0.226 psi/ft when the offset 1-mm fracture was located at $y=250$ ft, $y=125$ ft, and $y=25$ ft, respectively. When the direct fracture between the wells was plugged, pressure gradients in the outer half of the pattern averaged only 0.036 psi/ft, 0.037 psi/ft, and 0.051 psi/ft, respectively.

Effect of Fracture Width. The analysis to this point used fractures with widths of 1 mm. What if the fracture widths were larger or smaller? For fracture widths ranging from 0 to 2 mm, this question was addressed by Fig. 40. For the cases represented by the open circles and solid curve in Fig. 40, the direct fracture ($y=0$ ft) and the offset fracture (located at $y=250$ ft) had the same width. For the solid circle, $w_f = 1$ mm for the direct fracture, and no offset fracture was present. For fracture widths of 1 mm and above, the pressure gradients in the outer half of the pattern were extremely low—suggesting poor sweep and little oil production from this part of the pattern. For fracture widths of 0.5 mm and below, the pressure gradients were about the same as for the no-fracture case (Fig. 3, where $w_f = 0$ mm).

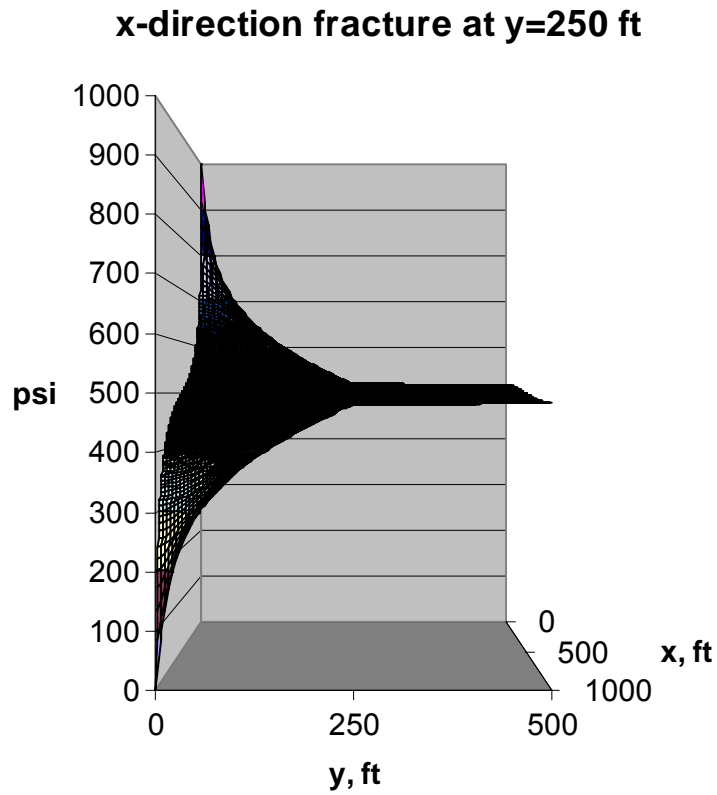
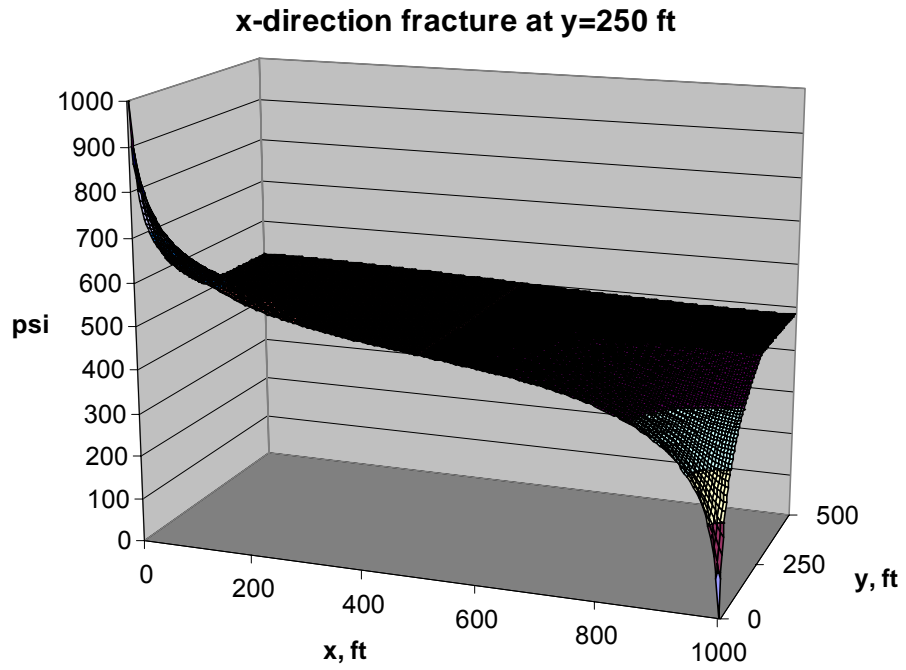


Fig. 37—Two views of pattern pressures when the main direct fracture was plugged.

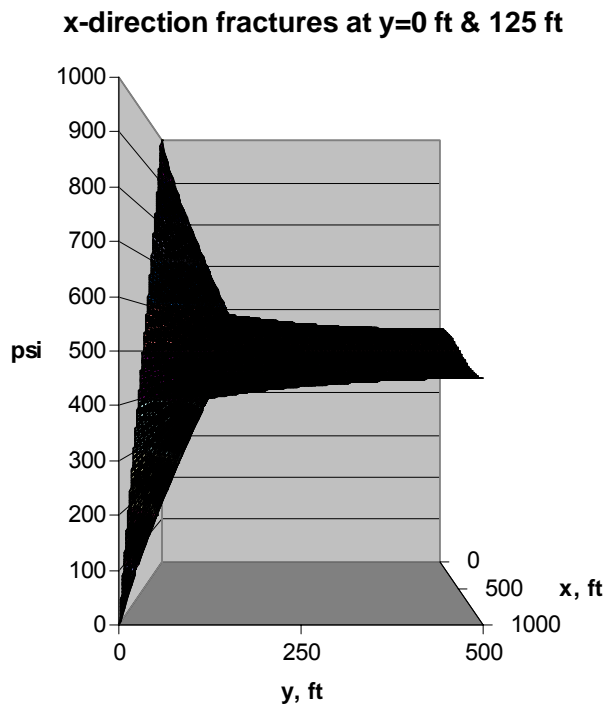


Fig. 38—Pattern pressures when the offset x-direction fracture was at y=125 ft.

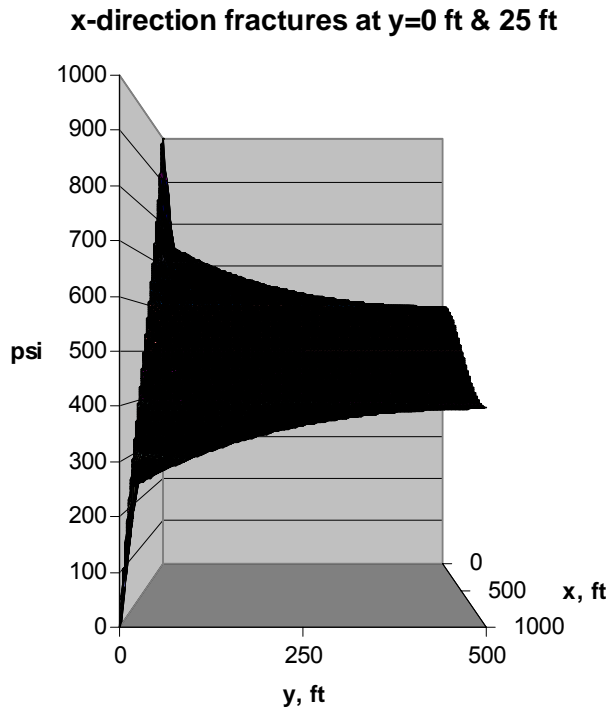


Fig. 39—Pattern pressures when the offset x-direction fracture was at y=25 ft.

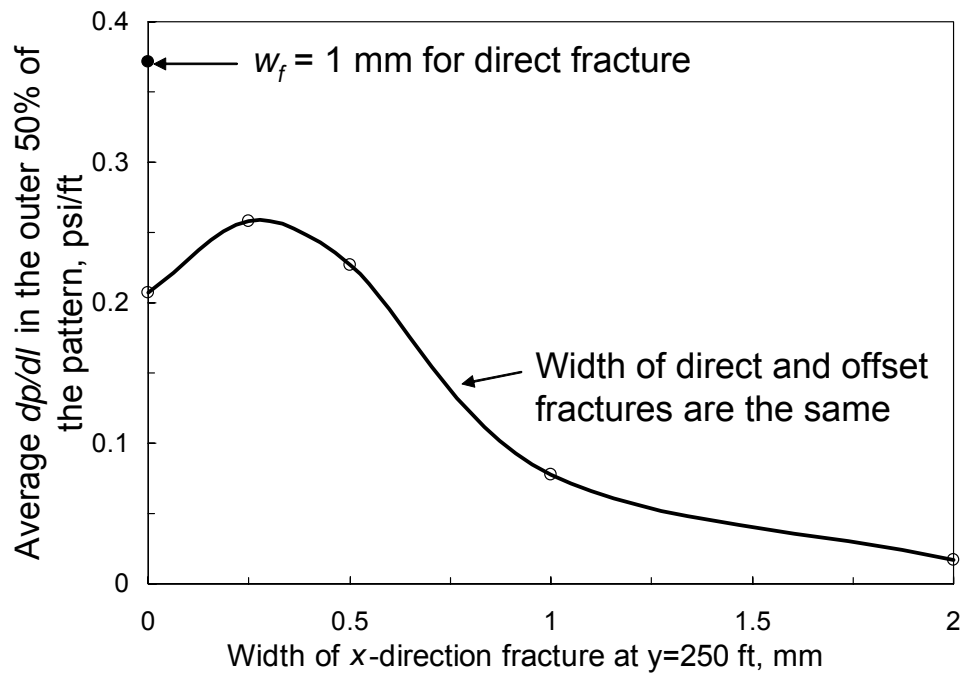


Fig. 40—Average pressures in the outer half of the pattern versus width of the offset fracture.

Effective Gel Placement in the Offset Fracture is Unlikely for Scenario 3. The results in this section indicated that plugging the most direct fracture will not significantly improve sweep in the pattern out beyond the parallel offset fracture. Is it possible to beneficially place gel or some other blocking agent within the offset fracture? Unless additional fractures are induced, the blocking agent must traverse through a significant distance of matrix rock to reach the offset fracture. When that blocking agent forms, substantial damage will occur within the matrix rock that will dramatically harm sweep efficiency (see Fig. 41). Consequently for Scenario 3, gel treatments are not expected to benefit sweep efficiency in the pattern beyond the offset fracture.

Summary for Scenario 3. In the third scenario, a vertical fracture connected a pair of vertical wells (as in Scenario 1). Additionally, a parallel fracture existed some distance away from the main direct fracture connecting the two wells. This parallel offset fracture had little effect on production rate but can greatly harm the pattern sweep efficiency. Plugging the main direct fracture did not aid sweep in the pattern beyond the offset fracture. Sweep of the outer portion of the pattern improved as the offset fracture approached the main direct fracture. However, in all cases, the sweep and pressure gradients in the outer parts of the pattern were much less desirable than in the inner portions of the pattern (i.e., between the main fracture and the offset fracture). For fracture widths of 1 mm and above (when $k_{matrix} = 100$ md), the pressure gradients in the outer half of the pattern were extremely low—suggesting poor sweep and little oil production from this part of the pattern. For fracture widths of 0.5 mm and below, the pressure gradients throughout the pattern were similar to those for the no-fracture case. Effective gel placement in the offset fracture is unlikely for Scenario 3. Gel treatments are only expected to be of value in improving sweep in the pattern between the main direct fracture and the offset fracture.

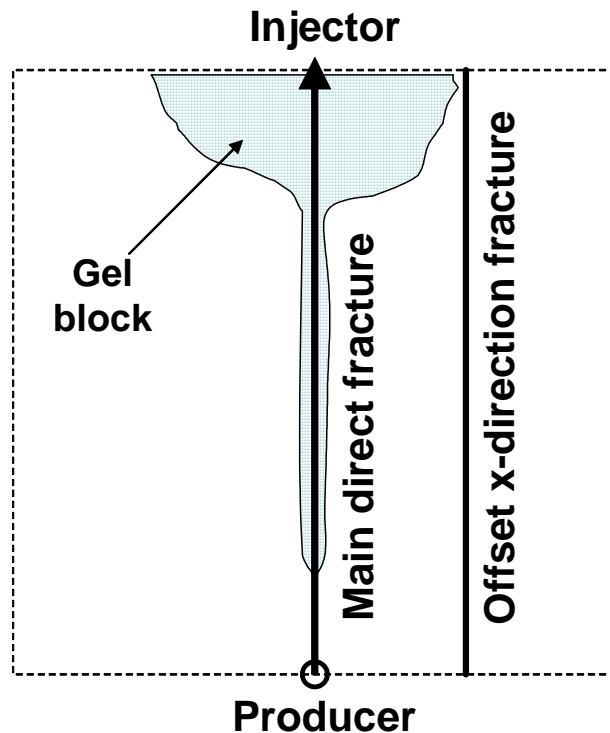


Fig. 41—Gel caused substantial damage to the matrix in reaching the offset fracture.

Scenario 4: Fractures Crossing the Main Direct Fracture

In the fourth scenario, a fracture (or fractures) crossed the main direct fracture (Fig. 42). Fig. 43 shows the pattern pressures when a 1-mm fracture (located at $x=500$ ft) crossed the main fracture ($y=0$ ft). This distribution of pressures was identical to that when no fracture existed at $x=500$ ft (Fig. 2). Plugging the main direct fracture led to a pressure distribution that was identical to that shown in Fig. 3, associated with no fractures in the pattern.

What happens if the y -direction fracture is not in the center of the pattern? Fig. 44 shows the pressure distribution for the case where $x=250$ ft. This distribution was very similar to that for the case with no y -direction fractures, except for a shelf of level pressures in the vicinity of $x=0$ ft, $y=500$ ft. Fig. 45 shows the pressure distribution for the case where $x=750$ ft. This distribution was also very similar to that for the case with no y -direction fractures, except for a pressure shelf in the vicinity of $x=1,000$ ft, $y=500$ ft. The average pressure gradient in the outer half of the pattern was 0.42 psi/ft for Figs. 44 and 45, compared to 0.372 psi/ft for that associated with Fig. 43. Thus, for the cases considered to this point, the crossing fractures had a fairly small influence on pressure gradients and sweep in the pattern. They also had little influence on production rates. For the cases represented in Figs. 43-45, the production rates were similar.

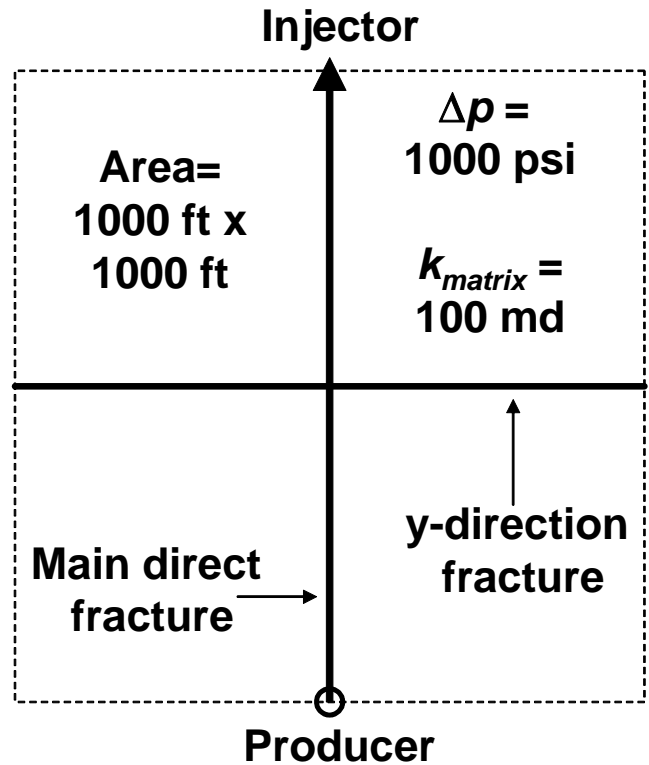


Fig. 42—Scenario 4: Areal view of a fracture crossing the main direct fracture.

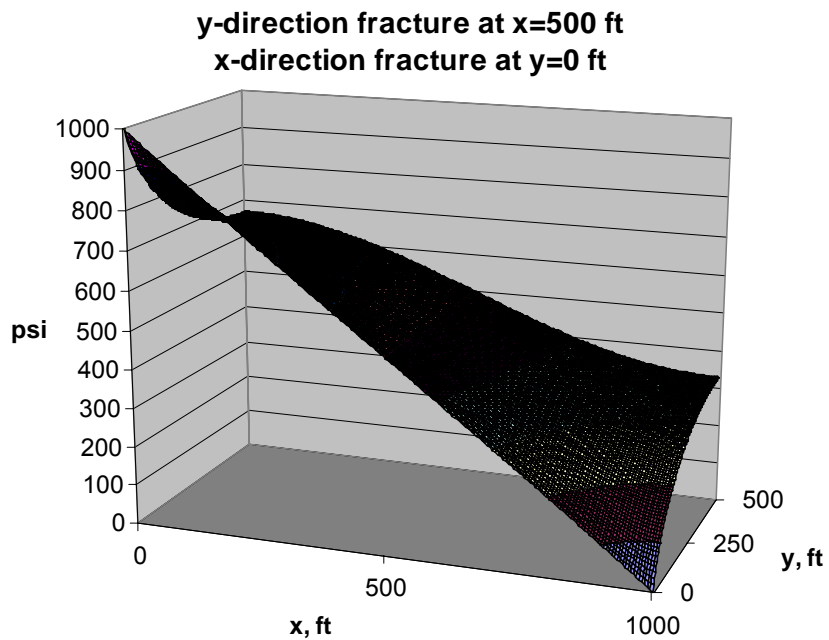


Fig. 43—Pattern pressures when a fracture at x=500 ft crossed the main direct fracture.

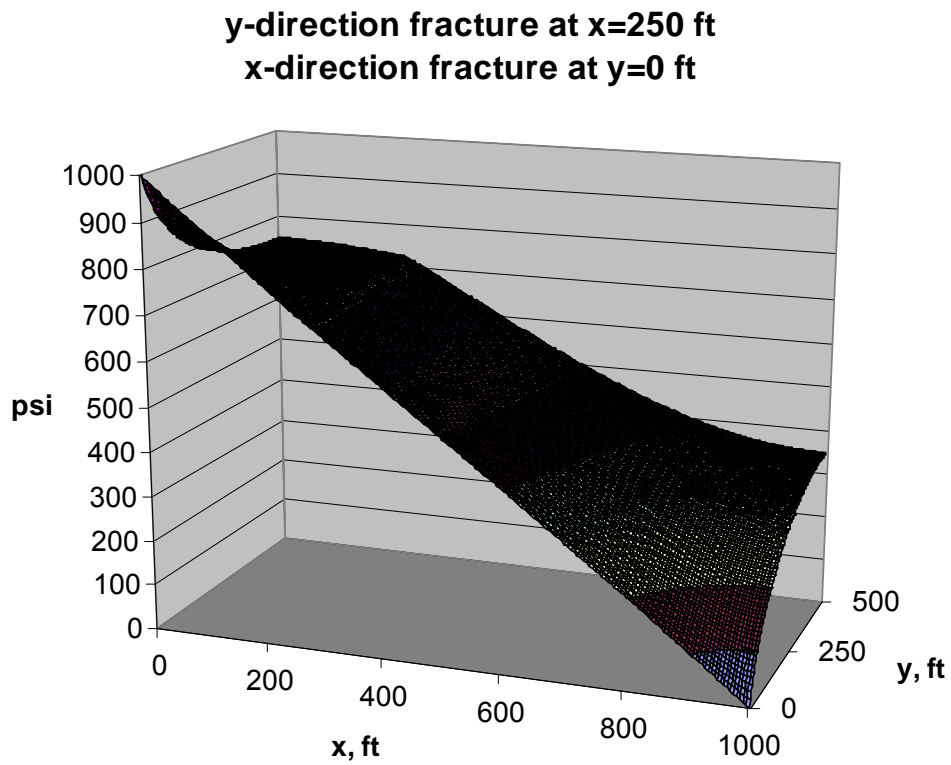


Fig. 44—Pattern pressures when a fracture at $x=250$ ft crossed the main direct fracture.

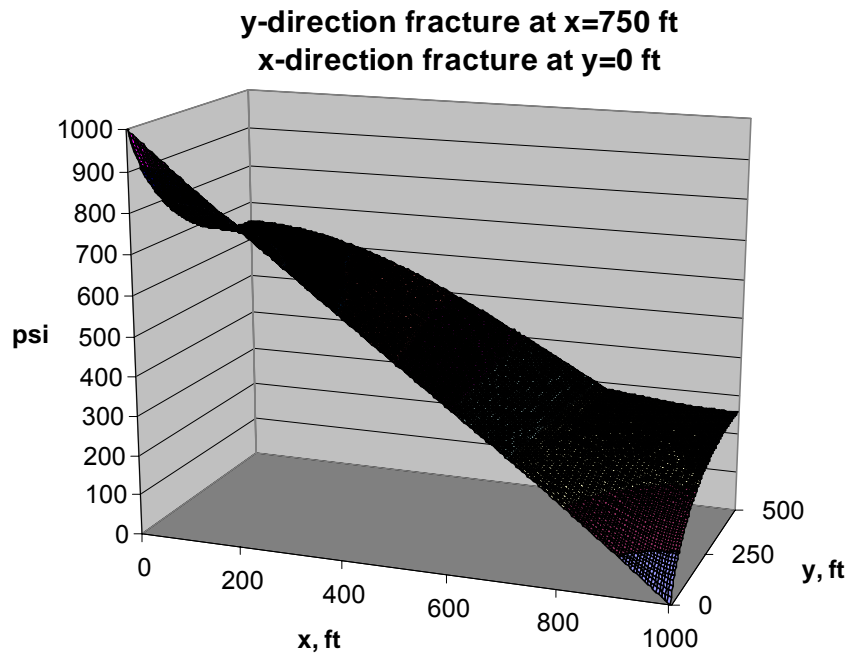


Fig. 45—Pattern pressures when a fracture at $x=750$ ft crossed the main direct fracture.

Sweep Improved as the Crossing Fracture Moved Away from the Pattern Center. As the crossing fracture moved away from $x=500$ ft, the sweep efficiency and average pressure gradients increased in the pattern. This was most evident when the crossing fracture was at an extreme position, such as $x=0$ ft. This case was equivalent to a fracture or horizontal well crossing the injection well in the y -direction. The pattern pressures for this case are shown in Fig. 46 (for 1-mm wide fractures). The average pressure gradient in the outer half of the pattern was 0.63 psi/ft. This value was 70% greater than that associated with Fig. 43 (for the crossing fracture at $x=500$ ft) and 63% of the value associated with two parallel y -direction fractures or horizontal wells (Fig. 26). Interestingly, the production rates were not particularly sensitive to the position or number of crossing (i.e., y -direction) fractures. Compared to the case with only the main direct fracture, the rates were a) 0% higher for the case with a fracture at $x=500$ ft (i.e. Fig. 43), b) 0.7% higher for the case with a fracture at $x=250$ ft (i.e. Fig. 44), c) 4.5% higher for the case with a fracture at $x=0$ ft, d) 7.5% higher for the case of fractures at $x=0$ ft and $x=1,000$ ft (i.e., two parallel y -direction fractures or horizontal wells as shown in Fig. 26), and e) 7.5% higher for the case with fractures at $x=0$ ft, $x=500$ ft, and $x=1,000$ ft (i.e., three parallel y -direction fractures).

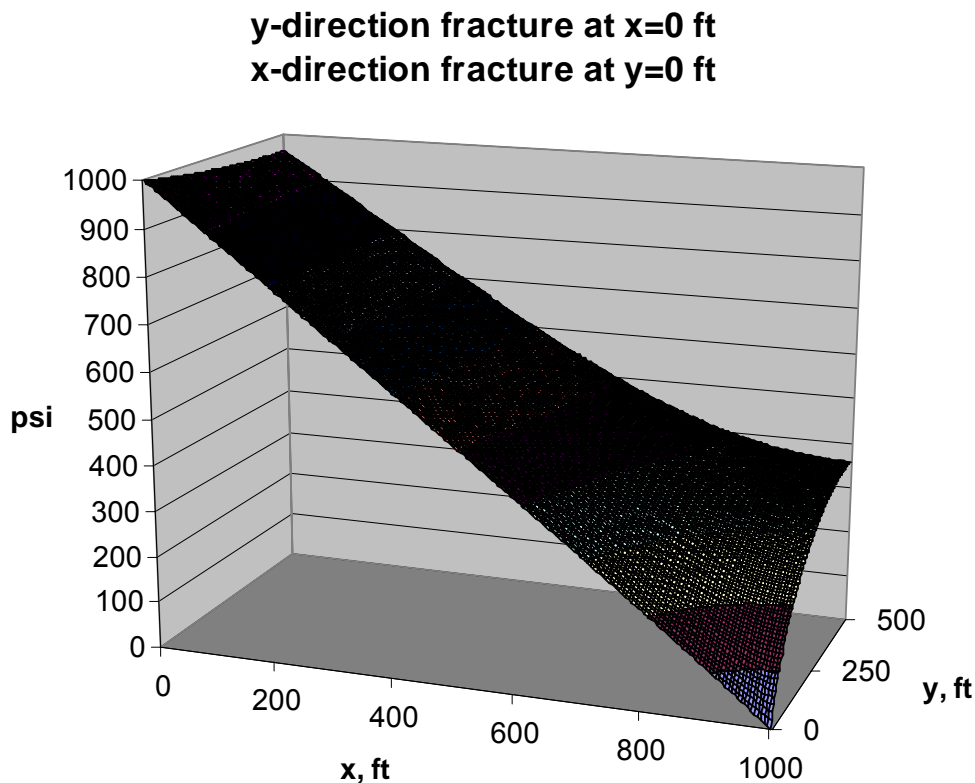


Fig. 46—Pattern pressures when a fracture at $x=0$ ft crosses the main direct fracture.

Plugging the Direct Fracture Reduced Channeling but May Not Improve Matrix Sweep. What happens when a gel treatment is applied to the main direct fracture? Fig. 47 shows the resulting pattern pressures when the main direct fracture in Fig. 42 was completely plugged. Plugging this fracture reduced the pattern flow rate to 4.7% of the value before plugging. For the

outer half of the pattern, the plug reduced the average pressure gradient from 0.372 to 0.206 psi/ft. For the inner half of the pattern, the plug reduced the average pressure gradient from 0.649 to 0.415 psi/ft. Thus, the plug (or gel treatment) certainly reduced channeling through the direct fracture, but it did not have a beneficial effect on pressure gradients in the pattern.

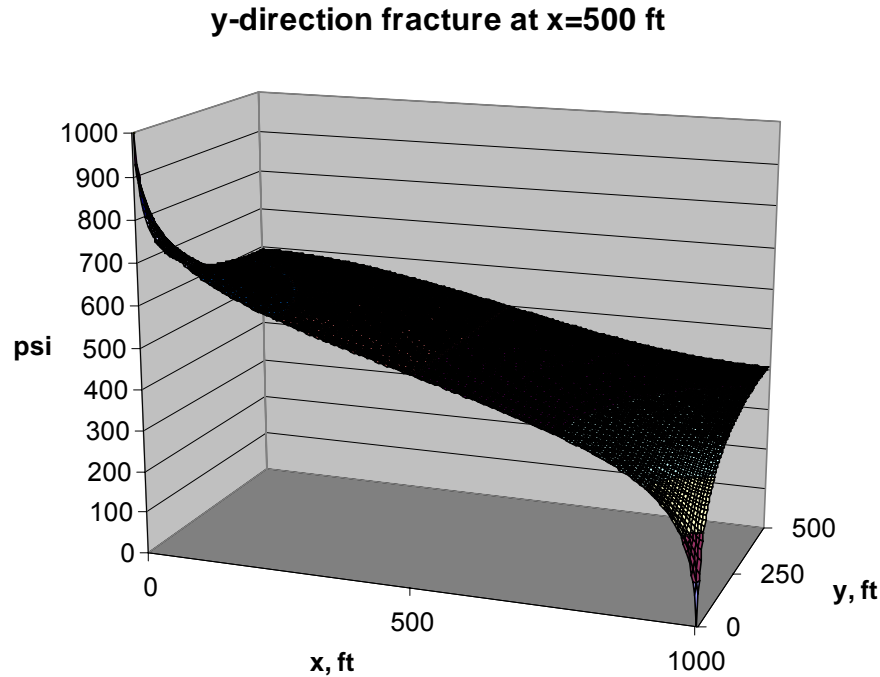


Fig. 47—Pattern pressures after complete plugging of the main fracture in Fig. 42.

A Centered Partial Plug in the Main Fracture Improved Sweep and Pattern Pressures. Fig. 48 shows the resulting pattern pressures when the main direct fracture in Fig. 42 was only half plugged (from the producer to the middle of the fracture). This half-plug reduced the pattern flow rate to 11.8% of the value before plugging. For the outer half of the pattern, the plug reduced the average pressure gradient from 0.372 to 0.202 psi/ft. For the inner half of the pattern, the plug reduced the average pressure gradient from 0.649 to 0.422 psi/ft. For both halves, the average pressure gradients were about the same when the main fracture was half plugged as when it was fully plugged. However, Fig. 48 shows that the pressure gradients were much lower in the upstream half of the pattern (i.e., closest to the injection well) than in the downstream half. Overall, the half-plug gel treatment substantially reduced channeling through the direct fracture, had a neutral to beneficial effect on pressure gradients in the downstream part of the pattern, but generated a negative impact on pressure gradients in the upstream part of the fracture.

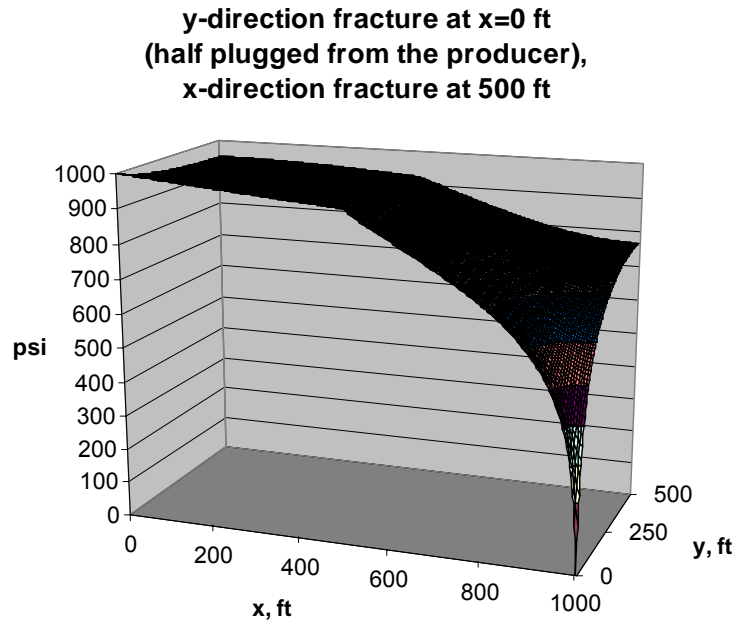


Fig. 48—Pattern pressures for a fracture at $x=500$ ft and a half-plugged main fracture.

The Most Effective Plugs Blocked the Entrances to the y-Direction Fractures. Fig. 49 shows pattern pressures when the main direct fracture in Fig. 42 was half filled with a 500-ft long plug that was centered halfway into the fracture. This half-plug reduced the pattern flow rate to 14.8% of the value before plugging. For the outer half of the pattern, the plug *increased* the average pressure gradient from 0.372 to 0.473 psi/ft. For the inner half of the pattern, the plug *increased* the average pressure gradient from 0.649 to 0.758 psi/ft. Thus, as was the case for Scenario 1, the best gel placement was a plug that was centered in the main direct fracture but that did not fill the entire fracture.

Fig. 50 shows pattern pressures when a 100-ft long plug was centered in the fracture, instead of the 500-ft long plug. This half-plug reduced the pattern flow rate to 27.4% of the value before plugging. Again, for the outer half of the pattern, the plug *increased* the average pressure gradient from 0.372 to 0.495 psi/ft. For the inner half of the pattern, the plug *increased* the average pressure gradient from 0.649 to 0.765 psi/ft. Thus, the centered 100-ft plug improved pressure gradients in the pattern as well as the centered 500-ft plug.

For the case in Fig. 50, the centered plug covered the entrance to the cross fracture at $x=500$ ft. Figs. 51 and 52 show pattern pressures when the 100-ft plug was close to the center of the main direct fracture, but did not cover the y-direction fracture at $x=500$ ft. When the plug was situated on the upstream side of the y-direction fracture, the pressure gradients and sweep were desirable for the downstream portion of the pattern (Fig. 51), but low on the upstream portion. When the plug was situated on the downstream side of the y-direction fracture, the pressure gradients and sweep were desirable for the upstream portion of the pattern (Fig. 52), but low on the downstream portion. So the most effective plugs should block the entrances of the cross-direction fractures.

**y-direction fracture at x=0 ft
(500-ft plug centered halfway),
x-direction fracture at 500 ft**

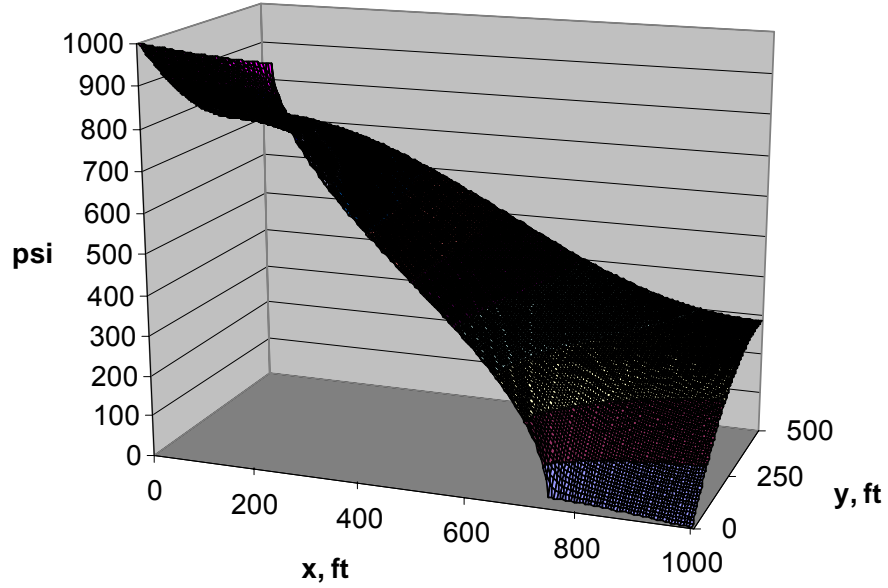


Fig. 49—Pattern pressures for a 500-ft plug centered in the main fracture.

**y-direction fracture at x=0 ft
(100-ft plug centered halfway),
x-direction fracture at 500 ft**

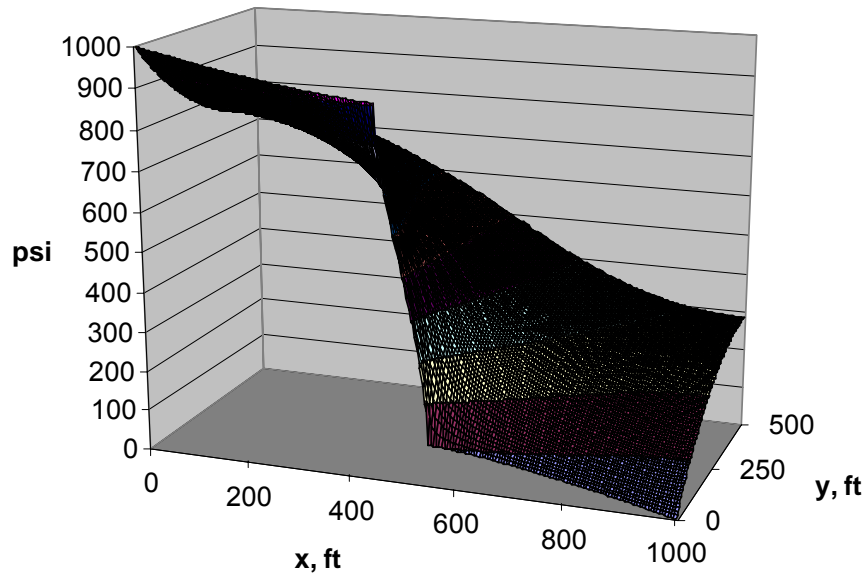


Fig. 50—Pattern pressures for a 100-ft plug centered in the main fracture.

**y-direction fracture at x=0 ft
(100-ft plug centered at 445 ft),
x-direction fracture at 500 ft**

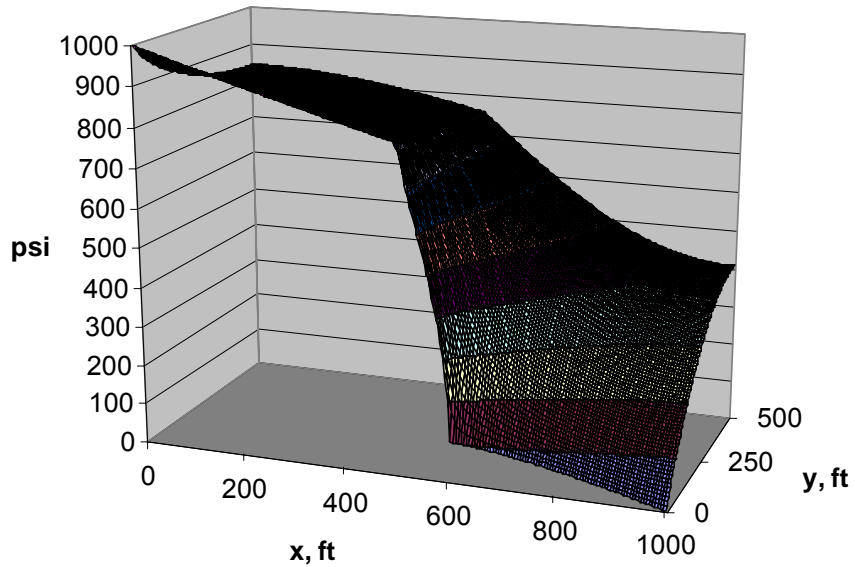


Fig. 51—Pattern pressures for a 100-ft plug centered at 445 ft in the main fracture.

**y-direction fracture at x=0 ft
(100-ft plug centered at 555 ft),
x-direction fracture at 500 ft**

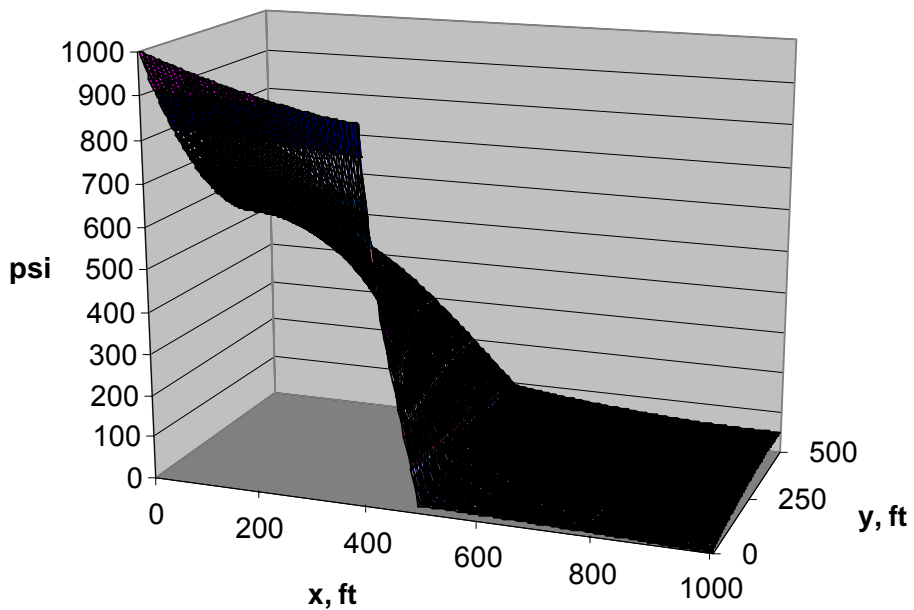


Fig. 52—Pattern pressures for a 100-ft plug centered at 555 ft in the main fracture.

Summary for Scenario 4. In the fourth scenario, where a fracture or fractures crossed the main direct fracture, sweep efficiency and average pressure gradients increased in the pattern as the cross-direction (y -direction) fractures moved closer to the wells. However, the number and position of these cross-direction fractures had only a minor effect on pattern production rates. Complete plugging of the main direct fracture reduced channeling but may not improve matrix sweep nor increase pressure gradients. A centered partial plug in the main fracture improved pattern sweep and increased pressure gradients. The most effective plugs blocked the entrances to the cross-direction fractures.

Scenario 5: Both Cross-Direction and Offset Fractures

Next, we consider the more complicated fracture system illustrated in Fig. 53. For the particular case shown (where a 1-mm wide crossing fracture existed at $x=500$ ft and 1-mm wide fractures occurred at $y=0$ ft and $y=250$ ft), the pattern pressures are shown in Fig. 54.

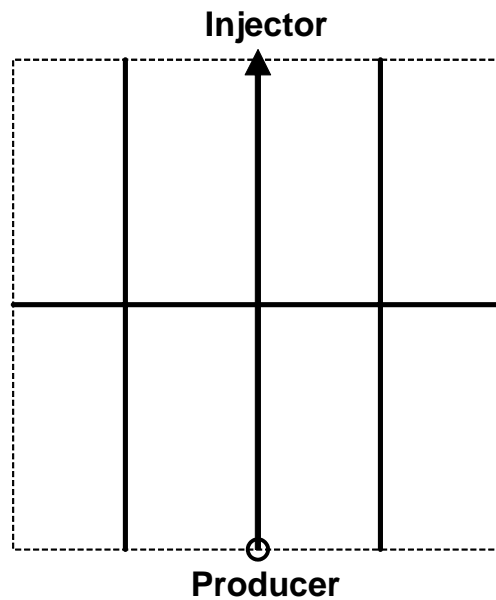


Fig. 53—Scenario 5: Both cross-direction and offset fractures.

The distribution of pressures shown in Fig. 54 was identical to that associated with Fig. 36, where no cross fracture occurred at $x=500$ ft. Consistent with the discussion for Scenario 4, cross fractures near the center of the pattern had little impact on either flow rates or sweep efficiency.

With Only One Cross-Direction Fracture, Sweep for the Outer Pattern Remained Poor.

Fig. 55 shows pattern pressures when the cross fracture was located at $x=250$ ft instead of at $x=500$ ft. Compared with Fig. 54, the flow rate increased by 7.1%, and the average pressure gradient in the outer half of the pattern increased by 44% (from 0.079 to 0.114 psi/ft). In both cases, the pressure gradients in the inner half of the pattern were substantially greater than those in the outer half (0.492 psi/ft versus 0.114 psi/ft for Fig. 55, and 0.477 psi/ft versus 0.079 psi/ft for Fig. 54).

**y-direction fracture at x=500 ft
x-direction fractures at y=0 ft & 250 ft**

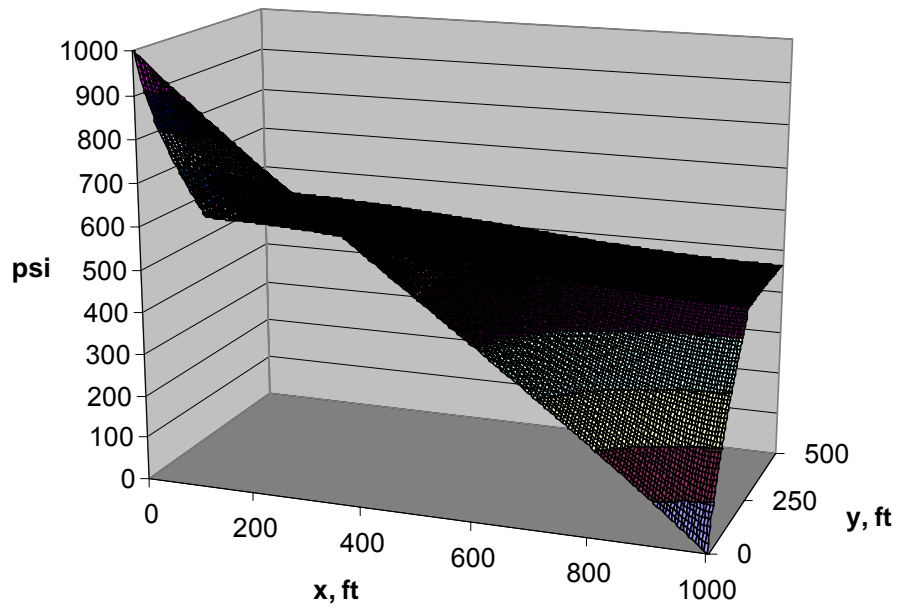


Fig. 54—Pattern pressures for fractures at x=500 ft, y=0 ft, and y=250 ft.

**y-direction fracture at x=250 ft
x-direction fractures at y=0 ft & 250 ft**

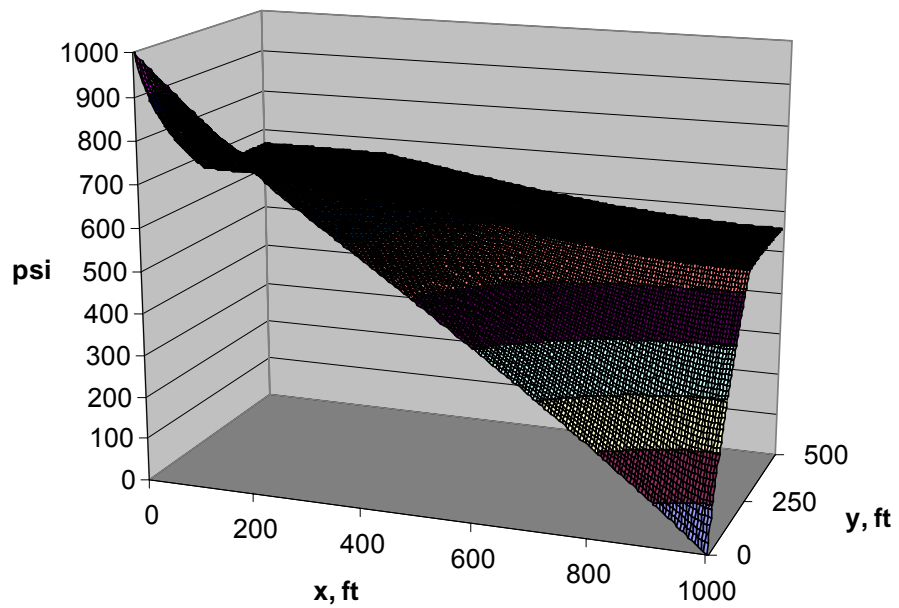


Fig. 55—Pattern pressures for fractures at x=250 ft, y=0 ft, and y=250 ft.

Fig. 56 shows pattern pressures when the cross fracture was located at $x=0$ ft instead of at $x=500$ ft. Compared with Fig. 54, the average pressure gradient in the outer half of the pattern increased by 186% (from 0.079 to 0.226 psi/ft). Again, the pressure gradients in the inner half of the pattern were significantly greater than those in the outer half (0.580 psi/ft versus 0.226 psi/ft).

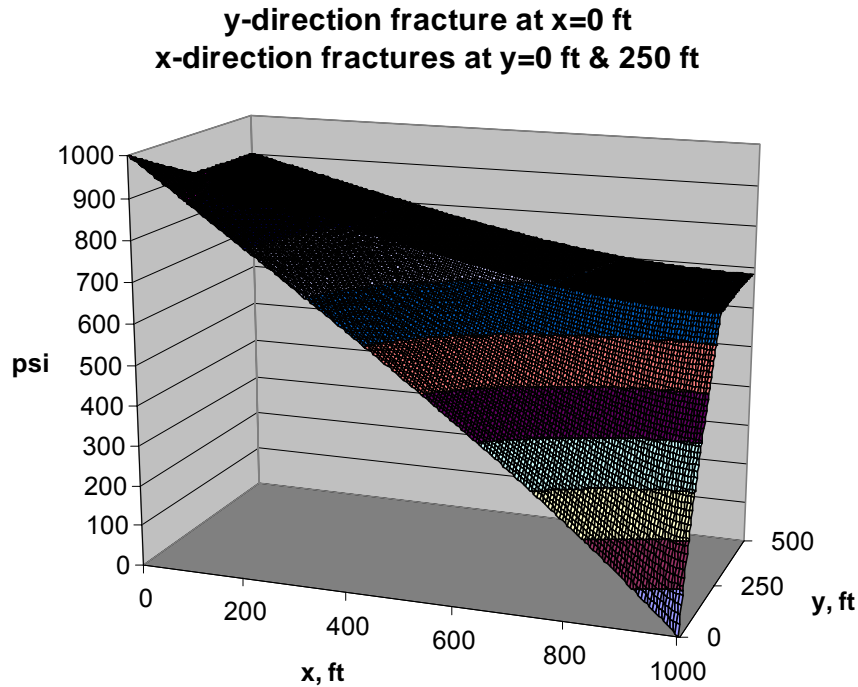


Fig. 56—Pattern pressures for fractures at $x=0$ ft, $y=0$ ft, and $y=250$ ft.

Parallel Cross-Direction Fractures Provided Good Pattern Pressure Gradients. Fig. 57 shows pattern pressures when two cross fractures were located at $x=0$ ft and $x=1,000$ ft (i.e., parallel fractures passing through each of the wells). Compared with Fig. 54, the average pressure gradient in the outer half of the pattern increased by 725% (from 0.079 to 0.652 psi/ft). In this case, the average pressure gradients in the outer half of the pattern were not greatly less than those in the inner half (0.652 psi/ft versus 0.827 psi/ft). For further comparison, when no offset x -direction fracture was present (i.e., no fracture at $y=250$ ft), the average pressure gradients were 0.937 psi/ft for the outer half of the pattern and 0.971 psi/ft for the inner half (Figs. 26 and 27).

Fig. 58 shows pattern pressures when three y -direction fractures were located at $x=0$ ft, $x=500$ ft and $x=1,000$ ft. This pattern is identical to that in Fig. 57.

Fig. 59 shows pattern pressures when two cross fractures were located at $x=0$ ft and $x=500$ ft. As expected, the sweep and pressure gradients were relatively uniform between the two cross-direction fractures (i.e., the upstream half of the pattern). Pressure gradients were greatest in the quadrant nearest the production well and smallest in the adjacent downstream quadrant in Fig. 59.

y-direction fractures at $x=0$ ft & 1000 ft
x-direction fractures at $y=0$ ft & 250 ft

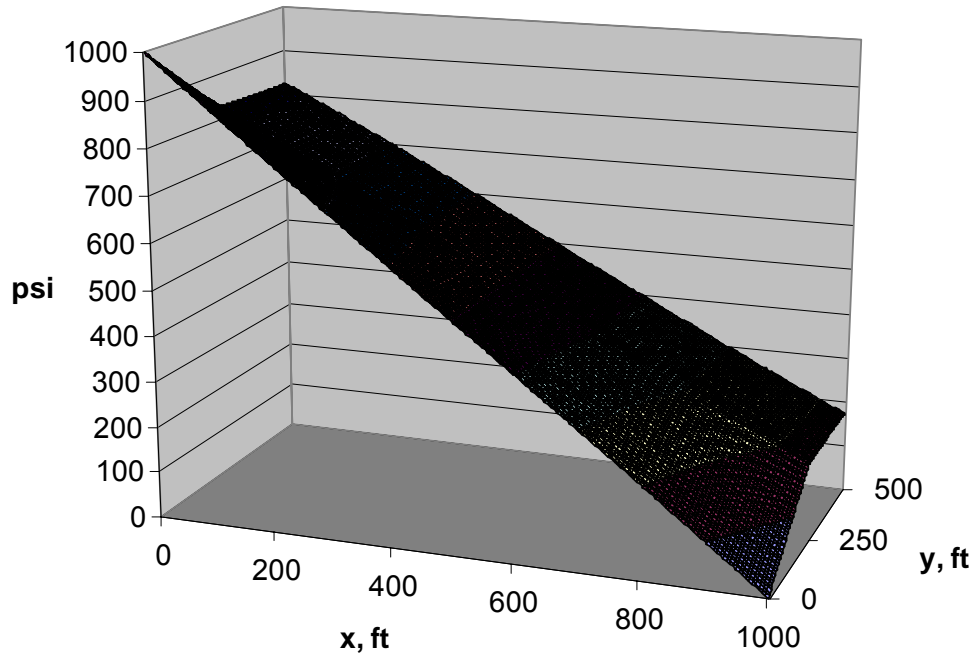


Fig. 57—Pattern pressures for fractures at $x=0$ ft, $x=1,000$ ft, $y=0$ ft, and $y=250$ ft.

y-direction fractures at $x=0$ ft, 500 ft & 1000 ft
x-direction fractures at $y=0$ ft & 250 ft

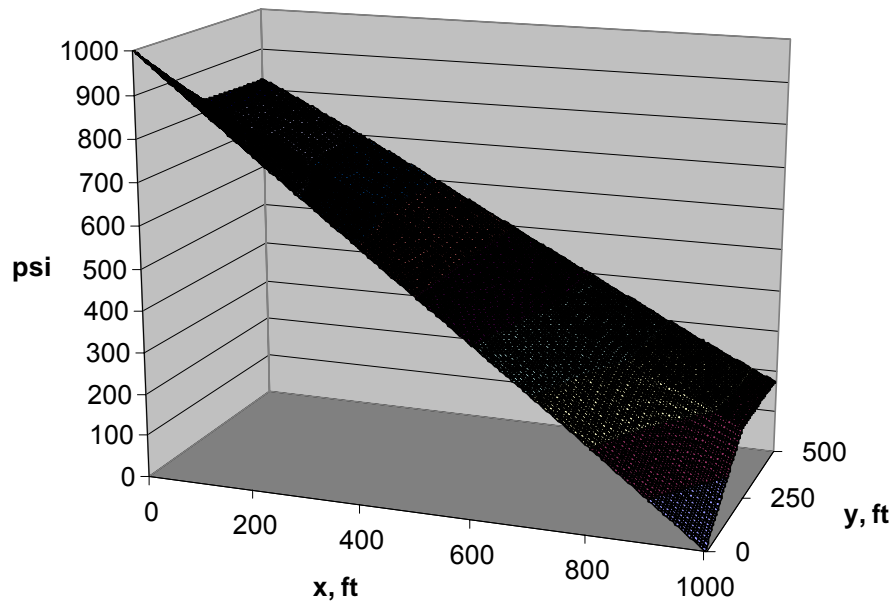


Fig. 58—Pattern pressures for fractures at $x=0$ ft, $x=500$ ft, $x=1,000$ ft, $y=0$ ft, and $y=250$ ft.

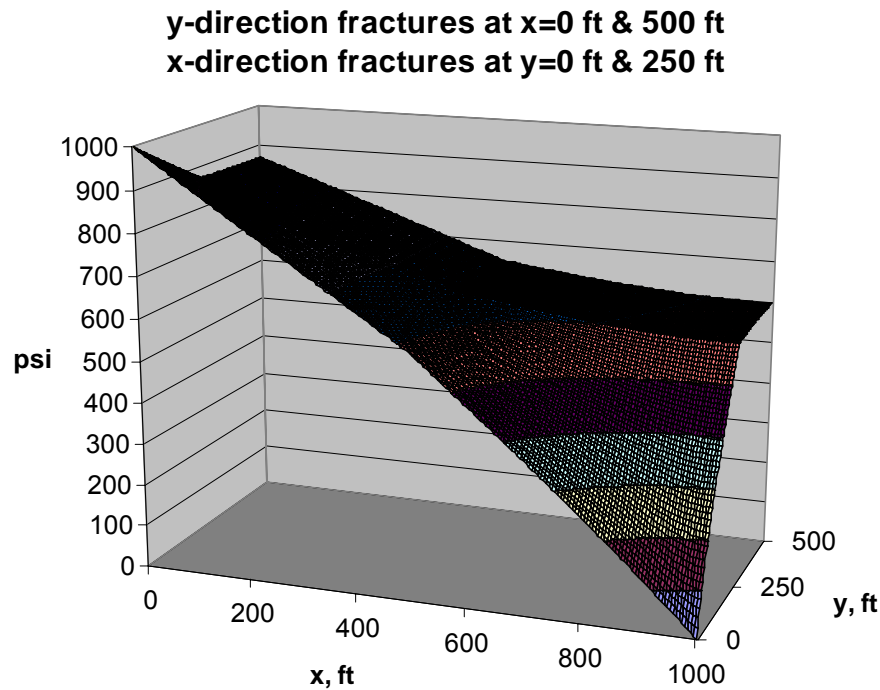


Fig. 59—Pattern pressures for fractures at $x=0$ ft, $x=500$ ft, $y=0$ ft, and $y=250$ ft.

Plugging the Direct Fracture Reduced Rates but Did Not Improve Pattern Pressures. If the main direct fracture shown in Figs. 53 and 54 was completely plugged, the resulting pressure distribution is shown in Fig. 60. The plug substantially reduced channeling by reducing the pattern flow rate to 5.3% of the original value. Average pressure gradients in the outer half of the pattern remained very low—in fact, decreased from 0.079 to 0.036 psi/ft because of the plug. The plug also resulted in a reduction in average pressure gradient in the inner half of the pattern—from 0.477 to 0.281 psi/ft. Thus, as in other scenarios, complete plugging of the main direct fracture significantly reduced channeling (i.e., total pattern flow rate), but it did not necessarily improve pattern sweep or pressure gradients.

Centered Partial Plugs Reduced Rate and Improved Sweep for the Inner Pattern. If the main direct fracture shown in Figs. 53 and 54 is plugged from 450 to 550 ft (a 100-ft long plug), the resulting pressure distribution is shown in Fig. 61. This plug reduced the pattern flow rate to 34% of the original value. Average pressure gradients in the outer half of the pattern increased slightly but remained very low—0.106 psi/ft after plug placement versus 0.079 psi/ft before. For the inner half of the pattern, the average pressure gradient increased slightly—from 0.477 to 0.537 psi/ft. However, a comparison of Figs. 60 and 61 reveals that this observation, by itself, is misleading. When the main fracture was completely plugged (Fig. 60), very high pressure gradients occurred within 100 ft of the wells, but pressure gradients were low elsewhere. In contrast, Fig. 61 reveals that pressure gradients were quite high throughout the inner half of the pattern (after placement of the centered 100-ft long plug). Expressed another way, the percentage

of the pattern that experienced pressure gradients exceeding 0.5 psi/ft was 20% for Fig. 60 and 50% for Fig. 61.

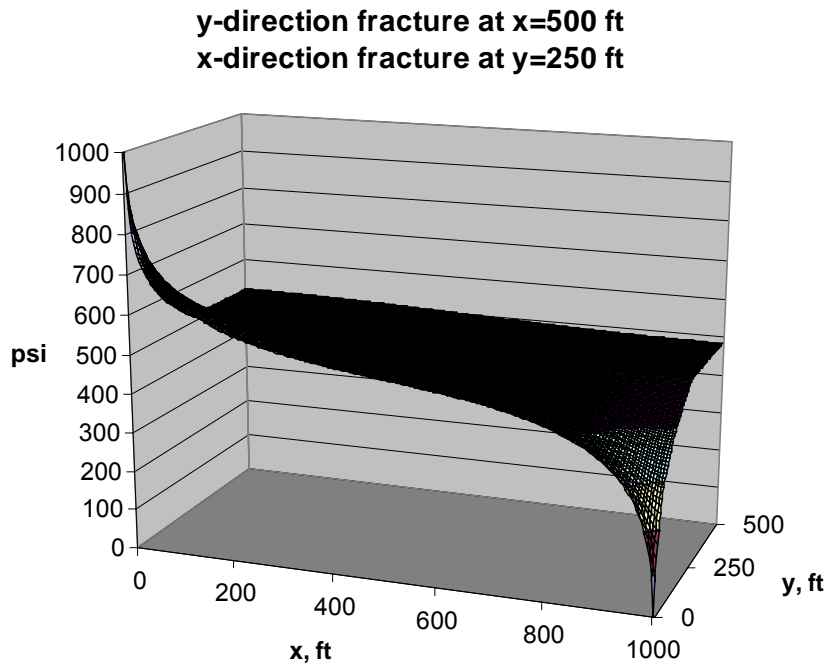


Fig. 60—Complete plugging of the main direct fracture in Figs. 53 and 54.

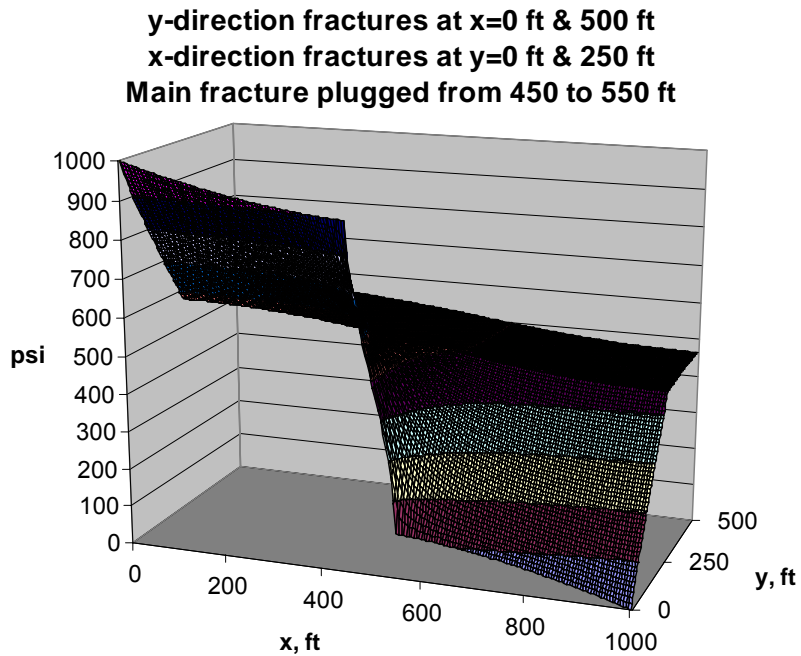


Fig. 61—Plugging from 450 to 550 ft in the main direct fracture in Figs. 53 and 54.

Fig. 62 shows results from the intermediate case where the main direct fracture was plugged from 250 to 750 ft (a 500-ft long plug). This plug reduced the pattern flow rate to 21% of the original value. Average pressure gradients in the outer half of the pattern increased slightly but remained very low—0.098 psi/ft after plug placement versus 0.079 psi/ft before. For the inner half of the pattern, the average pressure gradient increased slightly—from 0.477 psi/ft to 0.537 psi/ft. This result is quite similar to that for the 100-ft long plug. Again, pressure gradients for the inner half of the pattern were more favorable than for the case where the main direct fracture was completely plugged.

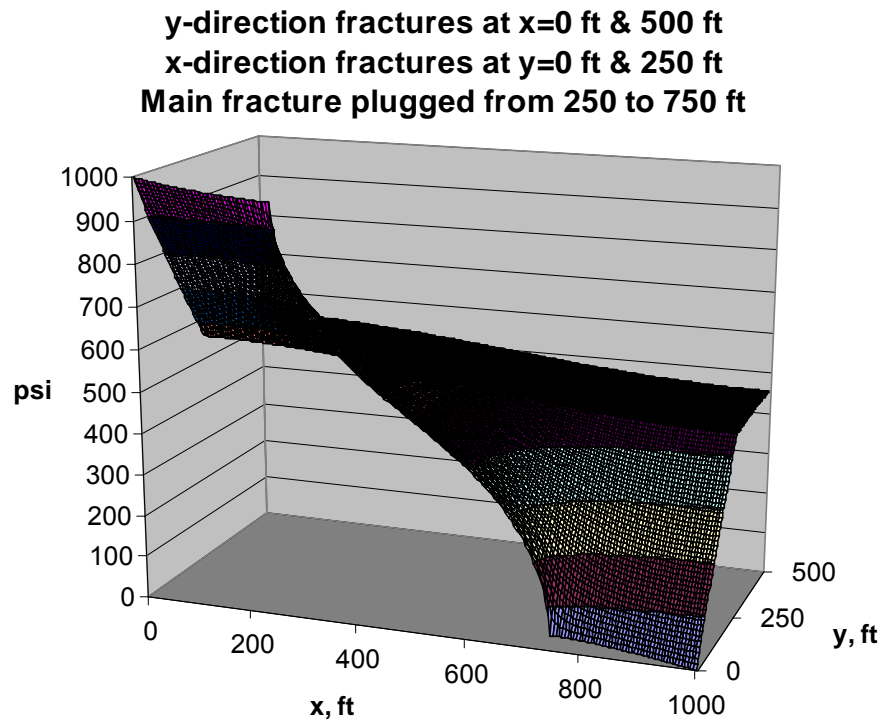


Fig. 62—Plugging from 250 to 750 ft in the main direct fracture in Figs. 53 and 54.

For Parallel Cross-Direction Fractures, Pattern Sweep Remained Good. Now, consider the case where three cross-direction fractures were present and part or all of the main direct fracture was plugged. In particular, take the case where a y -direction fracture (1 mm wide) passed through each of the wells and a third y -direction fracture occurs at $x=500$ ft (Fig. 58). If the main direct fracture was completely plugged, the resulting pattern pressures are shown in Fig. 63. The plug reduced the pattern flow to 13.9% of the value before plug placement. Compared with Fig. 58, the average pressure gradient in the outer half of the pattern remained essentially the same (0.652 psi/ft before plug placement versus 0.647 psi/ft after). Similarly, the average pressure gradient in the inner half of the pattern remained essentially the same (0.827 psi/ft before plug placement versus 0.824 psi/ft after). As with the previous case (Figs. 54 and 60) the gel plug dramatically reduced channeling (i.e., the total pattern flow), but did not greatly affect matrix sweep or pressure gradients.

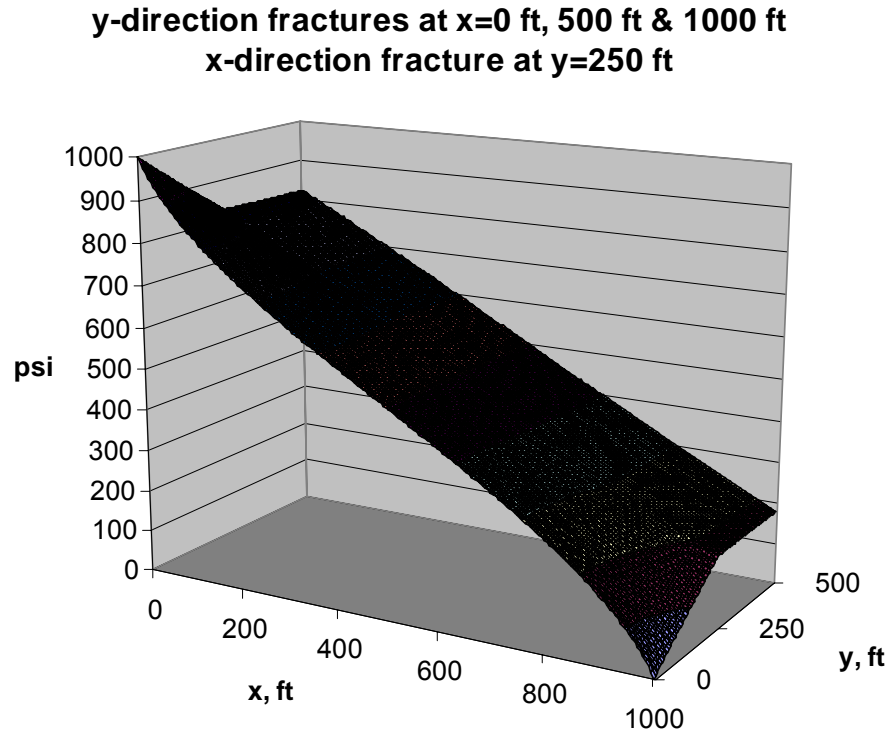


Fig. 63—Complete plugging of the main direct fracture in Fig. 58.

Any Fracture Pathways that Remain Unplugged Can Allow Severe Channeling. Fig. 64 shows pattern pressures when a 100-ft long plug was centered in the main direct fracture (between 450 and 550 ft), while Fig. 65 shows pattern pressures for a centered 500-ft long plug (between 250 and 750 ft). In both cases, the pressure gradients through the pattern were quite good. The gel plugs reduced pattern flow rates to 33.5% of the original (pre-plug) value for Fig. 64 and to 20.5% of the original for Fig. 65. Recall that the rate was reduced to 13.9% of the original when the direct fracture was completely plugged (Fig. 63). In considering the differences in flow rates for these cases, the higher rates associated with the smaller plugs (e.g., the difference between 33.5% and 13.9%) were put to good use in sweeping the inner half of the pattern (i.e., greater open fracture area allowed improved sweep of the two quadrants that were adjacent to the direct fracture). However, regardless of plug size, a significant volume of water channeled inefficiently from the injector, through the $x=0$ fracture to the $y=250$ fracture, to the $x=1,000$ fracture, and finally to the production well.

Fig. 66 shows pattern pressures when a 100-ft long plug was placed in the main direct fracture next to the production well (at x -values between 900 and 1,000 ft). This case also exhibited favorable pattern pressure gradients. Interestingly, the pattern flow rate was almost as great as when no plug was present. Even with the gel plug, two major fracture pathways allow severe channeling between the wells. One pathway leads from the injector through the $x=0$ fracture to the $y=250$ fracture, to the $x=1,000$ fracture, and finally to the production well. The second

pathway leads from the injector through the $y=0$ fracture to the $x=500$ fracture, to the $y=250$ fracture, to the $x=1,000$ fracture, and ultimately to the production well. These pathways would need to be plugged before all serious channeling through fractures could be suppressed.

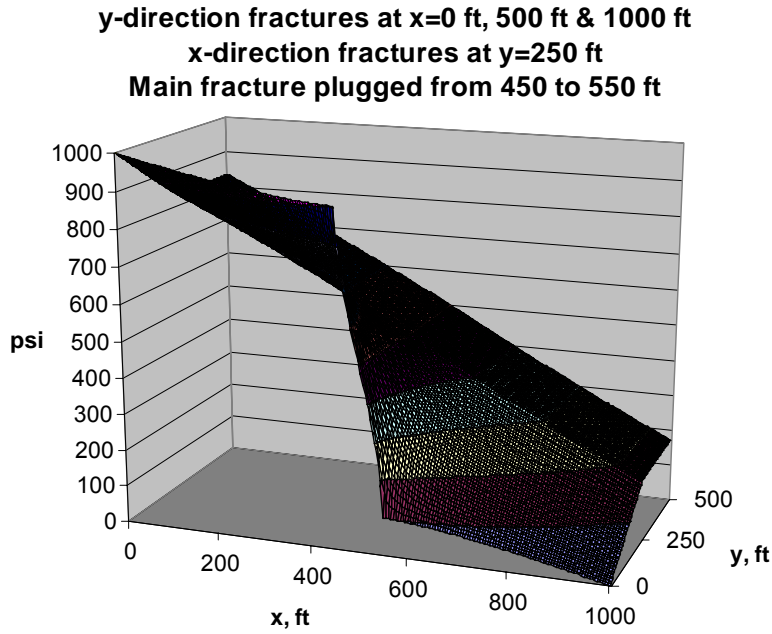


Fig. 64—Plugging from 450 to 550 ft in the main direct fracture in Fig. 58.

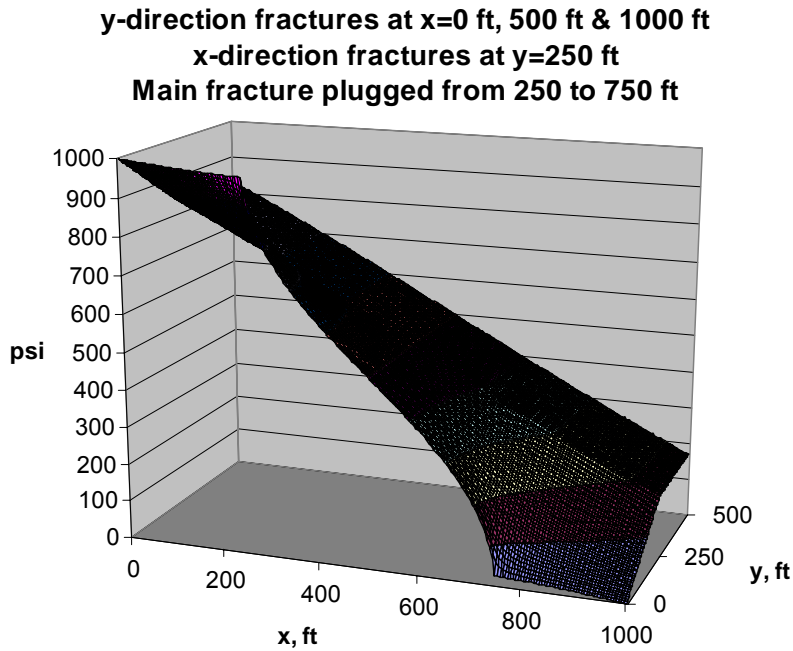


Fig. 65—Plugging from 250 to 750 ft in the main direct fracture in Fig. 58.

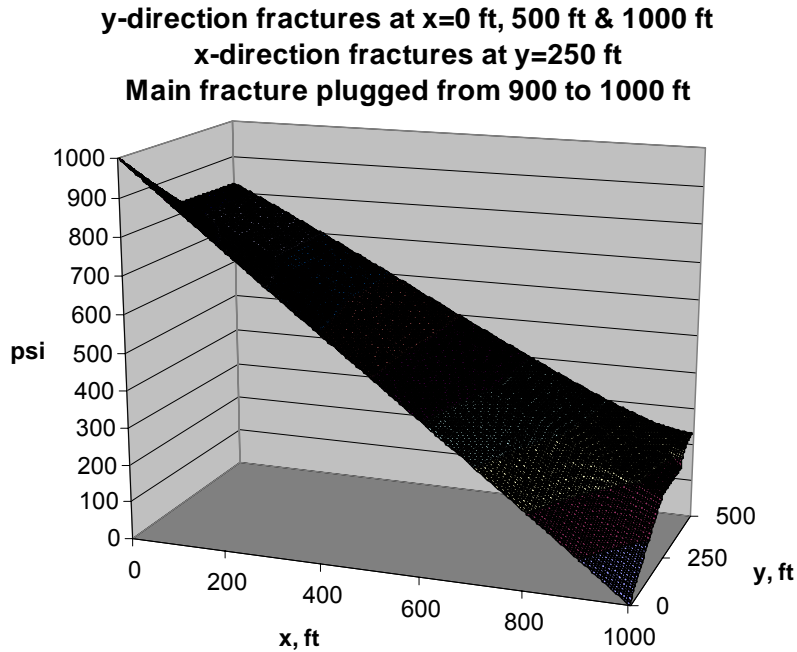


Fig. 66—Plugging from 900 to 1,000 ft in the main direct fracture in Fig. 58.

Summary for Scenario 5. Scenario 5 involved both cross-direction and offset fractures. With only one cross-direction fracture, sweep for the outer pattern remained poor. Plugging the direct fracture reduced rates but did not improve pattern pressures. Centered partial plugs reduced rate and improved sweep for the inner pattern. For parallel cross-direction fractures, pattern sweep remained good. Any fracture pathways that remained unplugged allowed severe channeling.

Scenario 6: More Complex Naturally Fractured Systems

In the analysis to this point, all fractures in the pattern had the same width. In Ref. 3, we considered many cases where fractures that were oriented in the *y*-direction (i.e., cross-direction) had different widths and conductivities than those oriented in the *x*-direction (Fig. 67). A conductivity ratio, *R*, was defined using Eq. 3.

$$R = (k_f w_f)_x / (k_f w_f)_y \dots \dots \dots (3)$$

For the analysis in Ref. 3, the degree of channeling was measured by the flow rate (*q*) through the most direct fracture, divided by the total pattern flow rate. A high degree of channeling indicated poor sweep efficiency, and *visa versa*. We studied the degree of channeling as a function of the fracture conductivity ratio, *R*, and the fracture intensity or spacing. Fracture intensity was assessed by the number (*n*) of *y*-direction fractures in the pattern. For the results shown in Fig. 68, the *y*-direction fractures were equally spaced and had the same spacing as the *x*-direction fractures. As in previous sections of this report, the pattern dimensions were fixed. So, the distance between adjacent parallel fractures decreased as *n* increased.

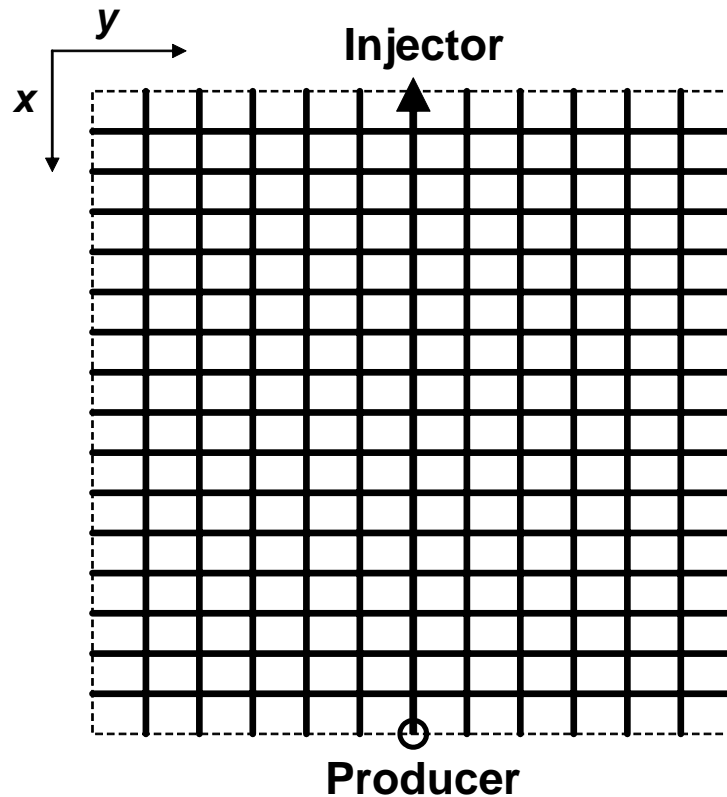


Fig. 67—Scenario 6: Simplified areal view of a naturally fractured pattern.

Fig. 68 shows that the most severe channeling occurred when the x -direction fractures were 10 or more times more conductive (two or more times wider) than the y -direction fractures (i.e., $R \geq 10$). Interestingly, channeling appeared less severe as the spacing decreased between adjacent fractures.

Fig. 69 shows the degree of sweep improvement that occurred when the most direct fracture was completely plugged. As indicated, sweep improvement was measured by the inter-well tracer breakthrough time after plug placement divided by breakthrough time before plug placement. A comparison of Figs. 68 and 69 revealed that the fracture systems associated with the most severe channeling (high R values and moderate to low n values in Fig. 68) were the most amenable to sweep improvement upon plugging of the most direct fracture (Fig. 69).

Figs. 68 and 69 apply to cases where the x -direction fractures had the same spacing as the y -direction fractures. Figs. 70 and 71 consider cases where the x -direction fractures were spaced differently than the y -direction fractures. As in Fig. 69, these figures investigated the sweep improvement that resulted from plugging the most direct fracture for various circumstances. Fig. 70 suggests that the effectiveness of gel treatments should be insensitive to fracture spacing for fractures that are aligned with the direct flow direction (i.e., the x -direction fractures). Especially if $R \geq 10$, Fig. 71 indicates that the effectiveness of gel treatments increased with increased fracture spacing for fractures that are not aligned with the direct flow direction (i.e., the y -direction fractures).

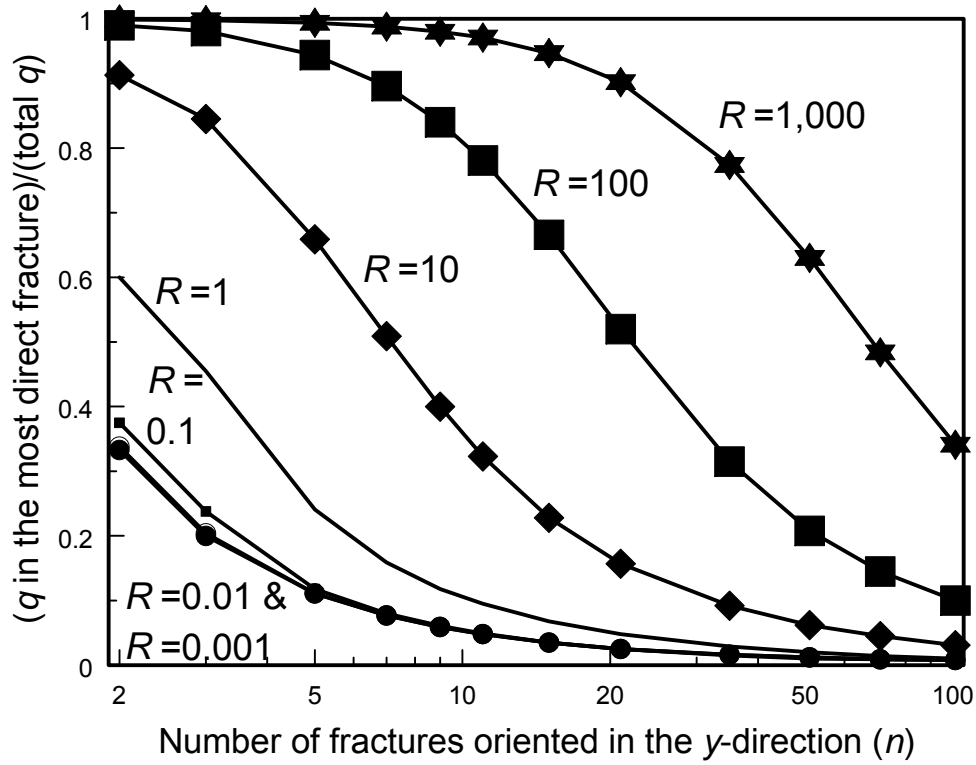


Fig. 68—Severity of channeling through the most direct fracture.

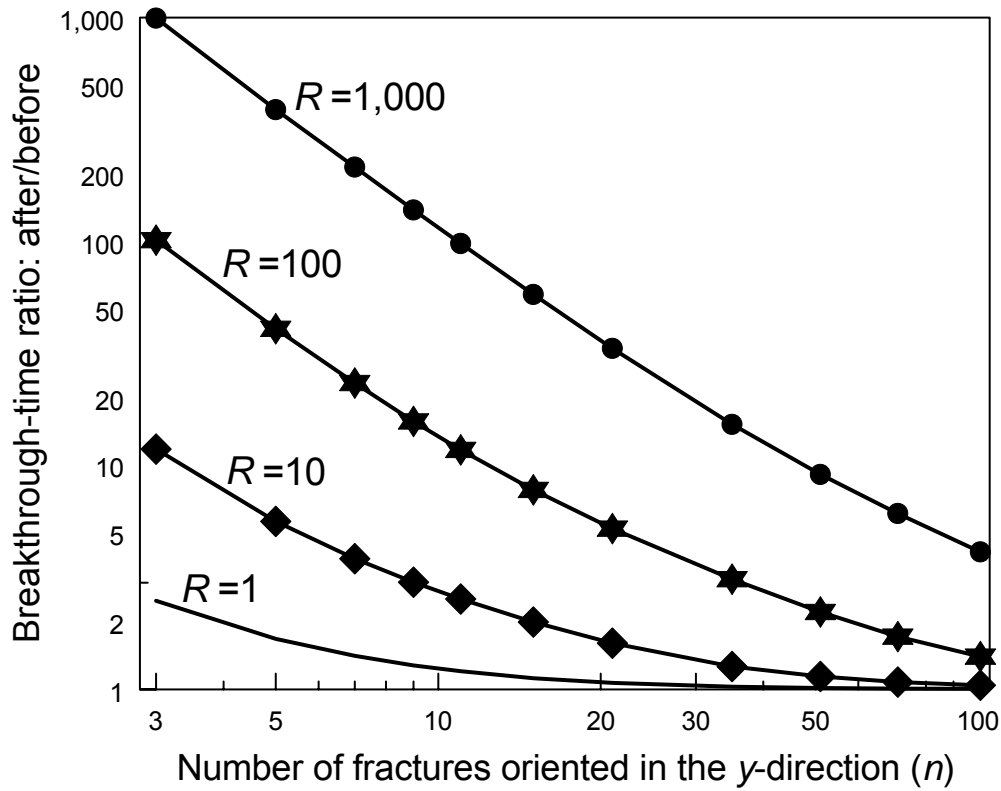


Fig. 69—Effect of plugging the most direct fracture.

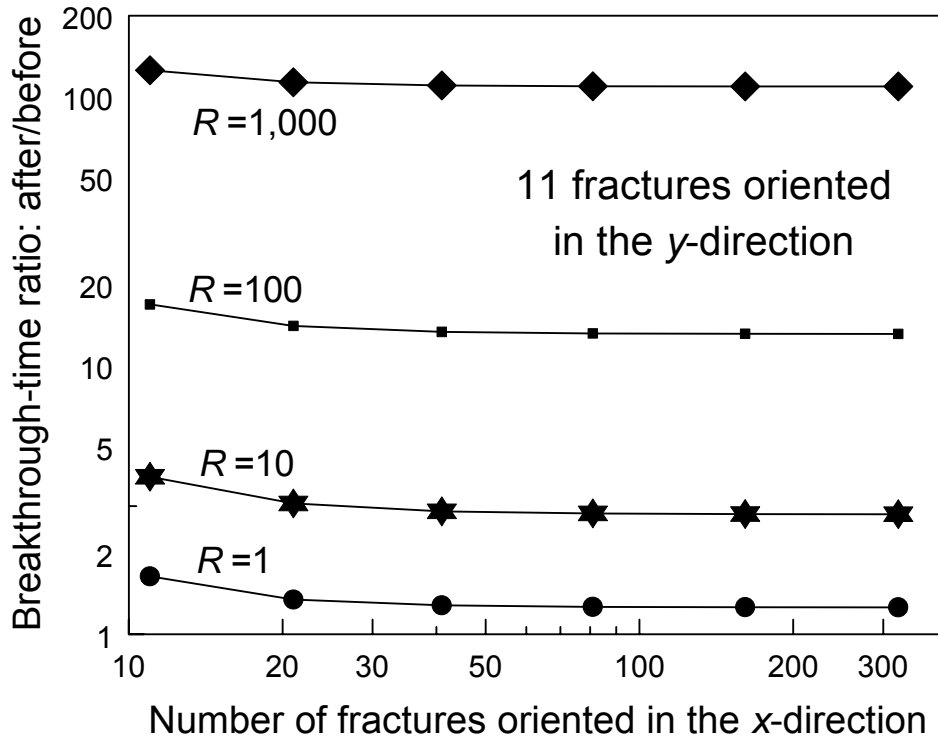


Fig. 70—Effect of plugging the most direct fracture (varied spacing for x -direction fractures).

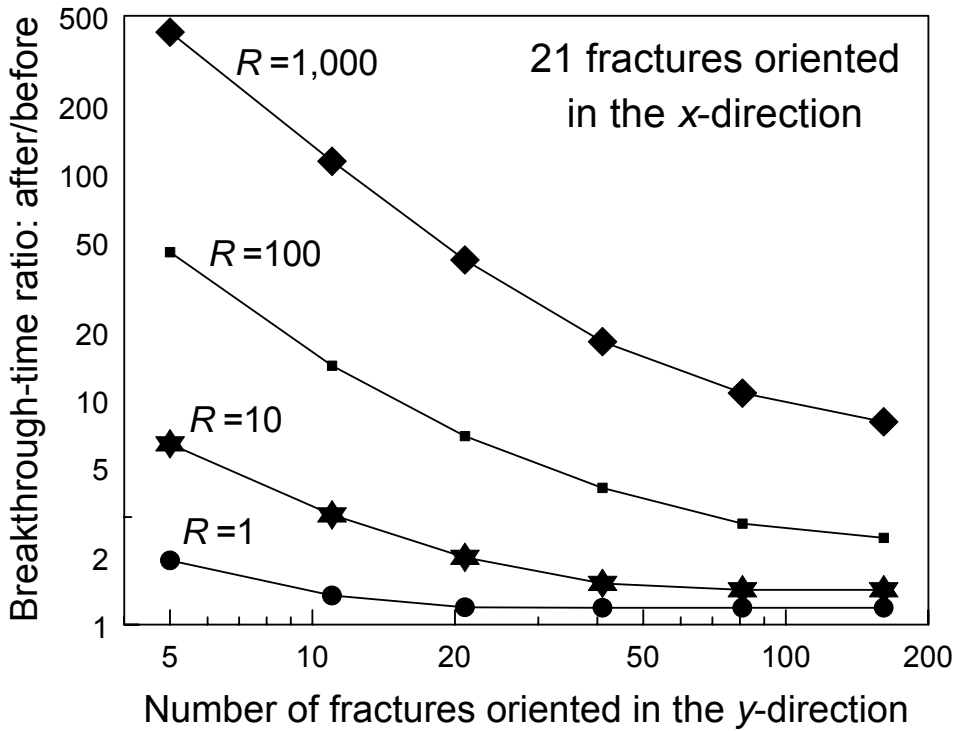


Fig. 71—Effect of plugging the most direct fracture (varied spacing for y -direction fractures).

Summary for Scenario 6. Scenario 6 involved many cross-direction (y -direction) and offset (x -direction) fractures. Results from a previous analysis (Ref. 3) indicated that the most severe channeling occurred when the x -direction fractures were ten or more times more conductive (two or more times wider) than the y -direction fractures. Channeling appeared less severe as the spacing decreased between adjacent fractures. These circumstances were also the most amenable to sweep improvement upon plugging of the most direct fracture. The previous analysis investigated the effects of variable fracture spacing on sweep and the potential for gel treatments. However, much additional work remains regarding the optimum size and placement of gel plugs in naturally fractured reservoirs.

Conclusions

This report considered several scenarios where a fracture (or fractures) allowed direct channeling between an injection well and a production well. We examined the effects of plug size and location on production rate, sweep efficiency, and pattern pressure gradients. Depending on the flow capacity of the fracture(s) relative to that of the reservoir rock, gel plugs may or may not be needed. For example, for fracture widths of 0.25 mm or less, channeling should not be a problem in 100-md rock. However, channeling can be a problem for fracture widths greater than 0.5 mm in this rock. A means is provided to apply these guidelines to rock with other permeabilities.

For vertical wells where channeling was dominated by a single vertical fracture, a small near-wellbore plug (e.g., 25 ft long) dramatically reduced pattern flow rates (i.e., water channeling), but did not improve pattern pressure gradients in a manner that enhanced oil displacement from deep within the reservoir. Significant improvements in oil displacement required plugging of at least 10% (and preferably more than 20%) of the length of the offending fracture, and ideally, this plug should be placed near the center of the fracture.

A second scenario considered an injector and a producer that had either parallel fractures or parallel horizontal wells and that were directly connected by a single vertical fracture. Pattern pressure gradients and sweep were very desirable for this scenario—with or without gel plugs. Small near-wellbore plugs were often sufficient to greatly reduce channeling.

A third scenario considered fractures that offset or parallel the main fracture that directly connected two wells. For vertical wells, these offset fractures had a negative impact on pattern sweep and pressure gradients that was difficult to overcome. These offset fractures presented less of a problem for cases similar to Scenario 2 (e.g., parallel horizontal wells).

In the fourth scenario, a fracture or fractures crossed the main direct fracture. Sweep efficiency and average pressure gradients increased in the pattern as the cross-direction (y -direction) fractures moved closer to the wells. However, the number and position of these cross-direction fractures had only a minor effect on pattern production rates. Complete plugging of the main direct fracture reduced channeling but may not improve matrix sweep nor increase pressure gradients. A centered partial plug in the main fracture improved pattern sweep and increased pressure gradients. The most effective plugs blocked the entrances to the cross-direction fractures.

Future Work

Much additional work remains regarding the optimum size and placement of gel plugs in naturally fractured reservoirs. Also, the work described in this report did not consider fractures that cut through multiple zones (i.e., at least one water zone and one hydrocarbon zone). In other words, the work in this report assumed that it was desirable to completely stop flow through the most direct and conductive fracture. Future work should consider fractures that allow flow of both water and hydrocarbon. Even for those cases where the plug is desired to completely block flow, issues remain on how to prevent gravity segregation within a given fracture from compromising the effectiveness of a gel plug.

3. INVESTIGATION OF GELS WITH LOW POLYMER CONCENTRATIONS

Part of our work is directed at gel propagation through and plugging of narrow fractures, as well as wide fractures. For many years, one Denver-based service company has advocated injection of gels with low concentrations of polyacrylamide. Unfortunately, much of the rationale that they use to justify their proposed gel designs violate well established physical principles and experimental observations. Some of this incorrect rationale includes:

1. The gels only enter and damage high-permeability, watered-out zones.
2. Crossflow does not impair the performance of the treatments.
3. The performance of the gel treatments can be modeled using a polymer flood simulator (in effect assuming that the gel acts as a super polymer flooding agent).
4. Aluminum propagates effectively through porous rock.
5. The gelant propagates deep into the high-permeability zone before gelation.

Over many years, we have consistently found no justification for the above claims (not laboratory, not theoretical, and not from detailed examination of field applications). However, in trying to keep an open mind that these low-concentration gels could have some value, we are searching for some mechanism by which these gels might improve reservoir sweep. In particular, we are investigating two types of problems. In the first case, we consider narrow fractures that cause channeling. In the second case, we consider channeling through a multi-darcy porous medium (without fractures).

Low-Concentration Gels in Narrow Fractures

Could low-concentration gels penetrate into and plug narrow fractures more effectively than more concentrated gels? Our previous work revealed that the pressure gradient required to extrude a gel through a fracture varied inversely with the square of fracture width.⁸ For a one-day-old Cr(III)-acetate-HPAM gel with 0.5% Alcoflood 935, 0.0417% Cr(III) acetate, 1% NaCl, and 0.1% CaCl₂, the pressure gradient needed for extrusion through a 0.1-mm wide fracture was over 1,000 psi/ft. We noted that a “partially formed” (i.e., gelant aged five hours before injection, when the gelation time was about four hours) Cr(III)-acetate-HPAM gel with 0.5% HPAM did not penetrate into a 0.05-mm wide fracture with a pressure gradient of 65 psi/ft.⁹ So for pressure gradients that are representative of field applications, Cr(III)-acetate-HPAM gels with concentrations over 0.5% HPAM will not penetrate significant distances into narrow fractures.

We wondered whether low concentrations of gel might show value in penetrating into and plugging tight fractures more effectively than conventional gels with higher concentrations. (Baojun Bai *et al.* performed preliminary work investigating this idea.^{10,11}) We performed experiments using gels with three concentrations: (1) 0.15% Alcoflood 935 HPAM and 0.0125% Cr(III) acetate, (2) 0.2% Alcoflood 935 HPAM and 0.0167% Cr(III) acetate, and (3) 0.25% Alcoflood 935 HPAM and 0.0209% Cr(III) acetate. All formulations contained 1% NaCl and 0.1% CaCl₂, and all experiments were performed at 41°C. Fig. 72 shows viscosity versus shear rate for HPAM solutions with no crosslinker. Within the experimental error, the viscosities were fairly Newtonian for shear rates from 1 to 100 s⁻¹, exhibiting average viscosities of 2.5 cp for 0.15% HPAM, 3.5 cp for 0.2% HPAM, and 6.5 cp for 0.25% HPAM.

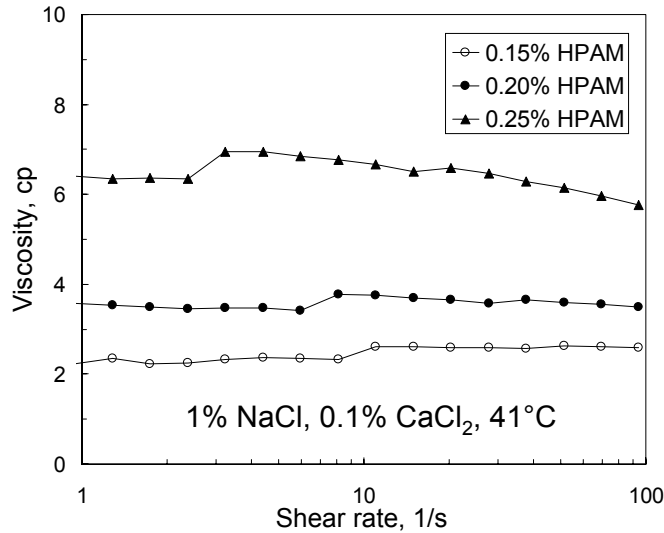


Fig. 72—Viscosity versus shear rate for HPAM solutions (no crosslinker).

With each gel composition, we performed experiments where 3,700 cm³ of one-day-old gel were extruded through fractures at 2,000 cm³/hr. All fractures were 3.8 cm high in Berea sandstone cores that were 4 ft (122 cm) long and 11.4 cm² in cross-section. Four internal pressure taps (drilled into the fracture) divided the core into five sections of equal length (0.8 ft). For each core, effluent could be produced from both the matrix and the fracture. For each gel composition, one experiment used a 0.5-mm-wide fracture, and another experiment used a closed fracture (with calculated fracture widths ranging from 0.08 to 0.15 mm). For two gel compositions, another experiment was performed using a 1-mm-wide fracture. All fractures had smooth-sawed faces. After gel placement, brine (1% NaCl and 0.1% CaCl₂) was injected at a rate of 100 cm³/hr. Table 1 shows the results.

Table 1—Use of low-concentration gels in tight fractures.
 $L_f = 4$ ft, one-day-old gel, gel rate=2,000 cm³/hr, brine rate=100 cm³/hr, 41°C

w_f , mm	Gel placement dp/dl , psi/ft	Effective viscosity of gel in fracture, cp	Brine breaching dp/dl , psi/ft	Stabilized brine dp/dl , psi/ft	Stabilized brine F_{rrw}	Matrix flow, %
0.15% high Mw HPAM, 0.0125% Cr(III) acetate						
0.15	7.4	3	0.25	0.21	3	0
0.5	0.27	4	0.13	0.11	53	0
1	0.096	12	0.088	0.063	243	0
0.2% high Mw HPAM, 0.0167% Cr(III) acetate						
0.1	31.0	7	20.0	8.8	40	100
0.5	0.21	3	0.076	0.056	27	7
1	0.028	4	0.056	0.036	138	0
0.25% high Mw HPAM, 0.0209% Cr(III) acetate						
0.08	61.8	4	61.8	58.9	116	100
0.5	1.0	16	0.74	0.72	347	0

Behavior during Gel Injection. The second column in Table 1 lists the stabilized pressure gradients during gel extrusion. As expected, for a given gel composition, the pressure gradient decreased dramatically with increased fracture width. The third column lists the effective viscosity exhibited by the gel in the fractures. In all cases, the effective viscosities were relatively low—on the order of the viscosities of the uncrosslinked polymer solutions. These low effective viscosities should aid deep placement in narrow fractures.

The values listed in Table 1 are averages taken over the middle three (of five total) fracture sections in the core. The pressure gradients were not the same along the length of the core. Figs. 73-75 show average pressure gradients in each of the five fracture sections for the various experiments. Note that the pressure gradients in the first (entry) section generally were not greater than any other section. Nor was there a consistent trend of pressure gradients through the fractures. Considering that these were smooth-sawed fractures of uniform width, the large variations in pressure gradient were somewhat surprising.

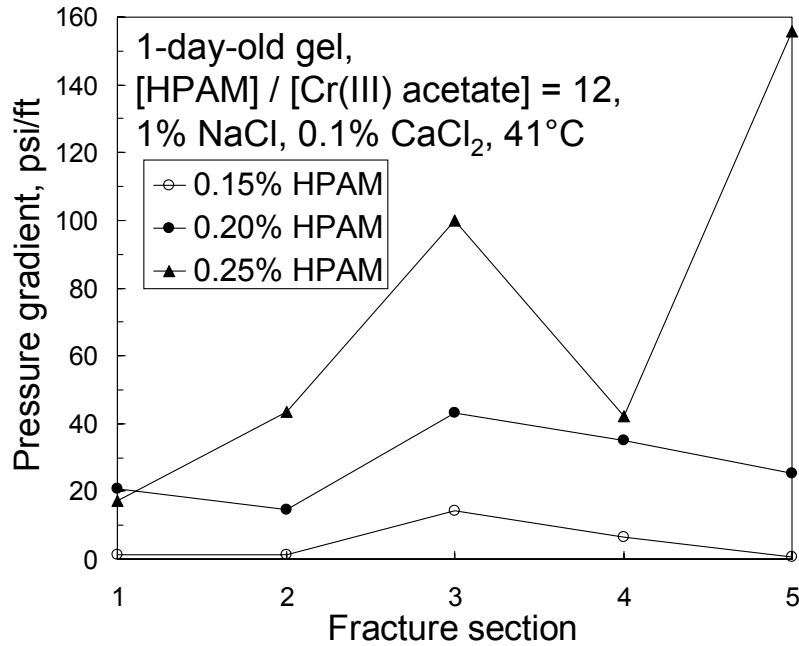


Fig. 73—Pressure gradients along closed fractures during gel injection.

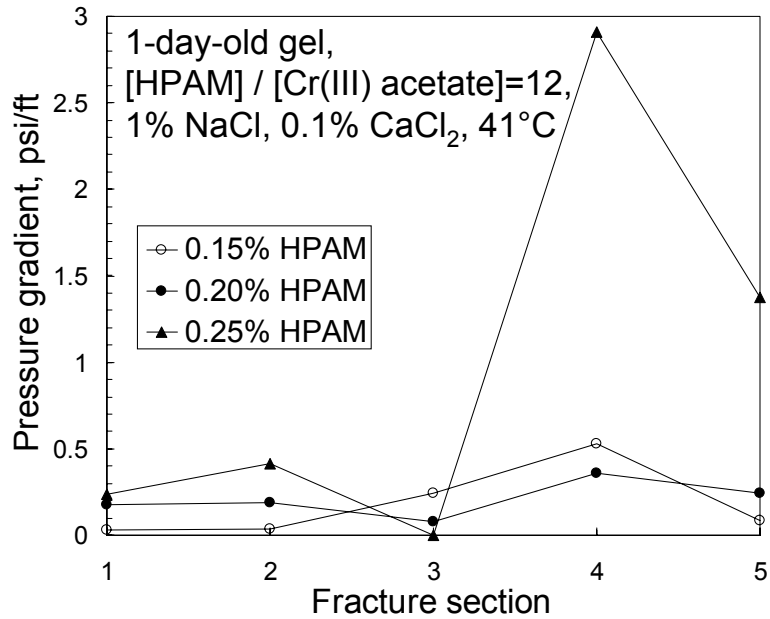


Fig. 74—Pressure gradients along 0.5-mm-wide fractures during gel injection.

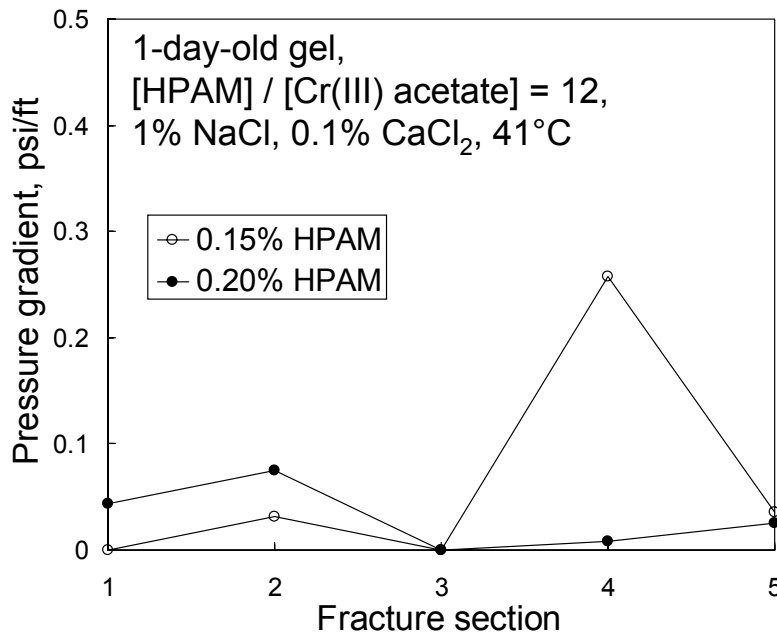


Fig. 75—Pressure gradients along 1-mm-wide fractures during gel injection.

Although substantial variations in pressure gradient were observed from section to section, pressure gradients were not particularly erratic within a given section (as a function of fracture volumes of gel injected). This fact is demonstrated in Figs. 76 and 77 for the 0.25% HPAM gel in closed and 0.5-mm-wide fractures. Certainly, some jumps occurred in various sections at particular times, and the pressure gradients trended upward or downward for some sections. However, in most cases, the pressure gradient behavior was fairly smooth.

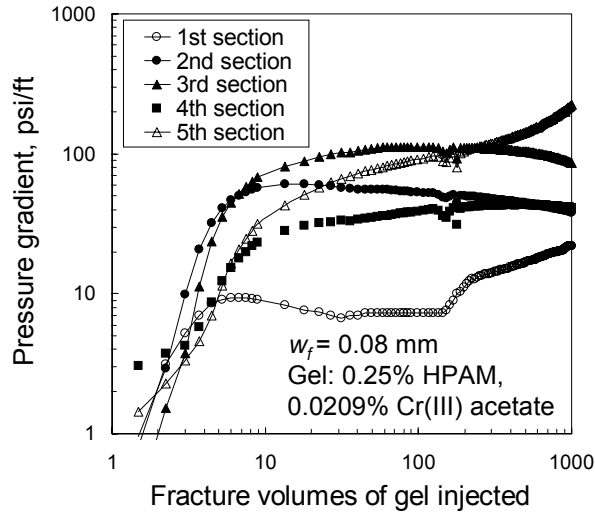


Fig. 76—Pressure gradients during gel injection: 0.08-mm fracture, 0.25% HPAM gel.

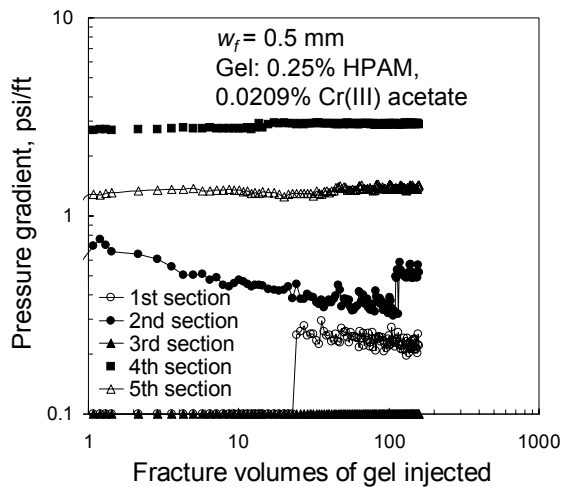


Fig. 77—Pressure gradients during gel injection: 0.5-mm fracture, 0.25% HPAM gel.

Behavior during Brine Injection after Gel Placement. The last four columns in Table 1 indicate how well the gel reduced the flow capacity of the fracture and how well the gel diverted water away from the fracture and into the matrix. The fourth column lists the maximum pressure gradient observed during the first brine injection (at $100 \text{ cm}^3/\text{hr}$) after gel placement. This pressure gradient indicates the point where brine first breached the gel.¹² For all but two of the cases in Table 1, the breaching pressure gradients were quite low—less than 1 psi/ft. The two exceptions involved two closed fractures—one for gel with 0.2% HPAM and one for gel with 0.25% HPAM. For those cases, the brine breaching pressures were significant and on the order of the pressure gradients during gel placement.

The fifth column of Table 1 reports the stabilized pressure gradient during brine injection, while the sixth column lists the residual resistance factor or factor by which the gel reduced the fracture

conductivity. The last column indicates that fraction of the injected brine that flowed through the matrix. The last column is particularly indicative of the diversion properties of the gel. Note that in two cases involving closed fractures (one for gel with 0.2% HPAM and one for gel with 0.25% HPAM), 100% of the brine flow occurred through the matrix (i.e., 0% of the flow occurred through the fracture) after the gel treatment. For all other cases, little or no brine flowed through the matrix after the gel treatment. Although two gel compositions showed promising behavior in penetrating into and plugging narrow fractures ($w_f \leq 0.15$ mm), they were ineffective in diverting flow into the matrix for wider fractures ($w_f \geq 0.5$ mm). Consequently, these compositions do not fulfill our requirements for aperture-tolerant plugging materials.

Low-Concentration Gels in Very Permeable Porous Media

In our second study, we considered whether low-concentration gels can propagate into and plug very high-permeability (multi-darcy) porous media that is not fractured. Ideally, in certain field applications, a gel would penetrate deep into the very high-permeability strata but not into adjacent, less-permeable strata. Achieving this ideal has been a sort of “holy grail” in conformance control for many years. Unfortunately, all credible investigations to date indicate that crosslinked polymers (e.g., gels, dispersions of gel particles, and “colloidal dispersion gels”) do not flow through normal porous rock using normal field pressure gradients. The question that we raise here is: Will the concept be viable in porous media with abnormally high permeability? More specifically, can low-concentration gels propagate effectively through a ~10-darcy porous medium (i.e., porous polyethylene)?

In this study, three porous polyethylene cores were 13.6 cm long with a cross-sectional area (circular) of 11.4 cm². These cores DID NOT CONTAIN FRACTURES. The cores had two internal pressure drops, located 2 cm from inlet and exit core faces. The central section of the core was 9.6 cm in length. In each experiment, one-day-old gel was forced into the core using a fixed rate of 2,000 cm³/hr. The three gel compositions used were similar to those mentioned in the previous section: (1) 0.15% Alcoflood 935 HPAM and 0.015% Cr(III) acetate, (2) 0.2% Alcoflood 935 HPAM and 0.02% Cr(III) acetate, and (3) 0.25% Alcoflood 935 HPAM and 0.0208% Cr(III) acetate. All formulations contained 1% NaCl and 0.1% CaCl₂, and all experiments were performed at 41°C.

The effective viscosities in the first (2 cm long) and second (9.6 cm long) core sections are plotted as a function of pore volumes injected in Figs. 78-80. For all three cases, these figures show serious plugging in the inlet (first) section. The degree of plugging was most severe for the gel with 0.25% HPAM (Fig. 80). The second sections revealed effective viscosities that were relatively low (Fig. 81). For the gel with 0.15% HPAM (Figs. 78 and 81), the effective viscosity in the second section was about the same as the viscosity of an uncrosslinked 0.15% HPAM solution (2.5 cp), and it increased gradually with increased throughput. Similarly, for the gel with 0.2% HPAM (Figs. 79 and 81), the effective viscosity in the second section was about the same as the viscosity of an uncrosslinked 0.2% HPAM solution (3.5 cp), but it decreased gradually with increased throughput. These results suggest that some free polymer may pass through the first core sections for the gels with 0.15% or 0.2% HPAM. However, for the gel with 0.25% HPAM, the low effective viscosity in the second core section suggests that virtually all polymer was filtered out by the first core section (Figs. 80 and 81).

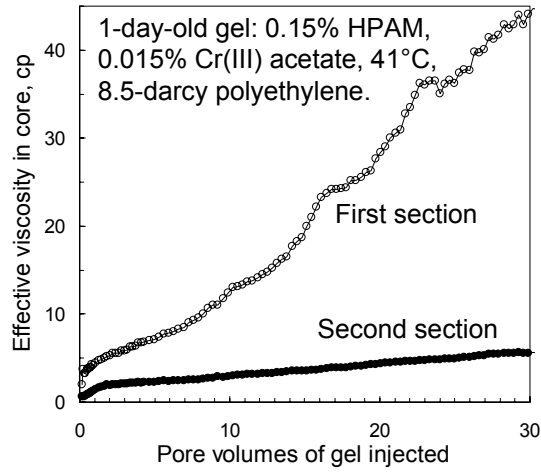


Fig. 78—Effective viscosities during gel injection: 0.15% HPAM gel.

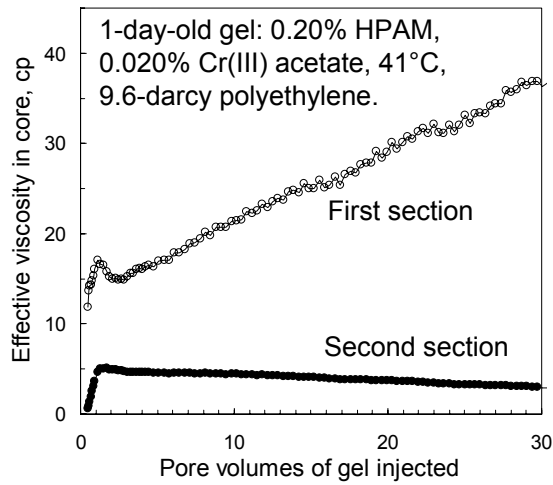


Fig. 79—Effective viscosities during gel injection: 0.2% HPAM gel.

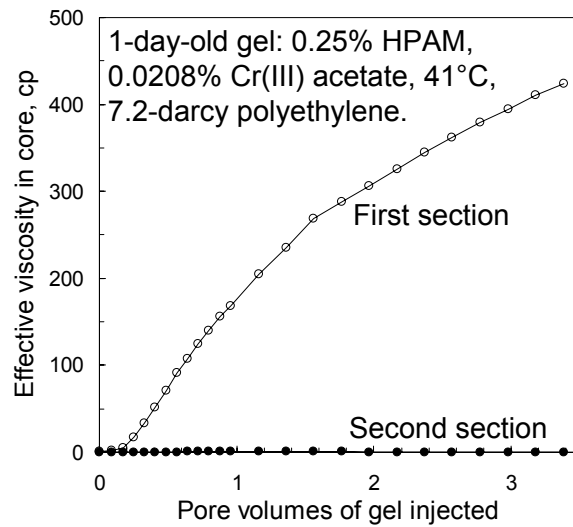


Fig. 80—Effective viscosities during gel injection: 0.25% HPAM gel.

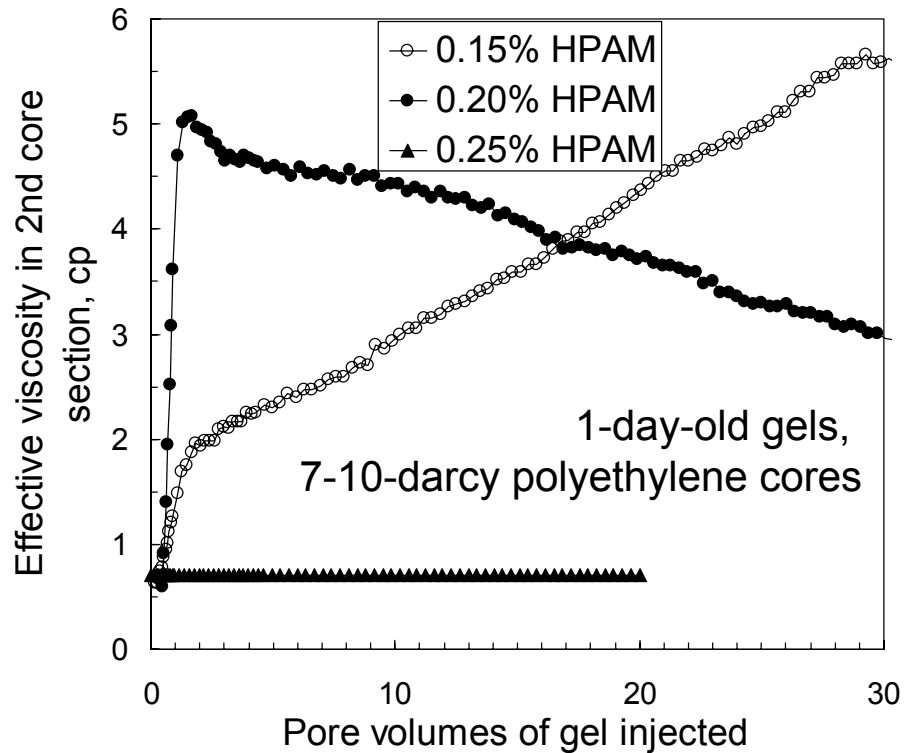


Fig. 81—Effective viscosities in the second sections during gel injection.

During brine injection after gel flow, the residual resistance factors (permeability reduction values) in the second core sections averaged 12 for the gel with 0.15% HPAM and 1 (i.e., no permeability reduction) for the other two gels. Overall, these results indicate poor propagation of the gel with 0.15% HPAM through 8.5-darcy polyethylene and no significant propagation through similar cores for the gels with 0.2% and 0.25% HPAM.

Another set of experiments were performed in a 1,570-md fused-silica core that was 13.1 cm (5.2 inches) long and 3.81 cm (1.5 inches) in diameter. The core had two internal pressure taps. The first was located 2 cm from the core inlet, while the second internal tap was 1.9 cm from the core outlet. These taps divided the core into three sections, with lengths of 2 cm, 9.2 cm, and 1.9 cm. As in our standard procedure, the core was first saturated with brine containing 1% NaCl and 0.1% CaCl₂. We prepared a gel that contained 0.15% Alcoflood 935 HPAM, 0.015% Cr(III) acetate, 1% NaCl, and 0.1% CaCl₂. This formulation was aged for four days at 41°C. Then, the gel was injected into the core at a rate of 100 cm³/hr (equivalent to a flux of 7 ft³/ft²/d) at 41°C. Fig. 82 shows the pressure gradients for each of the three sections during gel injection. This figure shows dramatic progressive plugging in the first core section, with pressure gradients rising to 30,000 psi/ft over the course of injecting 1.5 PV of gel. In contrast, the pressure gradients in the other two core sections remained stable and low. Thus, this gel with 0.15% HPAM did not penetrate very far into the 1,570-md core (i.e., less than 2 cm). Fig. 83 converts the pressure gradients from the first core section into resistance factors (effective viscosities). Resistance factors rose to 104,000 after 1.5 PV of gel injection.

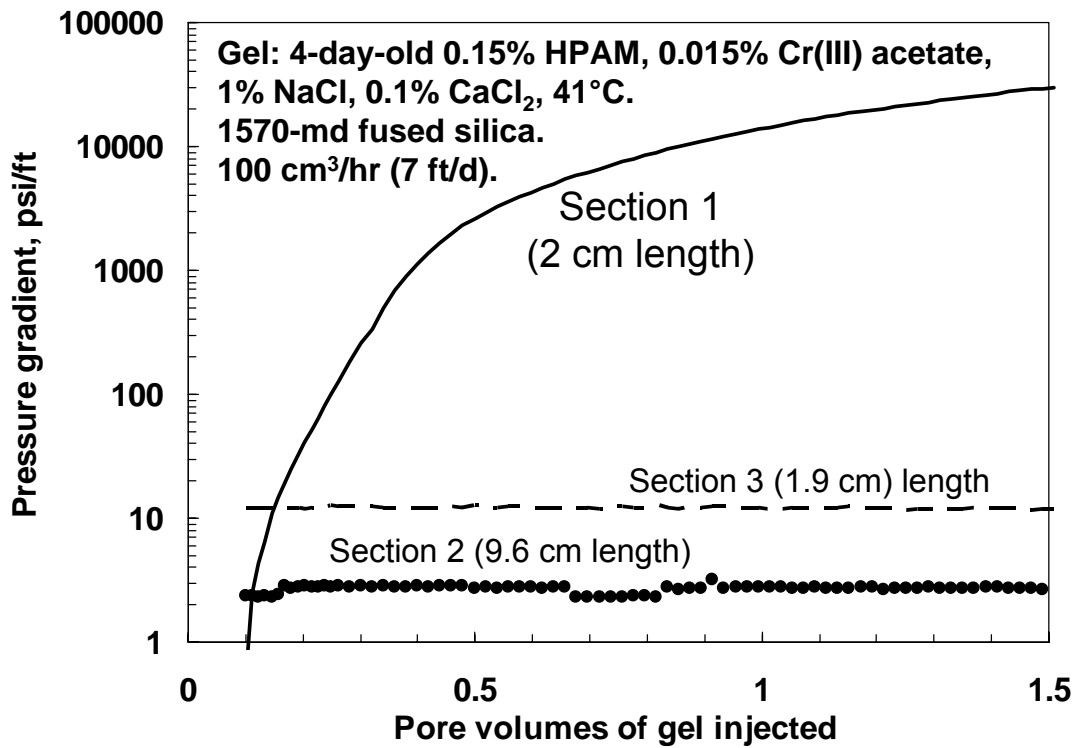


Fig. 82—Pressure gradients during gel injection into 1,570-md fused silica.

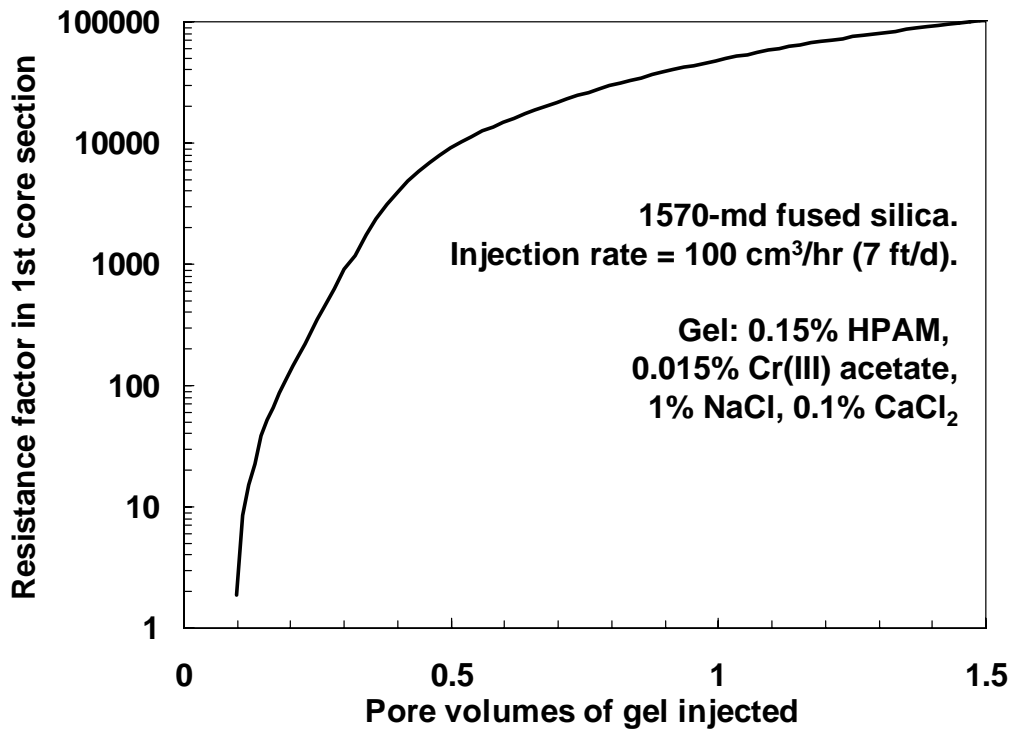


Fig. 83—Effective viscosities (resistance factors) in the first section during gel injection.

After gel injection, the core was shut in for three days, the flow direction through the core was reversed, followed by brine injection at $100 \text{ cm}^3/\text{hr}$ (7 ft/d) and 41°C . During the course of injecting 53 PV of brine (see Fig. 84), the residual resistance factor in the first core section (which is now located at the outlet of the core because the flow direction was reversed) was reasonably steady at 17,000 to 20,000. Thus, the gel did not simply wash off the sand face when the flow direction was reversed. For Sections 2 and 3, the residual resistance factors were near unity—indicating no significant damage to these sections.

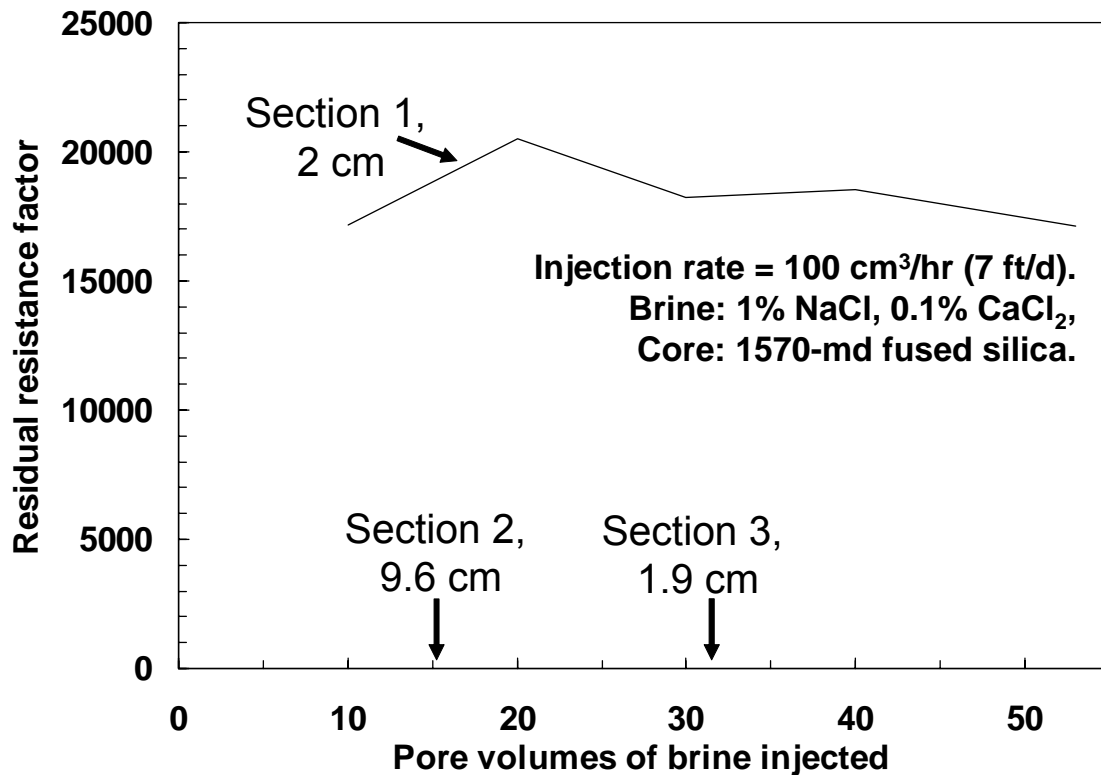


Fig. 84—Residual resistance factors during brine injection.

Next, brine was injected using a series of increasing rates. At each rate from 7 ft/d to $1,111 \text{ ft/d}$, the stabilized pressure gradient was recorded before moving up to the next rate. Upon reaching $1,111 \text{ ft/d}$, the rate was decreased in stages back to 7 ft/d . Fig. 85 shows the results. Interestingly, during the series of increasing rates, the pressure gradient held reasonably steady at $5,000$ to $6,000 \text{ psi/ft}$. This result suggests that $5,000$ to $6,000 \text{ psi/ft}$ is the critical level of pressure gradient needed to mobilize this gel in $1,570\text{-md}$ porous media.

During the series of decreasing rates, the stabilized pressure gradients consistently decreased with decreasing rate. However, Fig. 85 demonstrates that the relation between rate and pressure gradient was not conventional—i.e., halving the injection rate did not half the pressure gradient.

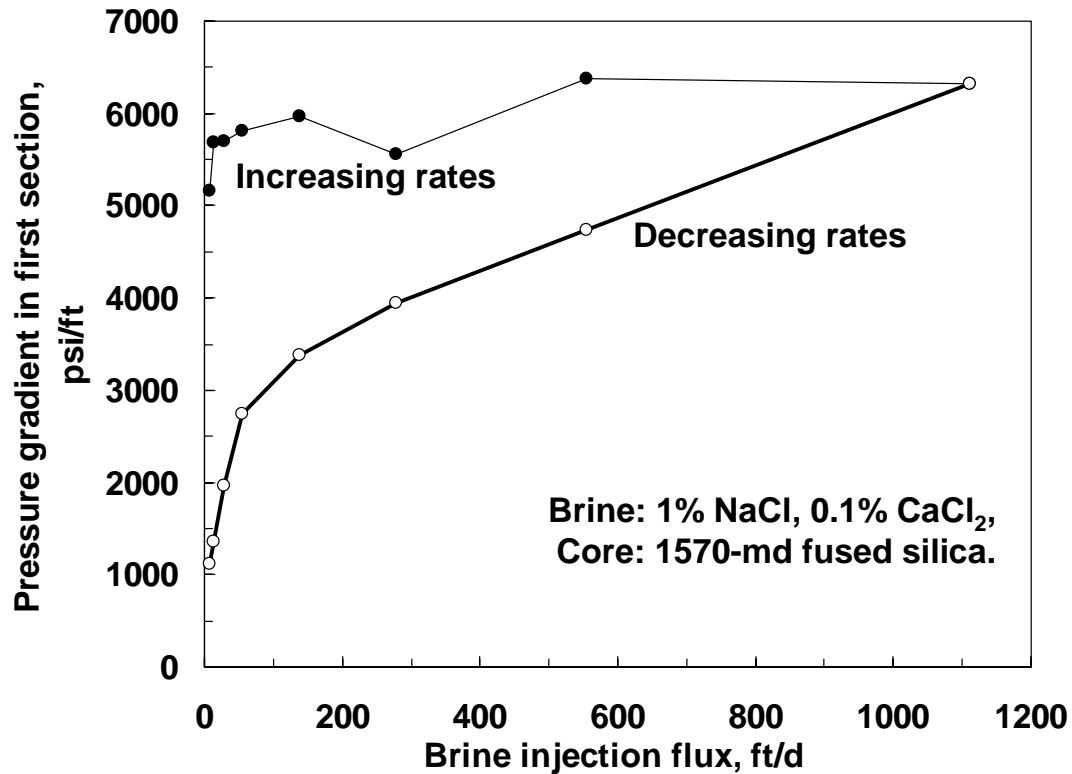


Fig. 85—Pressure gradients in the first section during brine flow at various rates.

In earlier work,¹³ we studied a “colloidal dispersion gel” with 0.03% Tiorco HiVis 350 HPAM, 0.0015% aluminum (as citrate), and 0.5% KCl at 41°C. For the first two hours after preparation, this formulation flowed through 707-md Berea sandstone without exhibiting progressive plugging of the inlet sandface. However, after two hours, severe plugging was noted at the inlet sandface, while the effective viscosity in the core (resistance factor) dropped to low values. Thus, once the crosslinking reactions occurred, even this “particle dispersion” gel with very low HPAM concentrations could not propagate through 707-md Berea.

We suspect that these gels can be made to flow through porous media if the permeability and/or the pressure gradient are large enough. In this work using a Cr(III)-acetate-HPAM gel with 0.15% HPAM in a 1,570-md core, the pressure gradient for gel mobilization in a core was greater than 5,000 psi/ft. Earlier, for a Cr(III)-acetate-HPAM gel with 0.5% HPAM in a 28-darcy sand pack, we found that the pressure gradient for gel mobilization was 200 psi/ft.¹⁴ However, our results indicate that the permeability that allows gel flow (as opposed to gelant flow) is greater than 10 darcys for pressure gradients that are typically encountered in field applications.

Conclusions

In fractures with widths around 0.1 mm, one-day-old Cr(III)-acetate-HPAM gels containing 0.15%, 0.2%, or 0.25% HPAM propagated effectively, exhibiting effective viscosities that were similar to the viscosity of polymer solutions without crosslinker (i.e., 3-7 cp). In contrast, our previous work revealed that Cr(III)-acetate-HPAM gels with 0.5% HPAM would not enter these narrow fractures unless extremely high pressure gradients were applied. The gels containing

0.2% or 0.25% HPAM effectively healed these narrow fractures, forcing all post-gel-treatment brine to flow through the Berea sandstone matrix rather than the narrow fractures. In contrast, the gel with 0.15% HPAM was ineffective at healing the fracture. Also, all three gels were ineffective at healing fractures that were 0.5 mm or 1 mm in width. Consequently, these compositions do not fulfill our requirements for aperture-tolerant plugging materials.

We tried to force formed Cr(III)-acetate-HPAM gels (again with 0.15%, 0.2%, and 0.25% HPAM) through 1.5- to 10-darcy porous media (not fractured). In all cases, severe face-plugging occurred, and the effective viscosities were low (i.e., similar to, or less than, the viscosity of uncrosslinked polymer solutions) for interior sections of the cores. We suspect that these gels can be made to flow through porous media if the permeability and/or the pressure gradient are large enough. However, the permeability that allows gel flow (as opposed to gelant flow) is greater than 10 darcys for pressure gradients that are typically encountered in field applications.

4. OPTIMIZING DISPROPORTIONATE PERMEABILITY REDUCTION

Many polymers and gels have shown an ability to reduce permeability to water more than that to oil or gas.¹⁵⁻¹⁹ This disproportionate permeability reduction (or “relative permeability modification”) is essential if polymers or gels are placed in production wells without protecting hydrocarbon-productive zones.²⁰ With existing polymers, gels, and technology, disproportionate permeability reduction has its greatest value when treating production wells that intersect a fracture or fracture-like features.^{1,2,21} Nonetheless, many people are very interested in exploiting this property to reduce excess water production from unfractured wells (i.e., radial flow into porous rock or sand). The idealistic goal or “holy grail” of this technology is to develop a material that can be injected into any production well (without zone isolation) and substantially reduce water productivity index without significantly impairing oil productivity. Several obstacles must be overcome before this ideal can be achieved.

Challenges for Applications of Disproportionate Permeability Reduction

Variable Performance. Several challenges currently limit the applicability of disproportionate permeability reduction. First, field applications of polymer and gel treatments have shown substantial variations in performance from one application to the next. In part, these variations arise from differences in reservoir conditions, well conditions, and mixing and injection procedures. However, significant performance variations appear inherent for some polymers and gels.²² During 16 replicate experiments (in Berea sandstone) with a commercially available “weak” gel, oil residual resistance factors (F_{rro} , permeability reduction factors) ranged from 2.7 to 59 (median of 5.9, average of 9.7, and standard deviation of 13.5), while water residual resistance factors (F_{rrw}) ranged from 1.5 to 317 (median of 6.6, average of 32, and standard deviation of 78).²²

Uncontrolled variability of residual resistance factors may be an inherent flaw for adsorbed polymers, “weak gels”, suspensions of particles (including gel particles), and “colloidal dispersion gels.” Permeability reduction by adsorbed polymers can be strongly influenced by mineralogy of the rock. In turn, rock mineralogy typically exhibits significant variations locally within a porous medium. Consequently, these mineralogical variations could lead to wide variations in performance for adsorbing polymers.

Weak gels are typically suspensions of gel particles that result from incomplete gelation.²³⁻²⁶ These particle suspensions have a particle size distribution—they are not monodisperse. Pores within a rock also have a size distribution. Since the particles reduce permeability by lodging in pore throats, the ratio of particle size to pore size is important in determining residual resistance factors for these suspensions. Variations in particle size distribution (especially resulting from unknown or uncontrolled particle generation) and variations in pore size distribution (resulting from normal geologic processes) may cause wide variations in performance for weak gels, suspensions of particles, and “colloidal dispersion gels.” We note that an extensive effort is underway at Institut Francais du Petrole (IFP) to address this issue. IFP is developing suspensions of “microgels” that are manufactured with very narrow particle size distributions.²⁷

F_{rro} Must Be < 2 for Radial Flow. A second challenge is presented by the requirements for successful application of disproportionate permeability reduction for different types of problems.

For example, consider an unfractured (i.e., radial flow) production well with one water zone, one oil zone, and a separating impermeable shale barrier. For this case, if a gelant is placed using unrestricted injection (i.e., no zone isolation), previous work demonstrated that the gel *must* provide a resistance factor less than 2 in the oil zone.^{20,24,28} Preferably, the gel should provide a residual resistance factor greater than 20 in the water zone (Fig. 86). The variations in residual resistance factors mentioned above point to the difficulties in reliably attaining permeability reductions to oil that are less than two.

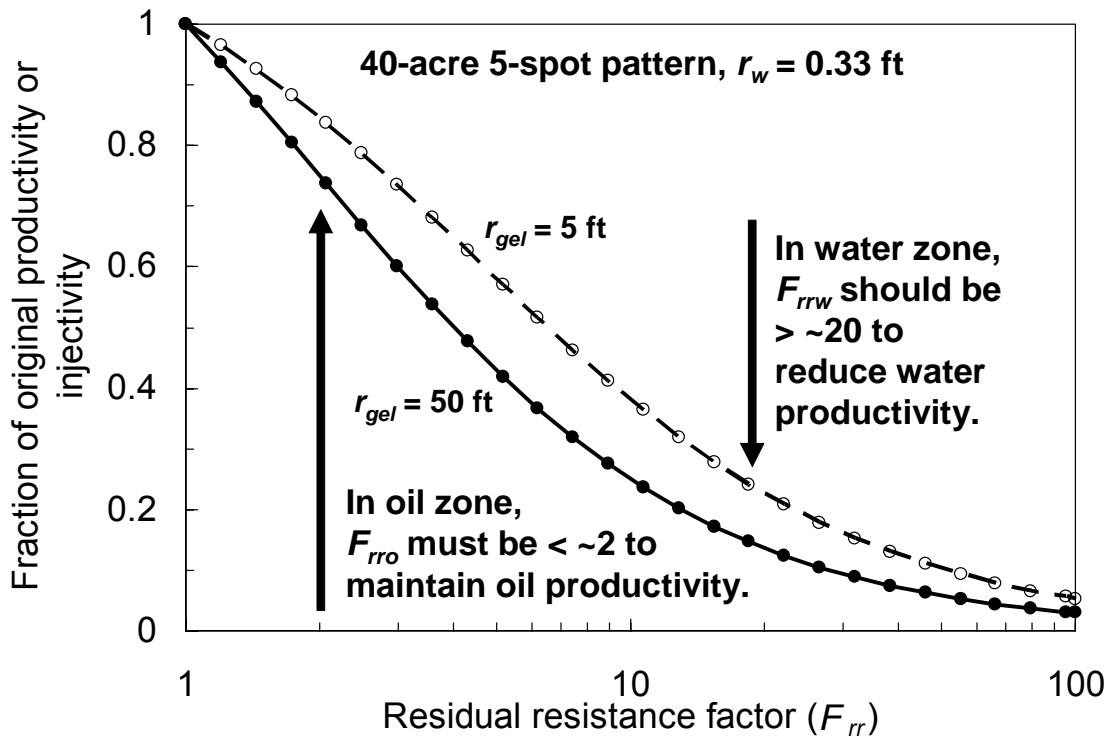


Fig. 86—Losses of zone flow capacity for radial flow.

Permeability Dependence of F_{rr} . A third challenge comes from the dependence of residual resistance factors on the permeability of the porous media. For adsorbing polymers and “weak” gels, residual resistance factors increased with decreased permeability (Fig. 87).²⁹ In other words, these materials damage low-permeability rock more than high-permeability rock. For the data shown in Fig. 87, the consequence of this behavior is shown in Table 2 after unrestricted polymer injection into an unfractured well with five non-communicating layers. The third column indicates the radius of polymer penetration into a given layer during placement with no zone isolation. (This is a simple calculation using the Darcy equation.^{24,28}) Note that the final (i.e., post-polymer-treatment) flow capacity decreased substantially with decreasing layer initial permeability. Thus, these polymers and gels can damage the flow capacity of low-permeability rock much more than high-permeability rock, even though the polymer or gelant penetrates significantly farther into the high-permeability rock.^{20,24,28}

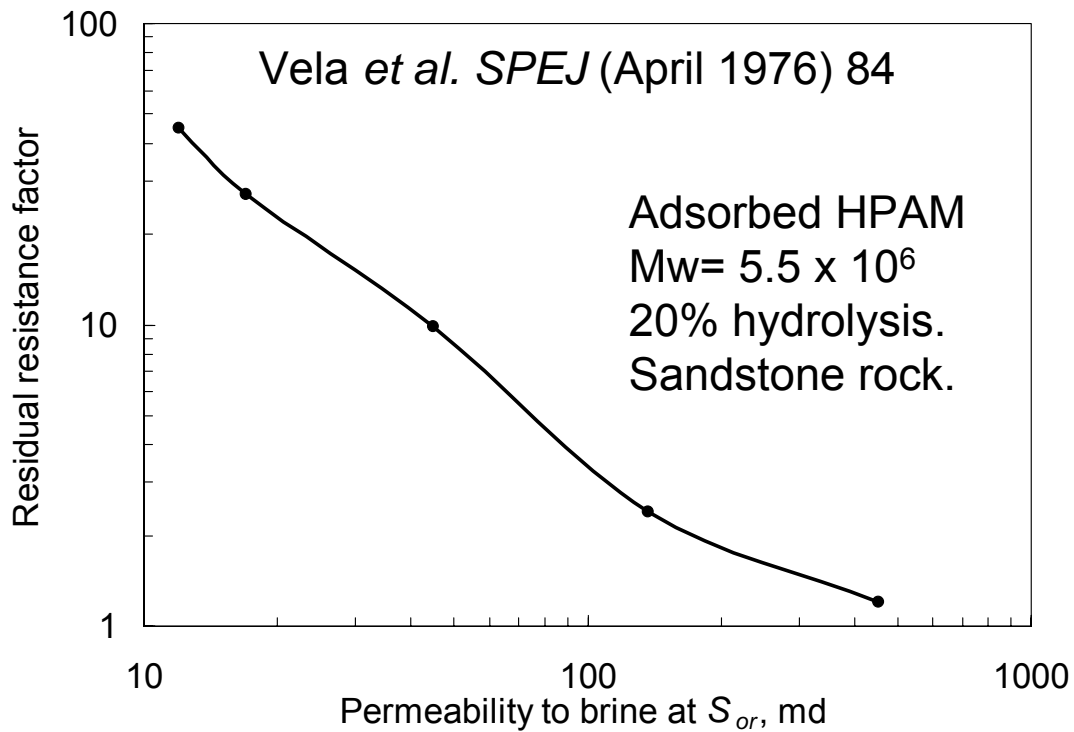


Fig. 87—Permeability dependence of water residual resistance factors (F_{rrw}).

Table 2—Adsorbed polymers and “weak” gels can harm flow profiles.

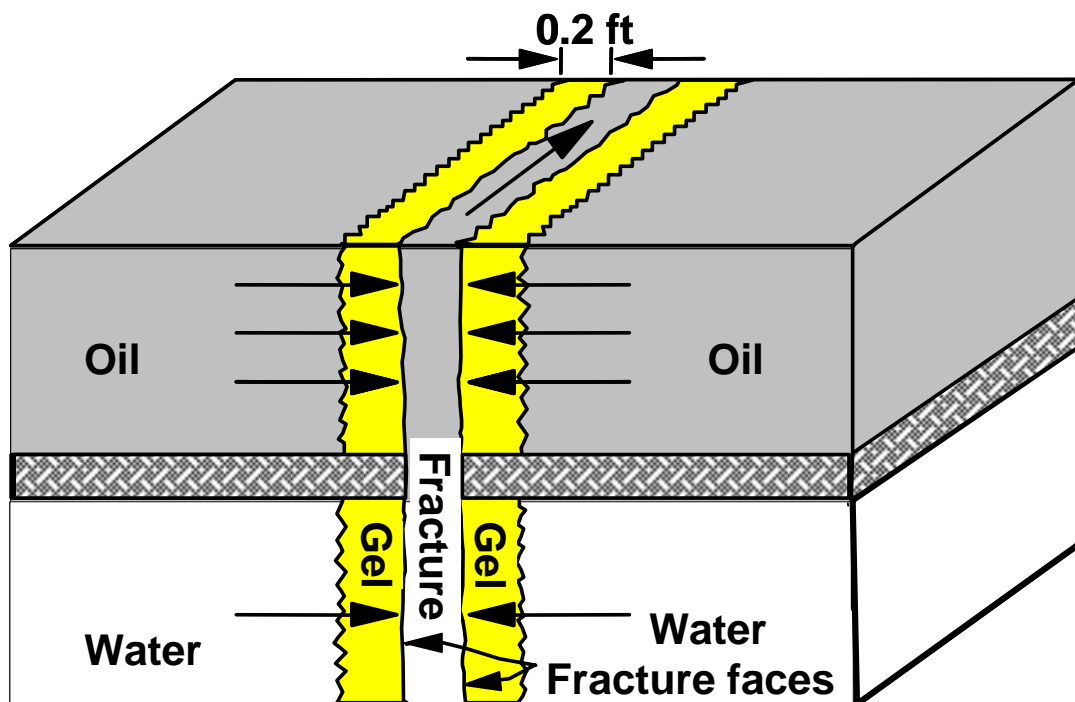
Layer	k_w @ S_{or} , md	Polymer radius, ft	Permeability reduction factor (F_{rrw}) from Fig. 87	Layer flow capacity, final/initial
1	453	30	1.2	0.94
2	137	16.5	2.4	0.71
3	45	9.5	9.9	0.31
4	17	5.8	27	0.15
5	12	4.9	45	0.10

Overcoming the Obstacles

Variability. Variability of residual resistance factors was the first challenge mentioned above. This variability was tied to uncontrolled particle size and size distributions for suspensions of gel particles and to mineralogical variations for both adsorbed polymers and suspensions of gel particles. Perhaps this variability in performance can be mitigated by using a permeability reduction mechanism with better control. In particular, if all aqueous pore space was filled with a uniform gel, the permeability reduction (at least for water flow) would be controlled by flow through the gel itself. If the inherent permeability of the gel to water was much less than the permeability of the original porous media, the permeability reduction would not be sensitive to variations in mineralogy, pore size, or pore size distribution.

Concerning variability of oil residual resistance factors, our recent work³⁰ suggested that re-establishing oil permeability in a gel-filled porous media can be predicted using concepts of mobility ratios and stable-versus-unstable displacements.

Linear versus Radial Flow. The second hurdle mentioned depended on the type of problem to be treated. Our work suggests that disproportionate permeability reduction currently has its greatest utility in treating fractures and fracture-like features.^{1,2,21} If gelant is allowed to leakoff a short, controlled distance from the fracture faces and if the gel provides predictable residual resistance factors, water entry into the fracture can be greatly impeded while causing minimal reduction in hydrocarbon productivity. This process does not require that the gel provide very low oil residual resistance factors—only that the gel provides water residual resistance factors that are reliably much greater than oil residual resistance factors (see Fig. 88 for an example).



Equivalent resistance to flow added by the gel

In oil zone: $0.2 \text{ ft} \times 50 = 10 \text{ ft}$.

In water zone: $0.2 \text{ ft} \times 50,000 = 10,000 \text{ ft}$.

Fig. 88—Gel restricting water entry into a fracture.

In contrast, for radial flow from wells into porous rock (i.e., unfractured production wells), the oil residual resistance factor (F_{ro}) must generally have a value below $2^{20,24}$ (see Fig. 86). Normally, we might not expect this to be achievable using a pore-filling gel, such as Cr(III)-acetate-HPAM. We typically expect pore-filling gels to provide high residual resistance factors for both oil and water. However, our recent work provides hope that low F_{ro} values may be attained.³⁰ For example, in one case before gel placement, a Berea core showed an endpoint

permeability to oil of 508 md (i.e., at S_{wr}) and an endpoint permeability to water of 120 md (i.e., at S_{or}). After placement of a Cr(III)-acetate-HPAM gel [with 0.5% HPAM and 0.0417% Cr(III) acetate], the permeability during brine injection quickly stabilized at 0.17 md (open circles in Fig. 89)—indicating a water residual resistance factor of 706 (i.e., 120/0.17). In contrast, during oil (hexadecane) injection after gel placement (solid circles in Fig. 89), the permeability rose gradually to 105 md over the course of 100 pore volumes (PV)—indicating an oil residual resistance factor of only 4.8 (i.e., 508/105). Since the permeability to oil was still rising at 100 PV (Fig. 89), hope exists that even lower oil residual resistance factors could be achieved.

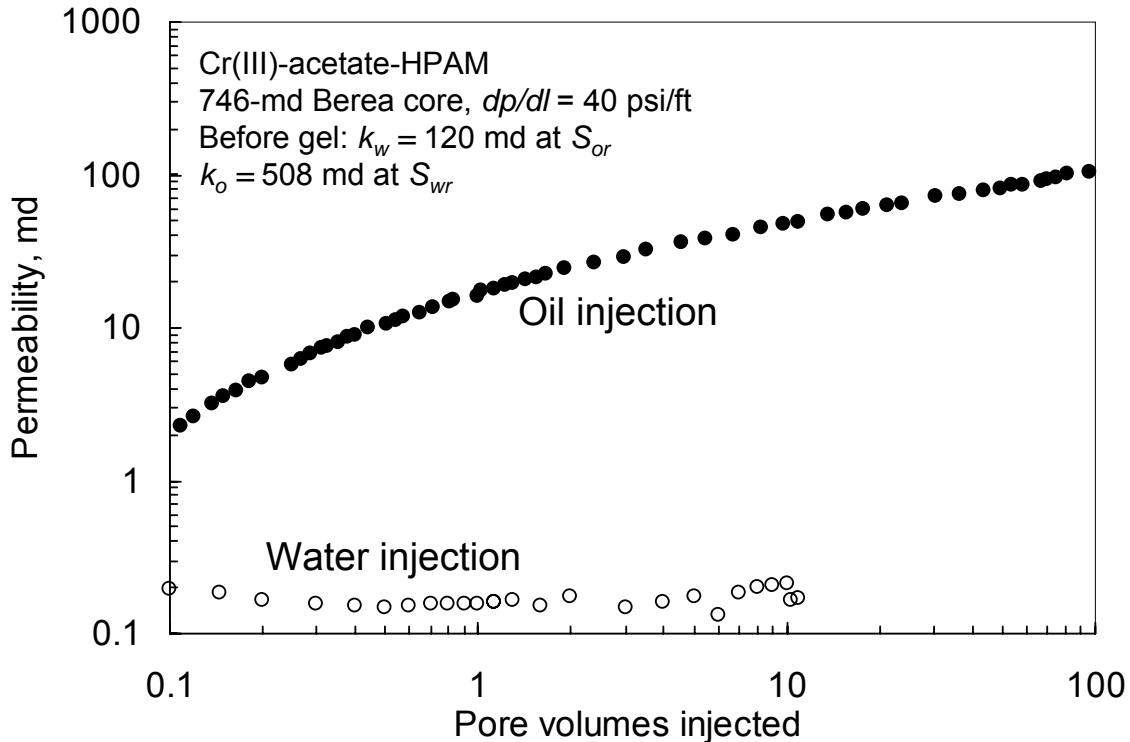


Fig. 89—Permeabilities to oil and water after gel placement in Berea.

Permeability Dependence. The third challenge mentioned above was the permeability dependence of residual resistance factors. For adsorbing polymers and suspensions of gel particles, residual resistance factors increased with decreased permeability. In contrast, pore-filling gels reduced the permeability to water of all porous media to the same low value—a value that approximates the inherent permeability of the gel to water.²³⁻²⁶ Consequently, use of pore-filling gels may provide a means to overcome some of the important challenges that have limited applications of disproportionate permeability reduction.

Permeability to Water after Gel Placement

k_w versus Initial Core Permeability and Core Material. With the above considerations in mind, we performed several experiments in an effort to use pore-filling Cr(III)-acetate-HPAM gels to optimize disproportionate permeability reduction. One goal was to ensure water residual resistance factors (F_{rrw}) are reliably high. For radial flow, Fig. 86 suggests that F_{rrw} values should

be greater than 20. For linear flow applications (e.g., fractured wells), much larger F_{rrw} values are desirable (see Fig. 88). Thus, we performed experiments to establish whether a pore-filling gel can provide reliable k_w and F_{rrw} values. In particular, for the first set of experiments (all at 41°C), we wish to confirm that a pore-filling gel reduces the permeability (k_w) of all porous media to the same low value—that reflects the inherent permeability of the gel to water. In Table 3, the first six entries describe experiments where cores at residual oil (hexadecane) saturation (S_{or}) were flooded with a Cr(III)-acetate-HPAM gelant [with 0.5% HPAM, 0.0417% Cr(III) acetate, 1% NaCl, 1% CaCl₂], followed by brine injection (1% NaCl, 0.1% CaCl₂) at a fixed pressure gradient. Initial core permeabilities ranged from 746 to 15,270 md in core materials including Berea sandstone, fused silica, and porous polyethylene. For the first six post-gel cases, k_w averaged 240 μ d (\pm 84 μ d), and no trend was evident when correlating with material type or initial core permeability. These results support our previous finding that pore-filling gels reduce permeability of all porous media to a value that reflects the inherent permeability of the gel to water.^{23,25,26}

Table 3— k_w during brine flow after gel placement.

Entry	Core material	Initial k , md	ϕ , %	k_w at S_{or} , md	HPAM in gel, %	S_{or} present?	dp/dl , psi/ft	Post-gel k_w , μ d	F_{rrw}
1	Berea	746	21	120	0.5	yes	40	170	706
2	fused silica	1,820	27	447	0.5	yes	30	230	1,940
3	fused silica	2,390	27	640	0.5	yes	10	120	5,330
4	polyethylene	6,400	40	4,810	0.5	yes	100	320	15,000
5	polyethylene	9,530	40	5,860	0.5	yes	30	240	24,400
6	polyethylene	15,270	40	6,500	0.5	yes	10	370	17,600
7	Berea	356	21	*	0.5	no	14	15	23,700
8	Berea	389	21	*	0.5	no	30	5	77,800
9	Berea	100	21	*	0.5	no	58	10	10,000
10	Berea	40	21	*	0.4	no	58	19	2,110
11	Berea	274	21	*	0.3	no	58	55	4,980
12	polyethylene	8,100	40	*	0.5	no	30	60	135,000
13	polyethylene	8,230	40	*	0.3	no	26	3,200	2,570
14	polyethylene	6,980	40	*	0.3	no	12	8,700	802
15	polyethylene	7,450	40	*	0.2	no	12	300	24,800
16	polyethylene	4,450	40	*	0.2	no	203	150	29,700
17	sand pack	8,100	35	*	0.5	no	0.5	29	279,000

* Since no residual oil was present, F_{rrw} was calculated using the initial core permeability.

k_w with/without S_{or} . Entries 7, 8, 9, 12, and 17 list results for the same gel (0.5% HPAM) but in porous media with no initial oil saturation (i.e., the cores were completely saturated with gel when brine was injected). For these five cases, a larger degree of variation was seen (average

post-gel k_w was $24 \mu\text{d} \pm 20 \mu\text{d}$), compared to that for the first six entries. Even so, the measured post-gel k_w values with no S_{or} were noticeably lower than those cases with a residual oil saturation. Why should permeability to water be higher (i.e., an average of ten times higher) when residual oil is present? To rationalize higher k_w values, several possibilities come to mind. First, brine could breach or fracture through the gel. With residual oil drops dispersed throughout the porous medium, breaking pathways through gel films (that separate oil drops) might be easier than breaking a path through one continuous large block of gel. However, such a breaking mechanism should depend on the pore size: gel breaching should be easier in large pores and very permeable media than in small pores and low-permeability rock. Since we did not see a significant trend for post-gel k_w values as initial core permeability increased (Entries 1-6 in Table 3), this mechanism seemed unlikely.

A second conceivable mechanism is that brine could force a pathway between the gel and the walls of the porous media. However, for this mechanism, the ability to form a pathway (i.e., higher k_w values) should be enhanced with (1) increased initial permeability (i.e., decreased rock-gel surface area) and (2) increased hydrophobic nature of the rock surface. Since these trends were not observed (Table 3), this mechanism also seemed unlikely.

The remaining mechanism is that water dominantly forces a pathway between the gel and the residual oil. Additional thought is needed to test whether this mechanism is viable.

k_w versus Polymer Content. In previous work with Cr(III)-acetate-HPAM gels,^{14,31} experimental results suggested that the inherent permeability of the gel to water (k_{gel} in μd) varied inversely with the third power of polymer concentration (C in %).

$$k_{gel} = 125 / C^3 \dots\dots\dots(4)$$

An important part of our current approach to optimizing disproportionate permeability reduction involves controlling the inherent permeability of the gel to water. So, we have begun investigating the performance of gels as a function of polymer content.

Entries 9 through 11 list k_w values for three Berea cores that were saturated with three different compositions of Cr(III)-acetate-HPAM gel, with HPAM concentrations of 0.5%, 0.4%, and 0.3%, respectively. The cores had the same dimensions and were cut from the same slab of Berea sandstone, but interestingly, the initial rock permeabilities (before gel placement) varied from 40 to 274 md. We should mention one “trick” to ensuring that pore-filling Cr(III)-acetate-HPAM gels form in Berea sandstone. That trick involved flushing the cores with a few pore volumes of brine containing 0.12% Cr(III) acetate before injecting the gelant. This saturates chromium adsorption sites and minimizes depletion of chromium from the gelant during placement. Prior to using this procedure, we often had problems with incomplete gel formation in Berea sandstone.

During brine injection (at 58 psi/ft) after gelation, post-gel k_w values were 10 μd , 19 μd , and 55 μd , respectively. For the gel with 0.5% HPAM, the 10- μd value (Entry 9) was similar to the 15- μd and 5- μd values associated with Entries 7 and 8—indicating a reasonable degree of reproducibility for the results. However, these values were substantially lower than the 1,000- μd value predicted from Eq. 4. On the other hand, if we accept the 10- μd value for the gel with 0.5%

HPAM, the post-gel k_w values for Entries 10 and 11 were consistent with the cubic relation of Eq. 4 between polymer concentration and inherent gel permeability. In particular, for Entries 9-11, k_w values of 10 μd , 19 μd , and 55 μd were observed, while Eq. 4 predicted values of 10 μd , 19 μd , and 46 μd (if 10 μd was accepted as correct for the 0.5%-HPAM case).

For Cr(III)-acetate-HPAM gels with 0.3% HPAM, post-gel k_w was 3,200 μd in a 8,230-md polyethylene core (Entry 13 in Table 3) and 8,700 μd in a 6,980-md polyethylene core (Entry 14). For comparison, post-gel k_w was 60 μd for a Cr(III)-acetate-HPAM gel with 0.5% HPAM in a similar core (Entry 12). Eq. 4 predicts an inherent gel permeability of 1,000 μd for gel with 0.5% HPAM and 4,630 μd for gel with 0.3% HPAM. The prediction from Eq. 4 was of the correct order for the gel with 0.3% HPAM, but was 17 times too high for the gel with 0.5% HPAM. On the other hand, it is possible that a gel did not fill all the aqueous pore space for the cases with Entries 13 and 14. As polymer concentration decreases, the certainty of creating a pore-filling gel decreases. If gel did not fill all aqueous pore space, a higher permeability was expected.^{25,26}

Two experiments were performed using Cr(III)-acetate-HPAM gels with 0.2% HPAM in polyethylene cores (Entries 15 and 16 in Table 3). For these cases, the post-gel k_w values were 300 μd and 150 μd , respectively. For comparison, Eq. 4 predicts a post-gel k_w value of 15.6 md for this gel composition. It is interesting that the gels with 0.2% HPAM provided lower post-gel k_w values than those for gels with 0.3% HPAM. We suspect this discrepancy was related to some unknown experimental factor that compromised gel formation for the gels with 0.3% HPAM. However, additional work will be performed to resolve this issue.

Another part of the discrepancy between the post-gel k_w values in Table 3 could be tied to differences in porosity of the porous media. In particular, Eq. 4 was based on flow through solid pieces of gel—i.e., 100% porosity with no rock. Except for the cases with residual oil, post-gel k_w values generally increased with increased porosity. Nonetheless, additional work is needed to establish how gel permeabilities vary with polymer concentration.

Stability of k_w . In the next section, we show that permeability to oil (k_o) after gel placement was a strong function of time and throughput. In contrast, if the gel was not compromised (e.g., by exposure to high pressure gradients), Fig. 90 demonstrates that the post-gel k_w was stable for a substantial period. In particular, for the gel associated with Entry 12 in Table 3, k_w held a value of about 60 μd for over one year during continuous exposure to a pressure gradient of 30 psi/ft at 41°C.

Are F_{rrw} Values High Enough? For radial flow, the residual resistance factor in the water zone should be at least 20 (Fig. 86). Will the results from Table 3 meet this requirement? Excepting Entries 13 and 14, the highest post-gel k_w value was 0.37 md (370 μd). Given the definition of water residual resistance factor (i.e., permeability to water before gel placement divided by permeability to water after gel placement), F_{rrw} will be ≥ 20 if the permeability to water before gel placement is greater than 7.4 md (i.e., 20×0.37). Many engineers and geologists (including me) believe that if a productive oil reservoir has a matrix permeability below 20 md, fractures or fracture-like features probably play a major role in allowing fluid to flow to the wells. Consequently, these gels would provide acceptable F_{rrw} values for radial flow applications.

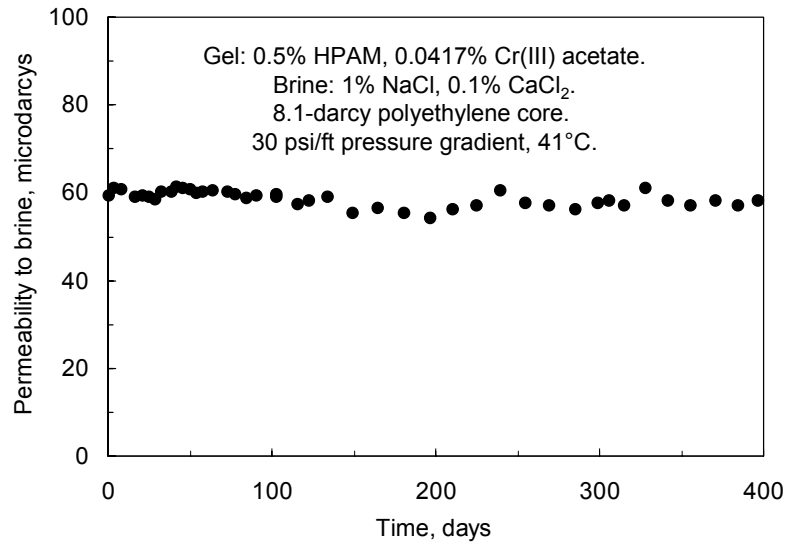


Fig. 90— k_w after gel placement versus time.

For Entry 13, the post-gel k_w was 3.2 md. To achieve $F_{rrw} > 20$ requires that the permeability to water before gel placement be greater than 64 md. For Entry 14, the post-gel k_w was 8.7 md. To achieve $F_{rrw} > 20$ requires that the permeability to water before gel placement be greater than 174 md. These requirements will be met in many, but not all reservoirs.

When treating fractures using the concept illustrated in Fig. 88, will the post-gel k_w values from Table 3 be satisfactory? The degree of productivity impairment (q/q_o) for flow into a fracture can be estimated using Eq. 5:

$$q/q_o \approx L_e / (F_{rr} L_p + L_e), \dots\dots\dots (5)$$

where L_p is the distance of polymer or gelant leakoff from the fracture face and L_e is the effective external drainage distance (roughly half the distance between two wells). Consideration of Eq. 5 reveals that reducing water productivity index by at least 50% requires that $F_{rrw} L_p \geq L_e$. If L_e is 500 ft, F_{rrw} must be at least 50 if L_p is 10 ft and at least 500 if L_p is 1 ft. If k_w after gel placement is 0.37 md (Table 3), a F_{rrw} value of at least 50 can be achieved if k_w before gel placement is at least 18.5 md (i.e., 50×0.37 md). A F_{rrw} value of at least 500 can be attained if k_w before gel placement is at least 185 md (i.e., 500×0.37 md).

These calculations reveal that gels can achieve beneficial reductions in water productivity for both linear and radial flow problems. However, they will not be effective in all situations. Effective applications require attention to ensure that the distance of gelant penetration is adequate for rock of a given permeability. For example, many West Texas fractured dolomite reservoirs have rock permeability around 10 md. If a gel provides a k_w after gel placement of 0.24 md (average of Entries 1-6 in Table 3), a fairly large gelant leakoff distance would be needed (i.e., > 10 ft) to reduce water productivity by more than 50%. Large gelant leakoff distances present challenges—especially with respect to penetration of high molecular weight

polymers into tight rock. Different gel formulations—e.g., using higher concentrations of lower molecular weight polymers—may require consideration for these applications.

Permeability to Oil after Gel Placement

Of course, the key to utilizing disproportionate permeability reduction is to identify conditions where a polymer or gel will reduce permeability to water much more than that to hydrocarbon. In the previous section, we were concerned with whether water residual resistance factors (F_{rrw}) were sufficiently high. In this section, we examine whether oil residual resistance factors (F_{rro}) can be sufficiently low. We also investigate how fast oil zones can regain permeability when oil is injected after gel placement.

Concepts from Previous Work. Previous work^{19,32,33} revealed that gels can dehydrate during oil injection, thus causing disproportionate permeability reduction. Although oil cannot enter or flow through the gel matrix, pressure applied by the oil forces water to flow through and out from the gel. In locations where the gel has been compressed and dehydrated, oil forms “fingers” or “wormhole” pathways (Fig. 91). These oil wormholes grow with time (and the entire gel structure continues to dehydrate with time under pressure), resulting in a gradual increase in permeability to oil. (Note the solid circles in Fig. 89.)

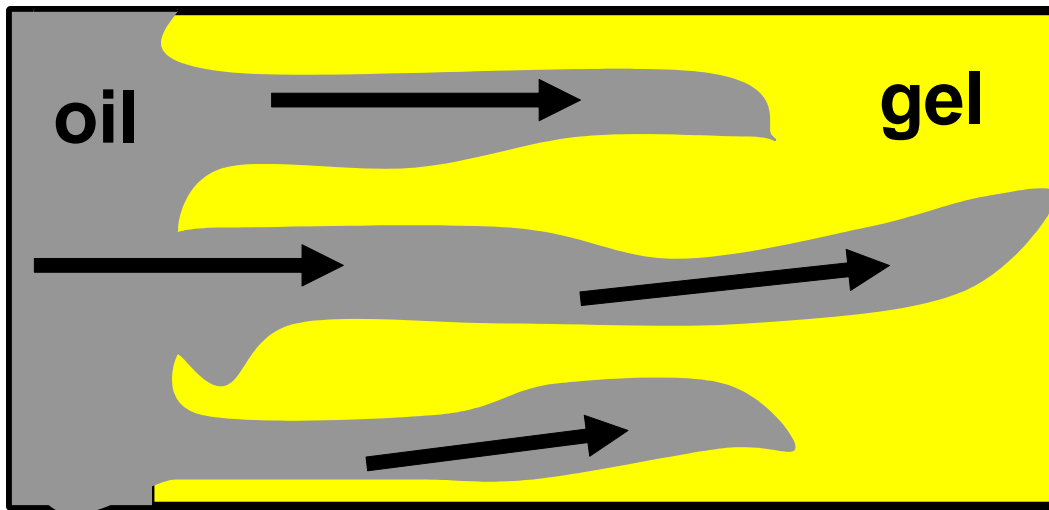


Fig. 91—Oil forming wormholes through gel.

This time- and throughput-dependent behavior during oil flow through gel-filled cores has important consequences with respect to the time required for wells to “clean up” or regain oil productivity after a gel treatment.³⁰ For applications where polymers and gelants are placed in production wells without protecting oil zones, the blocking agents necessarily penetrate some distance into the hydrocarbon zones. After the well is returned to production, oil can force its way through the gel to reach the well, but this process takes time. In particular, the clean up time varies (1) with the cube of the distance of polymer or gelant penetration from the well, (2) inversely with pressure drawdown, and (3) inversely with k_w in the gel-treated region.³⁰

This last finding (i.e., that clean up time varies inversely with k_w in the gel-treated region) inspired our current approach to optimizing disproportionate permeability reduction. A high k_w value is desired to allow rapid dehydration and clean up of gel-treated areas during hydrocarbon flow. In contrast, a low k_w value is desired to restrict flow from the water zones. Thus, an optimum k_w value may be needed to optimize disproportionate permeability reduction.

Experimental Results during Oil Injection. For many of the experiments described in Table 3, oil (hexadecane for Entries 1-6 and 14-16; and Soltrol 130™ for Entries 7-13 and 17) was injected after gel placement and determination of k_w . The apparent permeability to oil (k_o) for these experiments are summarized in Table 4 and are detailed in Figs. 92 through 105. The open circles in these figures show individual data points, while the solid curves indicate results from regressions. Equations and correlation coefficients from the regressions are also shown.

Table 4—Ultimate k_o and F_{rro} during oil flow after gel placement.

Entry	Core material	Initial k , md	k_o at S_{wr} before gel, md	HPAM in gel, %	Final k_o , md	Final F_{rro}	Final F_{rrw}/F_{rro}
1	Berea	746	508	0.5	105	4.8	147
4	polyethylene	6,400	6,400	0.5	515	12.4	1,210
5	polyethylene	9,530	9,530	0.5	531	17.9	1,363
6	polyethylene	15,270	11,410	0.5	637	17.9	983
7	Berea	356	242*	0.5	209	1.2	19,800
8	Berea	389	265*	0.5	ongoing		
9	Berea	100	68*	0.5	16.8	4.0	2,500
10	Berea	40	27.2*	0.4	13.4	2.0	1,050
11	Berea	274	186*	0.3	110	1.7	2,930
13	polyethylene	8,230	8,230**	0.3	1,320	6.2	415
14	polyethylene	6,980	6,980**	0.3	2,640	2.6	308
15	polyethylene	7,450	7,450**	0.2	ongoing		
16	polyethylene	4,450	4,450**	0.2	92	48	619
17	sand pack	8,100	8,100**	0.5	1,840	4.4	63,400

* Estimate based on Entry 1. ** Estimate based on Entries 4 and 5.

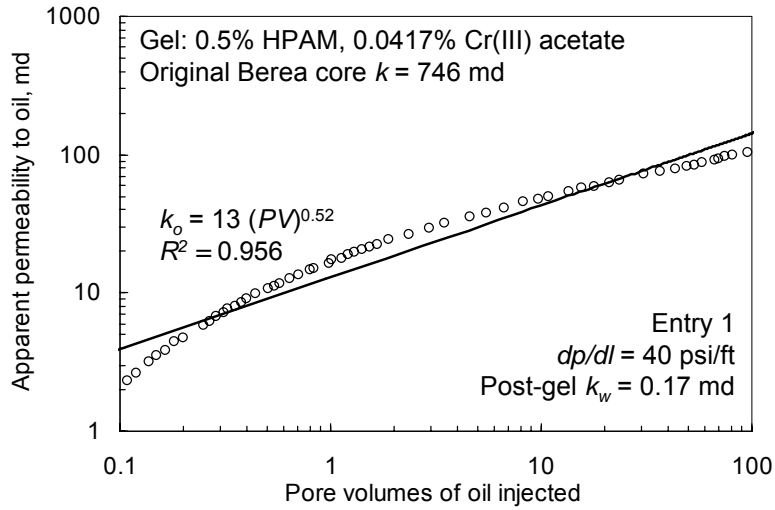


Fig. 92— k_o versus pore volume for Entry 1 in Tables 3 and 4.

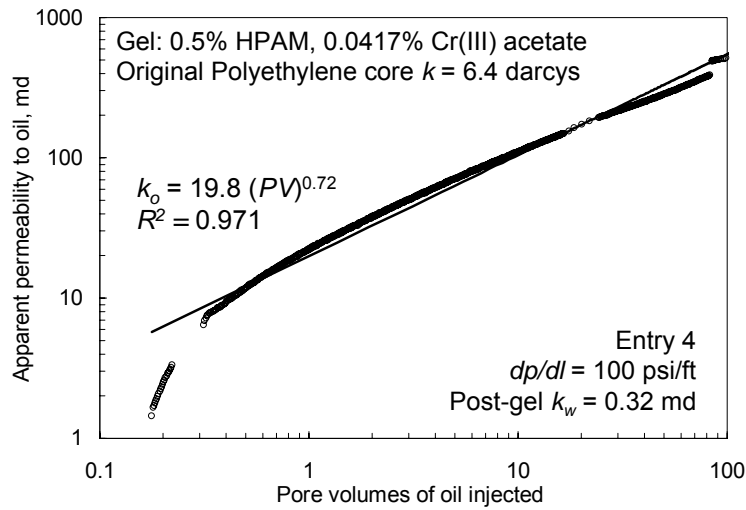


Fig. 93— k_o versus pore volume for Entry 4 in Tables 3 and 4.

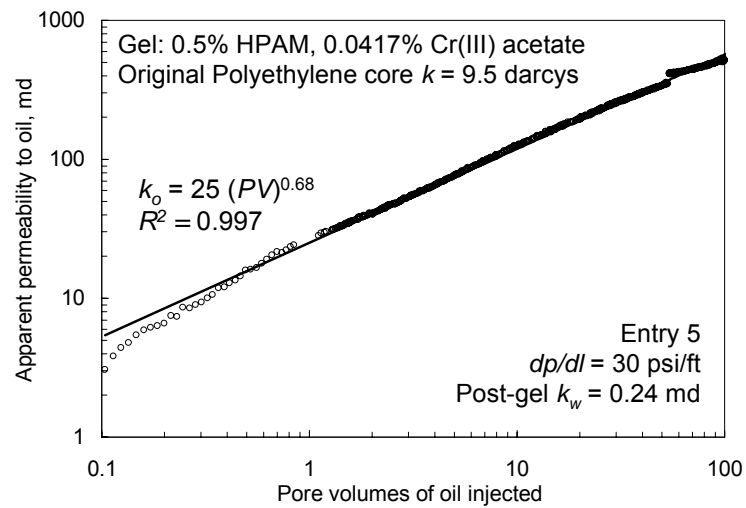


Fig. 94— k_o versus pore volume for Entry 5 in Tables 3 and 4.

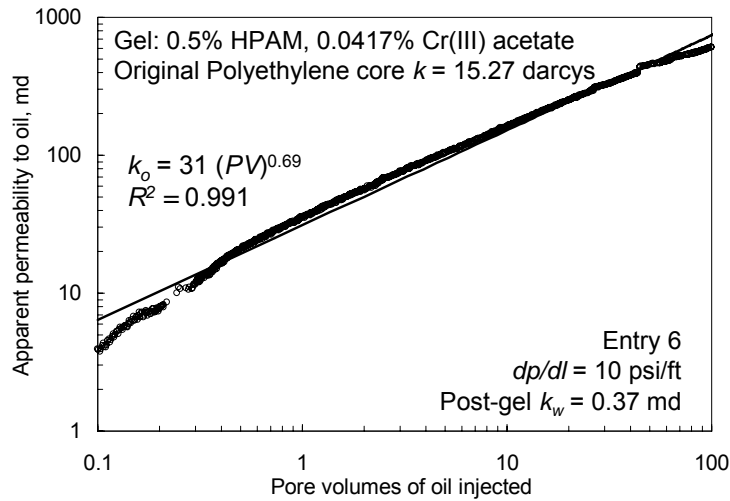


Fig. 95— k_o versus pore volume for Entry 6 in Tables 3 and 4.

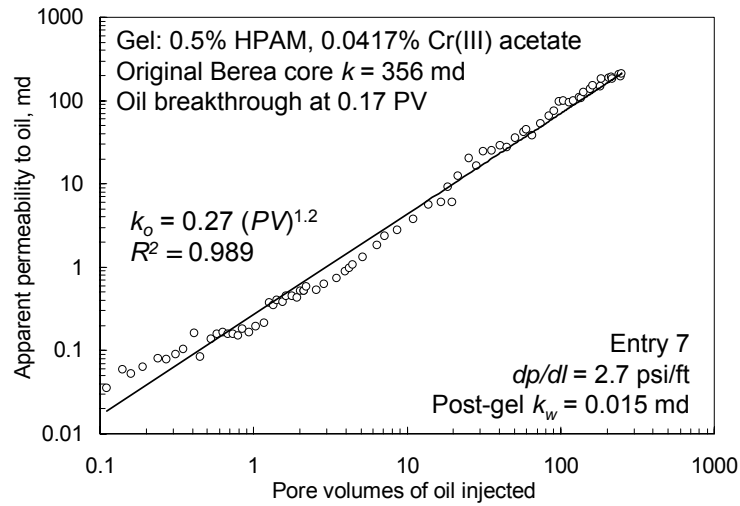


Fig. 96— k_o versus pore volume for Entry 7 in Tables 3 and 4.

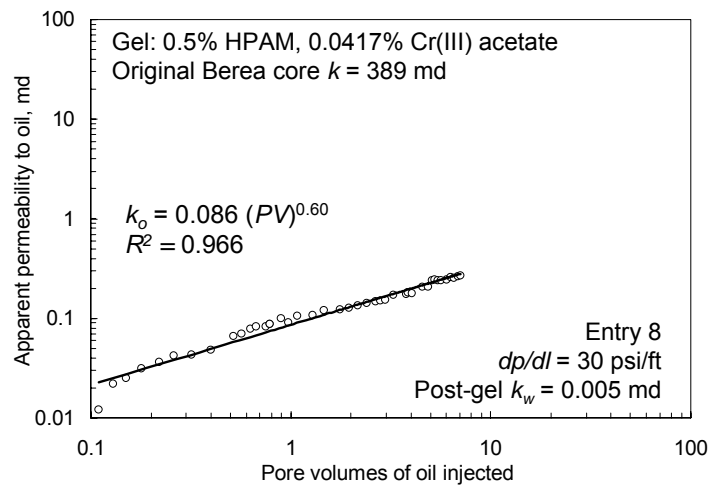


Fig. 97— k_o versus pore volume for Entry 8 in Tables 3 and 4.

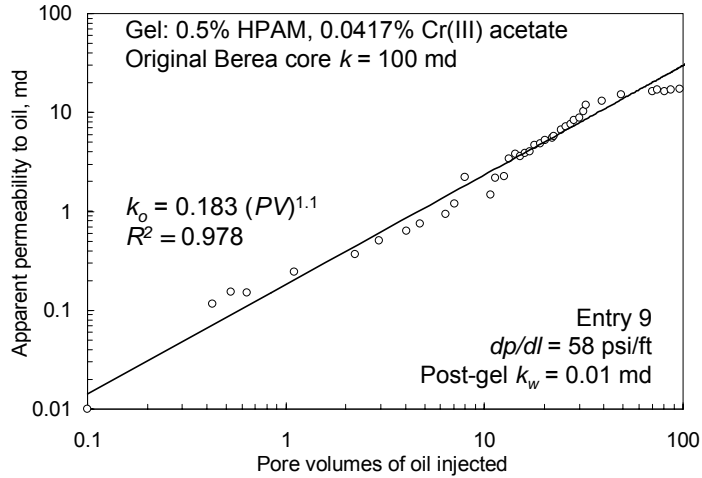


Fig. 98— k_o versus pore volume for Entry 9 in Tables 3 and 4.

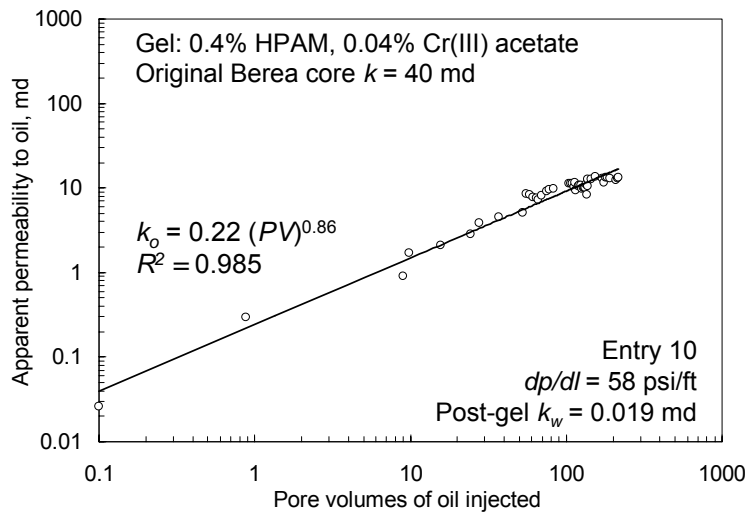


Fig. 99— k_o versus pore volume for Entry 10 in Tables 3 and 4.

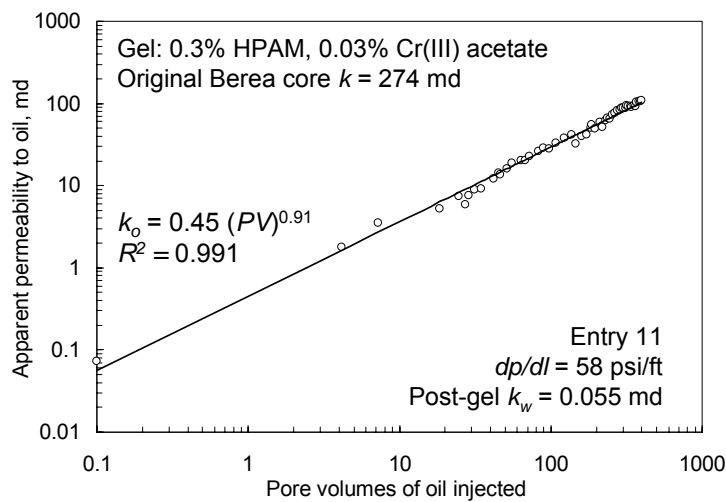


Fig. 100— k_o versus pore volume for Entry 11 in Tables 3 and 4.

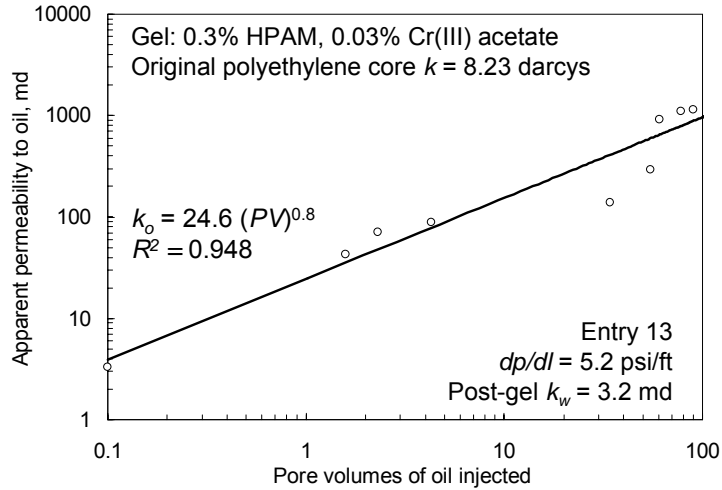


Fig. 101— k_o versus pore volume for Entry 13 in Tables 3 and 4.

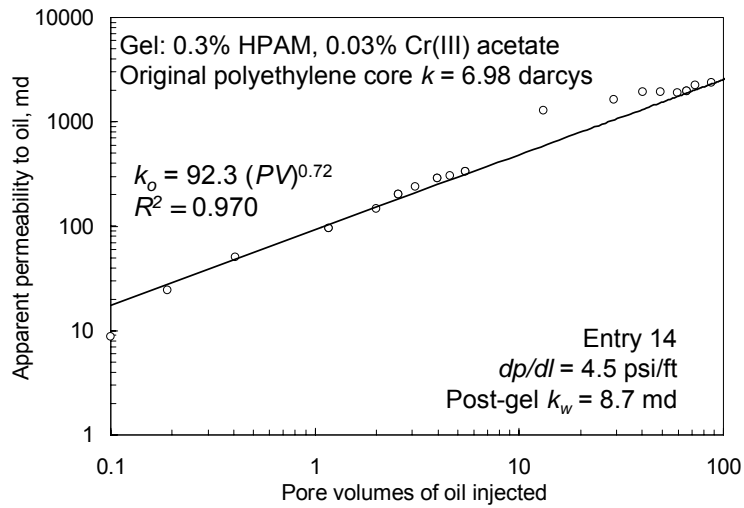


Fig. 102— k_o versus pore volume for Entry 14 in Tables 3 and 4.

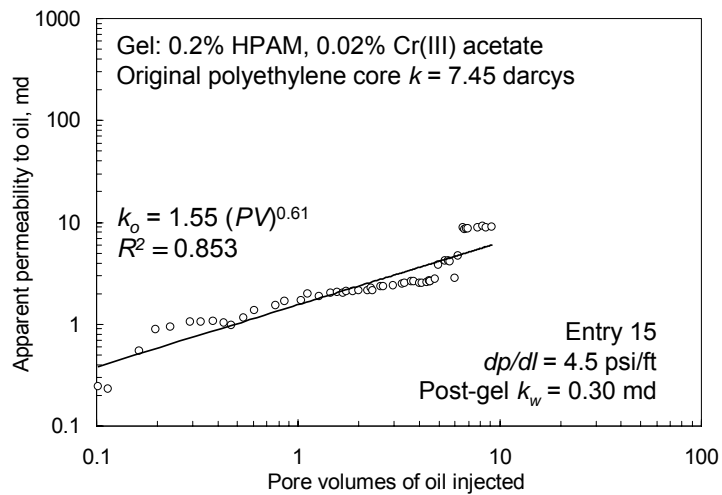


Fig. 103— k_o versus pore volume for Entry 15 in Tables 3 and 4.

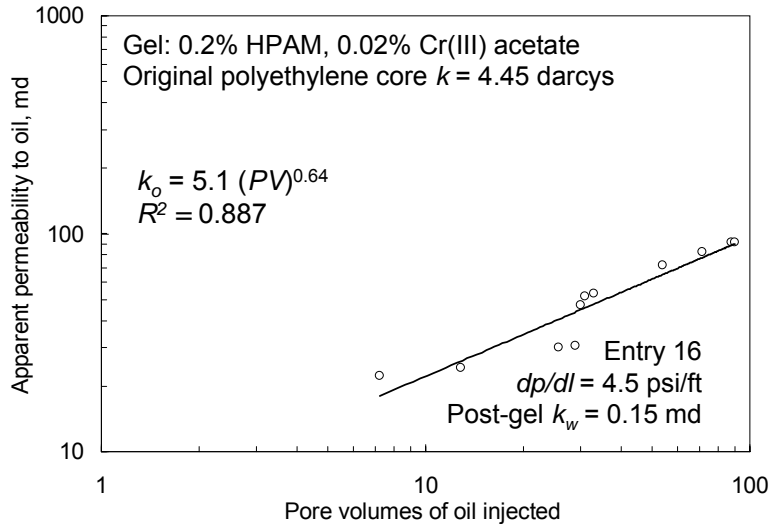


Fig. 104— k_o versus pore volume for Entry 16 in Tables 3 and 4.

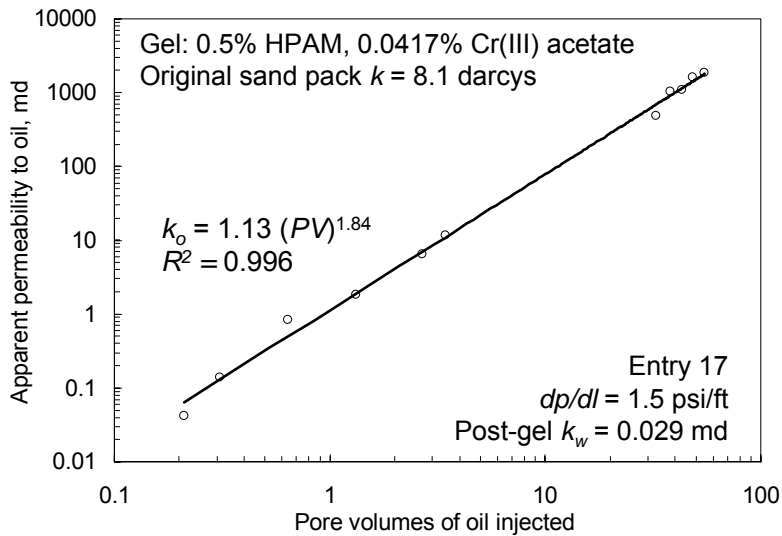


Fig. 105— k_o versus pore volume for Entry 17 in Tables 3 and 4.

In Figs. 92-105, k_o increased with PV throughput raised to a power between 0.52 and 1.2—averaging 0.8. (The sand pack results from Fig. 105 provided a notable exception.) The multiplier coefficient estimates k_o at one PV of oil throughput. For the very permeable polyethylene cores (4.45 to 15.27 darcys) and gels with 0.5% HPAM, the multiplier coefficient ranged from 19.8 to 31 md. For Berea sandstone, the multiplier ranged from 0.086 md for the 389-md core in Fig. 97 to 13 md for the 746-md core in Fig. 92. The reader should be cautioned not to extrapolate the regression results too far since the k_o values necessarily cannot exceed the pre-treatment k_o value.

Are F_{rro} Values Low Enough? With radial flow, oil residual resistance factors must be less than 2 to mitigate damage caused by polymer or gel to oil productive zones. Can F_{rro} values this low be attained using pore-filling Cr(III)-acetate gels? The sixth and seventh columns in Table 4 list

the final k_o and F_{rro} values for each case. Typically, these values were measured after over 100 PV of oil were injected. The lowest F_{rro} value was 1.2. We found three cases where gels provided water residual resistance factors greater than 2,100 and ultimate F_{rro} values of 2 or less (see Entries 7, 10, and 11 in Tables 3 and 4). These three cases used gels with 0.3% to 0.5% HPAM. As noted above, F_{rro} must be less than 2 for radial flow treatments where hydrocarbon zones are not protected during gel placement. So, our recent results provide hope that our current approach will identify a gel that can successfully and reliably treat either fractured or unfractured production wells without zone isolation.

For linear flow applications (wells that intersect fractures), our main requirement was that the gel reduce permeability to water much more than that to oil. The last column in Table 4 lists the ratio, F_{rrw} / F_{rro} . These ratios range from 147 to 63,400. The lowest ratio occurred in Berea sandstone, while the highest ratio was noted for the sand pack. These values would be very acceptable for applications in very permeable media. Unfortunately, fractures and fracture-like features are less likely to present channeling problems as the permeability of the media increases. The greatest need for high F_{rrw} / F_{rro} ratios exists in tight rock. As mentioned earlier, if the F_{rrw} value is too low when treating a fracture, the gelant must leakoff a substantial distance from the fracture faces. In addition to the expense of requiring large gelant volumes, this situation may be limiting because many polymer-based gelants cannot penetrate into tight rock.²⁹ On a positive note, the case for Entry 10 (using gel with 0.4% HPAM in 40-md Berea) exhibited $F_{rrw} = 2,110$, $F_{rro} = 2.0$, and $F_{rrw} / F_{rro} = 1,050$. These values would be quite acceptable for applications in either fractured or unfractured wells. Since they were measured in 40-md rock, we see hope that our approach will identify a gel that can successfully and reliably treat either fractured or unfractured production wells without zone isolation.

How Fast Will Oil Zones Clean Up? In Ref. 30, a means was described to use the data in Figs. 92-105 to predict how rapidly productivity can be restored to an oil zone that was invaded by a polymer or gel. For both linear and radial flow, clean up time varied with the cube of distance of gelant penetration (L_p^3). For cases with a pressure drawdown (Δp) of 100 psi and a k_w value of 0.26 md, the clean up time (t) followed Eq. 6.

$$t = 0.0006 L_p^3 \dots\dots\dots(6)$$

In this equation, t is the time for a gel-treated zone to regain half of its final productivity. Clean up time also varied inversely with pressure drawdown and k_w in the gel-treated region. With this information, Eq. 6 can be modified to Eq. 7.

$$t = 0.0156 L_p^3 / (k_w \Delta p), \dots\dots\dots(7)$$

where t has units of days, L_p is in ft, k_w is in md, and Δp is in psi. Fig. 106 illustrates Eq. 7 for the case where k_w is 0.24 md. For moderate to high pressure drawdown (i.e., >100 psi), clean up times were reasonably short if the distances of gelant penetration were not large (i.e., <10 ft).

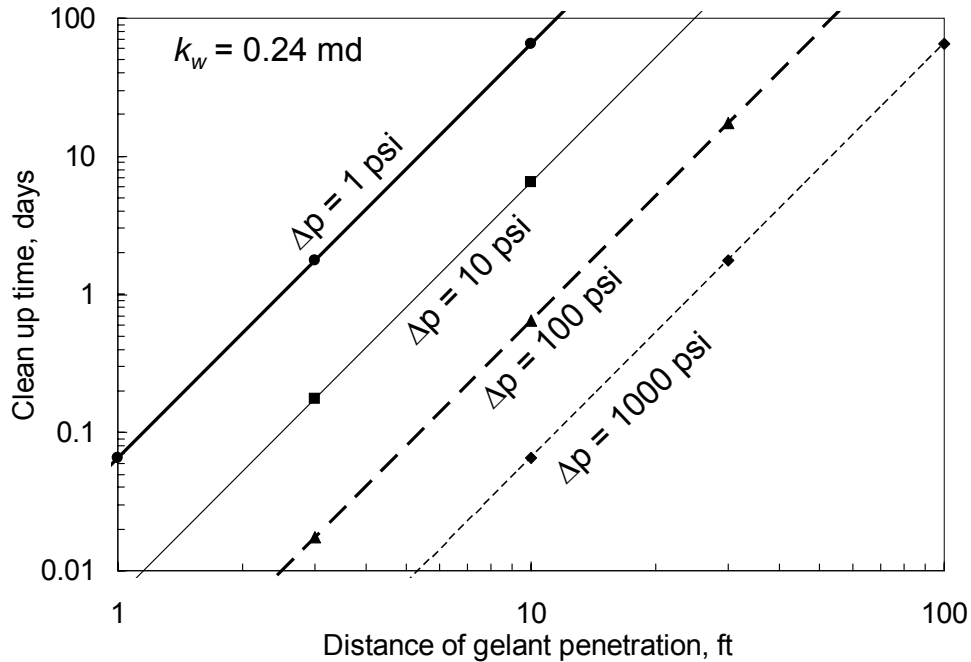


Fig. 106—Clean up times for the case where $k_w = 0.24$ md.

Second Water Flow after Oil Flow

In several experiments, water was injected again after the oil-flow experiments described in Table 4 and in Figs. 92-105. In all cases, the permeability to water stabilized quite quickly. Column 6 in Table 5 lists k_w values for these experiments. The last column in Table 5 converts the k_w values to water residual resistance factors. (For Entries 7 and 9-17, the initial core permeability to water was used when calculating F_{rrw} values because k_w values were not measured at S_{or} before gel placement.) For Entries 1, 4, and 5 in Table 5, the second k_w values were around 1 md. These values were higher than the first k_w values after gel placement (~ 0.24 md from Table 3), but were still very low relative to the k_o values (Table 4). An explanation for this behavior was provided in Refs. 32 and 33. (The explanation involves trapping of high residual oil saturations.)

For Entries 9-17 in Table 5, the second F_{rrw} values were between 100 and 30,000 times less than the values before oil injection (compare with the last column of Table 3). Thus, extended oil injection caused substantial damage to the gel for these cases. Interestingly, this damage was much less severe for the cases associated with Entries 1, 4, and 5, where residual oil was present during gel placement. For Entries 1, 4, and 5, the second F_{rrw} values were between two and seven times less than the values measured before oil injection. Additional work is needed to establish whether the presence of residual oil during gel placement was causally related to these differences.

The results in this section (i.e., for water flow following both gel placement and subsequent oil flow) are generally more of academic interest than of practical interest. After a polymer or gel treatment has been applied, brine is the first flowing fluid to contact the polymer or gel in the water zones, so the results from our "Permeability to Water after Gel Placement" section are of

direct practical interest. Similarly, oil is the first flowing fluid to contact the polymer or gel in the oil zones, so the results from our “Permeability to Oil after Gel Placement” section are also of direct practical interest. The results from this current section could have practical application only if an oil zone becomes watered out after being treated by a polymer or gel.

Table 5—Ultimate k_w and F_{rrw} during the second water flow after gel placement.

Entry	Core material	Initial k_w , md	k_w at S_{or} before gel, md	HPAM in gel, %	2nd k_w , md	2nd F_{rrw}
1	Berea	746	120	0.5	1.11	108
4	polyethylene	6,400	4,810	0.5	0.74	6,500
5	polyethylene	9,530	5,860	0.5	1.17	5,008
6	polyethylene	15,270	6,500	0.5	106	61.3
7	Berea	356	*	0.5	42	8.5
8	Berea	389		0.5	ongoing	
9	Berea	100	*	0.5	2.5	40
10	Berea	40	*	0.4	2.4	16.7
11	Berea	274	*	0.3	18.5	14.8
13	polyethylene	8,230	*	0.3	1,000	8.2
14	polyethylene	6,980	*	0.3	1,430	4.9
15	polyethylene	7,450	*	0.2	ongoing	
16	polyethylene	4,450	*	0.2	23.3	191
17	sand pack	8,100	*	0.5	850	9.5

* Since no residual oil was present, F_{rrw} was calculated using the initial core permeability.

After measuring k_w values for Entries 9, 10, and 11 in Table 5 (Berea sandstone cores), distilled water was injected to determine whether the gel can be swelled—thus reducing permeability to water. Very shortly after the start of injecting distilled water, k_w values dropped from 2.5 to 0.84 md for Entry 9, from 2.4 to 1.8 md for Entry 10, and from 18.5 to 4.1 md for Entry 11. We cannot discount the possibility that these permeability reductions were caused by clay swelling in these Berea cores. However, in separate experiments where gel was not present, we observed no clay swelling when distilled water flowed through our Berea sandstone. Therefore, we suspect that during the gel experiments, the reduced k_w values resulted from swelling of the gel in the presence of distilled water. After distilled water, we re-injected brine with 1% NaCl and 0.1% CaCl₂. The k_w values rose from 0.84 to 2.4 md for Entry 9, from 1.8 to 2.9 md for Entry 10, and from 4.1 to 15.1 md for Entry 11. Thus, contact with brine appears to have reversed the swelling caused by the distilled water. During the final cycle of distilled water injection, k_w values decreased from 2.4 to 0.83 md for Entry 9, from 2.9 to 1.4 md for Entry 10, and from 15.1 to 4.1 md for Entry 11.

Because of a concern that the above swelling and shrinking behavior may have been caused by clays in the Berea, a separate experiment was performed in a polyethylene core (Fig. 107). This

core had an initial permeability of 10.75 darcys and was saturated with a gel containing 0.25% HPAM, 0.025% Cr(III) acetate, 1% NaCl, 0.1% CaCl₂. All injection steps were performed at 41°C using a pressure gradient of 12 psi/ft. After gelation, 130 PV of brine (1% NaCl, 0.1% CaCl₂) was injected, resulting in an average permeability of 2,830 md. Next, 67 PV of distilled water were injected. The permeability immediately dropped and leveled at a value averaging 345 md. Then, 30 PV of brine were injected, resulting in an immediate permeability increase to 3,920 md. Finally, 30 PV of distilled water were injected, and permeability dropped to 1,990 md. These results strongly suggest gel swelling, restriction of pore pathways, and permeability reduction during injection of distilled water. They also suggest gel shrinking, opening of pore flow pathways, and permeability increase during injection of brine. In all cases, the permeability changed rapidly and stabilized when the injection fluid was switched. Since no clays or other minerals were present, the observations must be attributed to the gel. We noted that the permeability was higher during the second cycle of brine injection than during the first cycle (3,920 md versus 2,830 md). Similarly, the permeability was higher during the second cycle of distilled water injection than during the first cycle (1,990 md versus 345 md). This result suggests some gel degradation through the injection cycles.

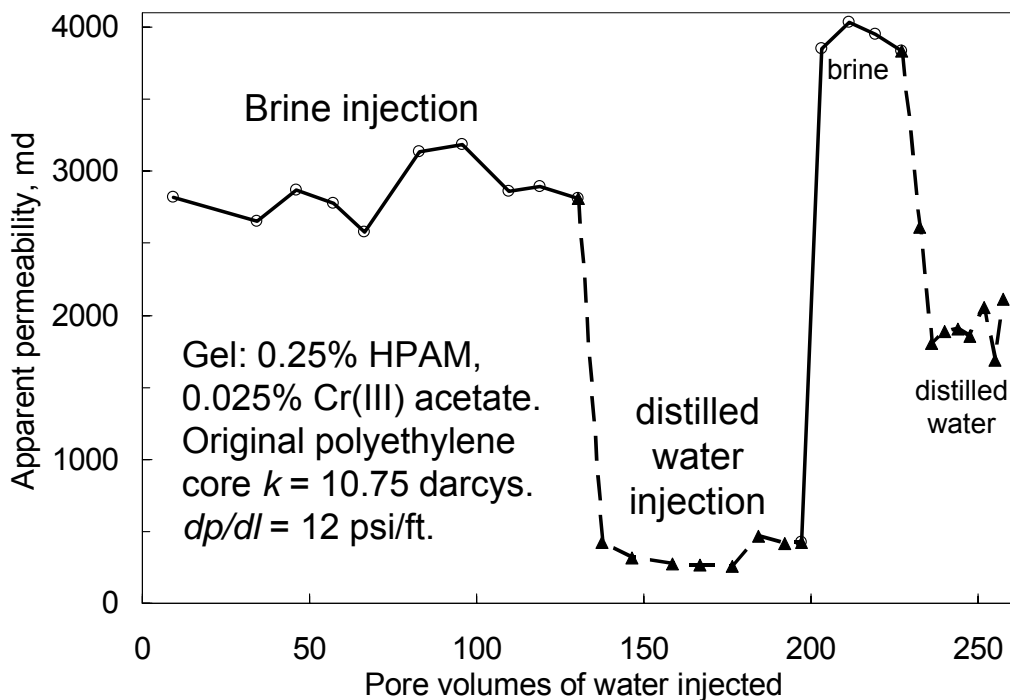


Fig. 107—Apparent gel swelling and shrinking in a polyethylene core.

Summary

Although some polymers and gels reduce permeability to water more than to oil, several factors currently limit widespread field applications of this property. First, adsorbed polymers, “weak” gels, and suspensions of gel particles show large variations in performance. Second, in unfractured wells (i.e., radial flow into porous sand or rock), the oil residual resistance factor, F_{rro} , (permeability reduction factor) must be reliably less than 2. Third, adsorbed polymers,

“weak” gels, and particle suspensions reduce permeability by greater factors in low-permeability rock than in high-permeability rock. We are investigating pore-filling gels to overcome these limitations, beginning with Cr(III)-acetate-HPAM gels. For porous media at residual oil saturation with initial permeability to water (k_w) ranging from 120 to 6,500 md, a Cr(III)-acetate-HPAM gel (with 0.5% HPAM) consistently reduced k_w to 240 μ d (± 84 μ d). For porous media with initial k_w values ranging from 100 to 8,100 md (0.5% HPAM, no residual oil), the gel reduced k_w to 24 μ d (± 20 μ d). Thus, pore-filling gels can provide greater reliability and behavior that is insensitive to the initial rock permeability.

With sufficient oil throughput, pore-filling gels can be dehydrated, thus increasing permeability to oil. We found three cases where gels provided water residual resistance factors greater than 2,100 and ultimate F_{rro} values of 2 or less. As noted above, F_{rro} must be less than 2 for radial flow treatments where hydrocarbon zones are not protected during gel placement.

For linear flow (wells that intersect fractures), F_{rro} values for pore-filling gels are sufficiently low, and F_{rrw} values are adequate for applications in moderate to high-permeability rock (>100 md). However, higher F_{rrw} values are needed for applications in low-permeability rock. In one case in 40-md Berea, a gel with 0.4% HPAM exhibited $F_{rrw} = 2,110$, $F_{rro} = 2.0$, and $F_{rrw}/F_{rro} = 1,050$. These values would be quite acceptable for applications in either fractured or unfractured wells. Since they were measured in 40-md rock, we see hope that our approach will identify a gel that can successfully and reliably treat either fractured or unfractured production wells without zone isolation.

5. REHYDRATION OF GEL IN FRACTURES

Review of Gel Extrusion Behavior

Formed gels (i.e., the product from gelation) can be extruded through fractures. Although some gels exhibit progressive plugging (or “screen outs”) during this extrusion process, other gels can be formulated to extrude with stable pressure gradients (i.e., no progressive plugging).^{8,34,35} When gels extrude through fractures, they dehydrate to some extent. Specifically, water is squeezed out from the gel and leaks off through the fracture faces. In contrast, the crosslinked polymer remains in the fracture—becoming increasingly concentrated with time and retarding movement of the gel front through the fracture.^{8,35} Dehydrated gel in the fracture is frequently 20 times more concentrated than the injected gel, and can be over 50 times more concentrated.^{8,35}

When gel dehydrates, its mobility becomes less than that of the original gel. Consequently, gel of the original or injected concentration forms “finger” or “wormhole” pathways through the less mobile dehydrated gel.^{8,35} In fact, gel of the original injected concentration is virtually the only mobile gel in the fracture. Near the end of the gel placement process, the fracture is filled (1) mostly with concentrated gel that is difficult to mobilize and (2) relatively mobile gel of the injected concentration that resides in wormholes through the concentrated gel.³⁵

When water or oil is injected after gel placement, the wormholes provide the point of failure where gel in the fracture is first breached.^{12,35} These wormholes also provide the dominant pathway for brine flow through the gel-filled fracture. For the most part, the dehydrated gel remains immobile and substantially reduces the flow capacity of the fracture (relative to that for the original open fracture).^{12,35-37}

Do Gels Rehydrate during Brine Flow After Gel Placement?

Since gel was concentrated by large factors during gel extrusion, will these gels swell or rehydrate during water flow after gel placement? Swelling of the concentrated gel should restrict or close the wormhole flow paths during brine injection. However, no evidence of rehydration was noted—i.e., no reduction in core flow capacity was observed—while injecting up to 80 fracture volumes of brine.¹² Also, concentrated gel was removed from a fracture and placed in a vial of brine (10:1 ratio of brine to gel). This gel exhibited no visible swelling over the past seven years.

New Experiments. Three new corefloods were performed to assess the degree of gel rehydration after gel placement in fractures. All cases used 700-md Berea sandstone cores that were 122 cm long, 3.8 cm high, and 3.8 cm wide. In each core, a 1-mm wide fracture was sawed lengthwise down the center of the core. (So the fracture faces were fairly smooth.) The cores had four internal pressure taps that were equally spaced along the fractures, thus dividing each core and fracture into five sections. The outlet end of the core allowed effluent to be simultaneously collected from three locations—from the fracture and from the porous rock on either side of the fracture (see Fig. 108). The cores were cast in epoxy and initially saturated with brine containing 1% NaCl and 0.1% CaCl₂. All flow experiments were performed at 41°C.

After saturation with brine, 4,000 cm³ (~80 fracture volumes) of gel were injected at a rate of 2,000 cm³/hr (equivalent to 4,133 ft/d if all injected fluid flowed only through the fracture).

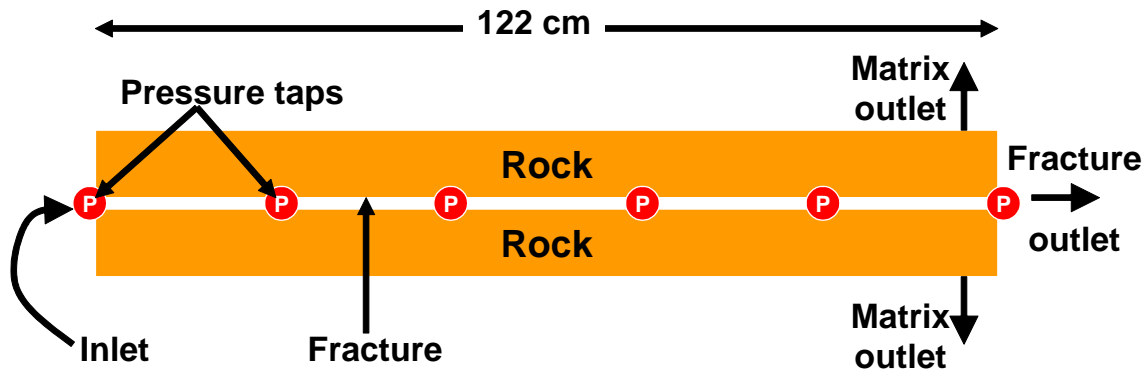


Fig. 108—Top schematic view of a fractured core.

Each coreflood used a different gel composition. All three gels contained 0.5% Alcoflood 935™ HPAM, 1% NaCl, and 0.1% CaCl₂. The HPAM polymer had a molecular weight (Mw) of about 5 million Daltons and a degree of hydrolysis of 5% to 10%. Each of the three gels used a different crosslinker and a different aging time and temperature before injection into a given fractured core. In one experiment, the polymer was crosslinked using 0.0417% Cr(III) acetate (our standard crosslinker), and the gel was aged for one day at 41°C before injection. In a second experiment, the HPAM was crosslinked with 0.25% resorcinol and 0.25% formaldehyde (at pH=9.3), and the gel was aged for two weeks at 60°C before injection (at 41°C). In the third experiment, the polymer was crosslinked with 0.05% polyethyleneimine (Mw=750,000), and the gel was aged for two months at 60°C before injection (at 41°C).

We chose to investigate resorcinol/formaldehyde and polyethyleneimine because they form covalent bonds with HPAM. In contrast, Cr(III) forms *coordinate* covalent crosslinks with the polymer. The covalent bonds are thought to be irreversible, whereas the Cr(III) *coordinate* covalent crosslinks are reversible. Why does this matter? When the Cr(III)-acetate-HPAM gel dehydrates, polymer chains are brought much closer together. If the Cr(III) crosslinks are reversible, the gel structure can be reformed (i.e., crosslinks can be remade) to tie polymer chains into a concentrated state and retard the gel from swelling in the presence of excess brine. In contrast, if the crosslinks are irreversible covalent bonds, the polymer chains should not experience irreversible chemical confinement after dehydration. When excess water is introduced, swelling should occur relatively easily. Our experiments tested these ideas.

During gel injection, pressure gradients averaged 16 psi/ft for the Cr(III)-acetate-HPAM gel, 99 psi/ft for the resorcinol-formaldehyde-HPAM gel, and 11 psi/ft for the polyethyleneimine-HPAM gel. After gel placement, the cores were shut in for one day. The pressure gradients for the Cr(III)-acetate-HPAM gel and polyethyleneimine-HPAM gels were consistent with previous experimental results, whereas the pressure gradient for the resorcinol-formaldehyde-HPAM gel was quite high. We noted that the resorcinol-formaldehyde-HPAM gel had 10-12 times the mass of crosslinker as the other two gels. This may have increased the degree of intermolecular crosslinking and led to a stiffer gel for the resorcinol-formaldehyde-HPAM formulation.

Injecting Large Volumes of Brine Did Not Rehydrate the Gel. After the one-day shut-in, a large volume of brine was injected at a rate of 100 cm³/hr. The brine contained 1% NaCl and 0.1% CaCl₂—the same brine used to prepare the gels. Fig. 109 plots the pressure gradients across the fractures during the first period of brine injection after gel placement. In each case, the pressure gradient rose to a peak—at 0.6 to 1 fracture volume—followed by a decline and stabilization. The peak indicates the pressure gradient where brine first breaches the gel, by displacing relatively mobile gel from the wormholes that remained from the gel placement process. For the Cr(III)-acetate-HPAM, the peak pressure gradient was about 3 psi/ft—significantly less than the 16 psi/ft value that was noted during placement of the gel. In previous work,¹² we often found that the peak pressure gradient during first brine injection was typically around the pressure gradient during gel placement. However, cases like that observed for the Cr(III)-acetate-HPAM gel in Fig. 109 have been observed on occasion.

For the resorcinol-formaldehyde-HPAM, the peak pressure gradient was about 6 psi/ft—substantially less than the 99 psi/ft value that was noted during gel placement. For the polyethyleneimine-HPAM, the peak pressure gradient was about 2 psi/ft—again, significantly less than the 11 psi/ft value that was noted during gel placement.

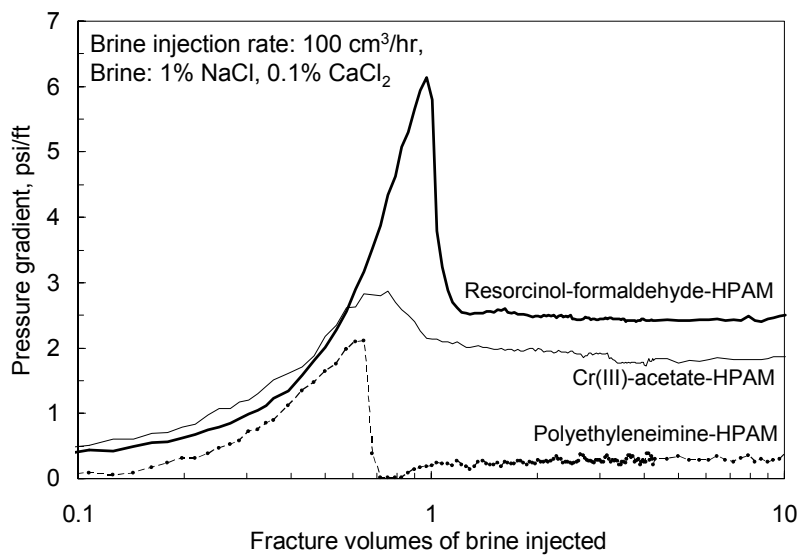


Fig. 109—Pressure gradients during first brine flow after gel placement.

After the peak, the pressure gradients declined and leveled at values around 1.8 psi/ft for the Cr(III)-acetate-HPAM gel, 2.4 psi/ft for the resorcinol-formaldehyde-HPAM gel, and 0.3 psi/ft for the polyethyleneimine-HPAM gel. These pressure gradients indicate that the gels reduced the fracture flow capacities by factors of 7,000, 9,330, and 1,170, respectively.

Fig. 110 plots pressure gradients for the rest of the 200+ fracture volumes of brine injection. These curves show no indication of pressure gradients increasing with increased throughput, no evidence of closure of the wormholes, and therefore, no evidence of gel swelling or rehydration. (Injecting 200 fracture volumes at 100 cm³/hr required about four days.)

Fig. 111 plots the percentage of the injected brine that was produced from the matrix as a function of brine throughput after gel placement. In all cases, before the peak pressure gradient was reached, 100% of the injected brine was produced from the matrix taps (i.e., 0% of the brine was produced from the fracture outlet tap)—indicating that the fracture was completely plugged by gel. After the peak, the percentage of fluid flowing through the fracture was 48% for the Cr(III)-acetate-HPAM gel, 75% for the resorcinol-formaldehyde-HPAM gel, and 96% for the polyethyleneimine-HPAM gel. These values held fairly constant throughout injection of 200+ fracture volumes of brine. Given stabilized brine pressure gradients and flow rates through the fracture after the peaks in Fig. 109, one can calculate effective average wormhole radii, assuming that brine wormholes were tubes of constant radii. These brine wormhole radii averaged 150 μm for the Cr(III)-acetate-HPAM gel, 160 μm for the resorcinol-formaldehyde-HPAM gel, and 290 μm for the polyethyleneimine-HPAM gel.

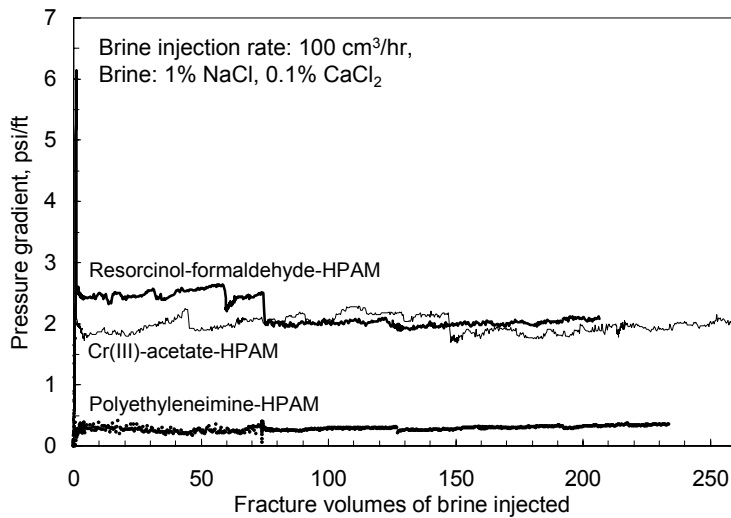


Fig. 110—Pressure gradients during >200 fracture volumes of brine after gel placement.

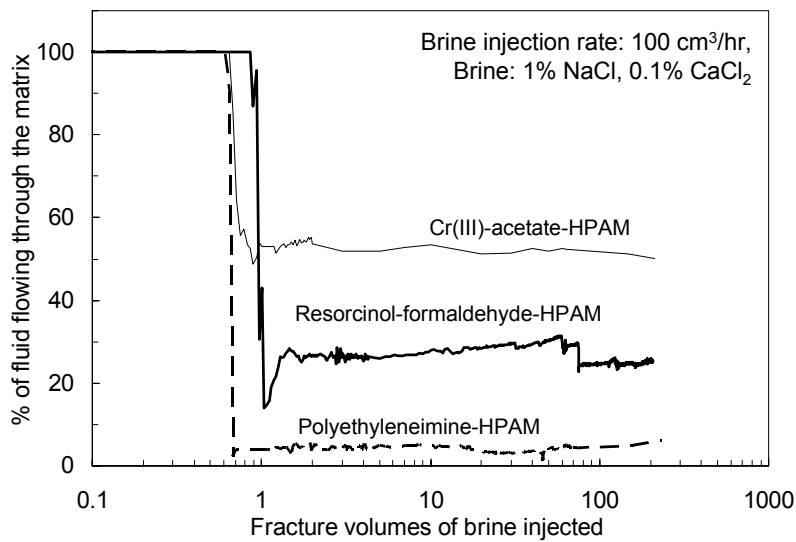


Fig. 111—Percent of brine flowing through the matrix after gel placement.

Injecting Less Saline CaCl₂ Brine Rehydrated the Gel Slowly. Since no rehydration was evident when injecting the brine with 1% NaCl and 0.1% CaCl₂, we examined whether rehydration would occur after injecting brine that contained only 0.1% CaCl₂. This brine was injected into the three fractured cores immediately after obtaining the results shown in Figs. 110 and 111. We did not change immediately to distilled water for fear that distilled water might swell clays and substantially reduce permeability in the Berea sandstone.

Fig. 112 shows pressure gradients during the course of injecting many fracture volumes of the 0.1% CaCl₂ brine. Complementing this figure, Fig. 113 plots the fraction of brine flowing through the porous rock (i.e., the matrix) during injection of the 0.1% CaCl₂ brine. For the Cr(III)-acetate-HPAM gel, the pressure gradient gradually doubled over the course of 300 fracture volumes, then remained stable at about 4.2 psi/ft. At the same time, the fraction of fluid flowing through the matrix gradually increased from 52% to 82.5%. With this information, the effective average radius of a brine wormhole through the gel was estimated to decrease from 150 μm to 97 μm. Thus, some gel swelling occurred, but it required injection of hundreds of fracture volumes of the 0.1% CaCl₂ brine.

For the resorcinol-formaldehyde-HPAM gel, the pressure gradient gradually doubled over the course of 242 fracture volumes, then fell sharply to 1.5 psi/ft. From 0 to 230 fracture volumes, the fraction of fluid flowing through the matrix gradually increased from 25% to 37%. From 230 to 242 fracture volumes, this fraction jumped to 97%, and then suddenly fell to 9.7%. This information suggests that the brine wormhole almost completely closed during injection of the 242 fracture volumes of 0.1% CaCl₂ brine, and then the gel experienced failure (at 5.3 psi/ft) to re-open the wormhole—now, with a new average radius of 190 μm.

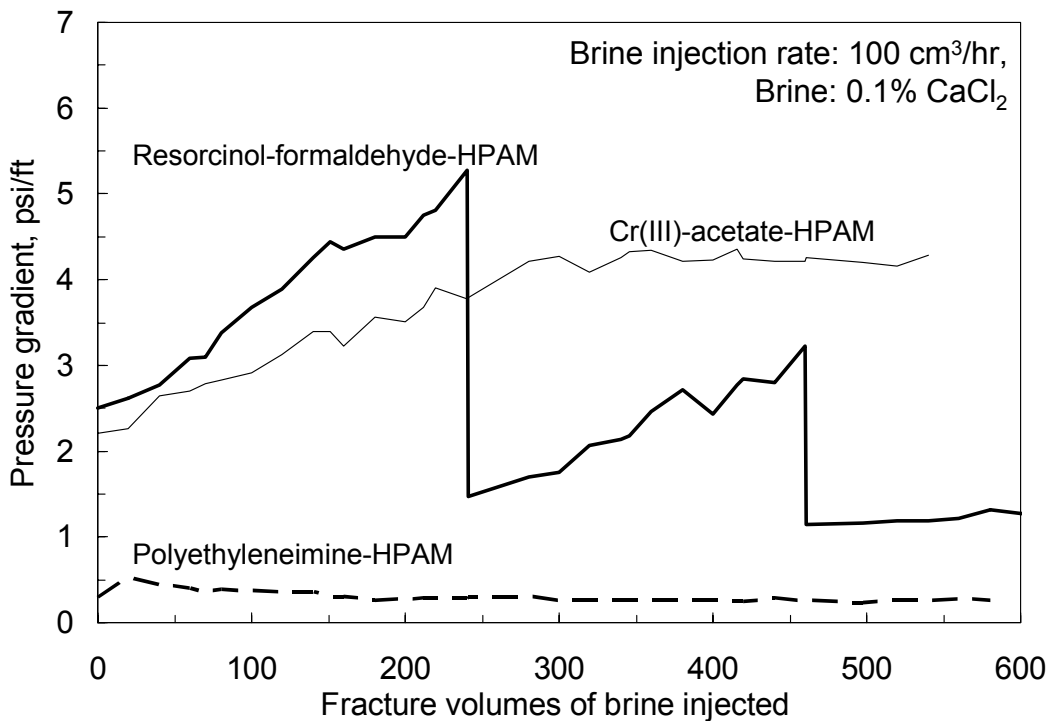


Fig. 112—Pressure gradients during flow of brine with 0.1% CaCl₂.

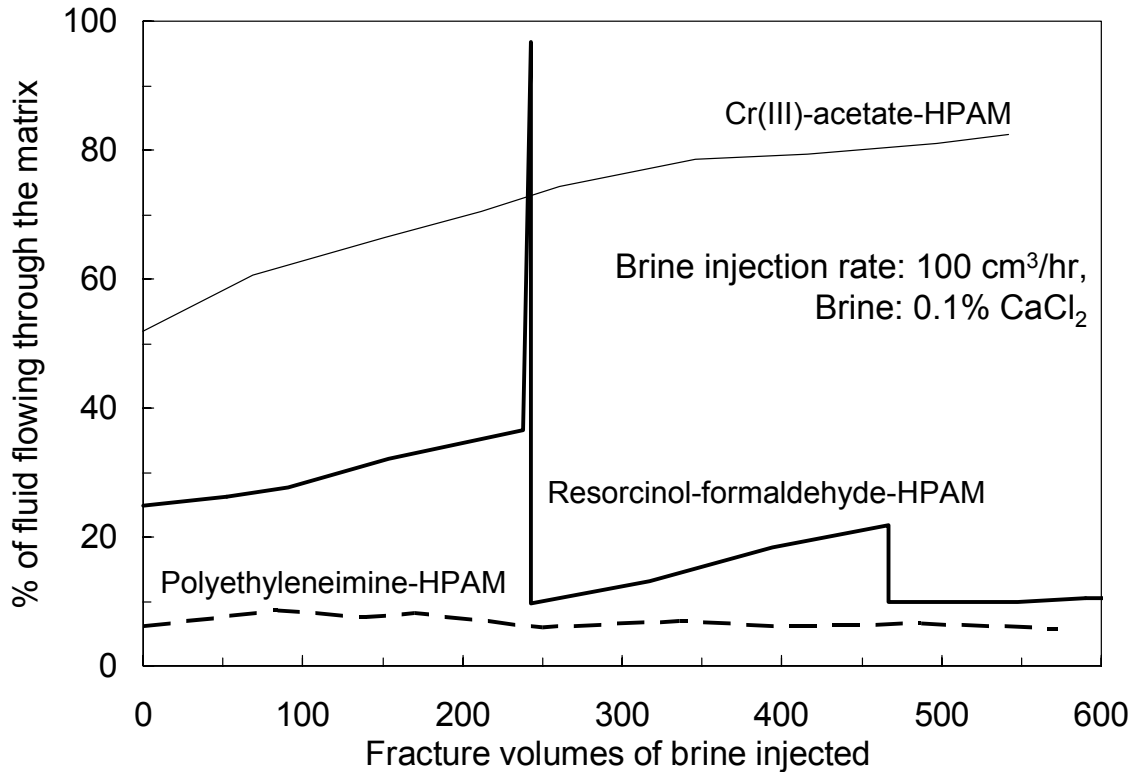


Fig. 113—Percent of flow through matrix for brine with 0.1% CaCl_2 .

From 242 to 460 fracture volumes of 0.1% CaCl_2 brine injection, the pressure gradient again rose gradually to 3.2 psi/ft (Fig. 112) and the percent of fluid flowing through the matrix rose from 9.7% to 21.8% (Fig. 113). These trends suggested that additional gel swelling and restriction of the wormhole was occurring. At 460 fracture volumes, the pressure gradient again dropped sharply (to 1.2 psi/ft) and the percent of fluid flowing through the matrix fell sharply to 9.9%. This behavior suggested additional failure of gel and enlargement of the brine wormhole.

During injection of the brine with 0.1% CaCl_2 through the polyethyleneimine-HPAM gel, the pressure gradient averaged 0.3 psi/ft (Fig. 112), and the fraction of fluid flowing through the matrix averaged 7% (Fig. 113). No significant plugging of the wormhole or swelling of this gel was observed.

Higher Rates and Pressure Gradients Widened Wormholes. For the Cr(III)-acetate-HPAM gel, we examined pressure gradient and percent of fluid flowing through the matrix as a function of brine injection rate. This experiment was performed at the end of injection of the 0.1% CaCl_2 brine (i.e., after injecting 540 fracture volumes of 0.1% CaCl_2 brine at $100 \text{ cm}^3/\text{hr}$ shown in Figs. 112 and 113). In this rate experiment, the 0.1% CaCl_2 brine was injected at increasingly higher rates (100, 200, 400, 800, 2,000, 4,000, 8,000, and $16,000 \text{ cm}^3/\text{hr}$). For each rate, we recorded the stabilized pressure gradient and percent of brine flowing through the matrix. These values are plotted in Fig. 114. With each exposure to a higher rate, the pressure gradient increased, and the fraction of fluid flowing through the matrix decreased. As expected, these results indicate that exposure to higher flow rates and pressure gradients eroded gel in the fracture, widened brine

wormholes, and caused more of the brine to channel through the fracture rather than flow through the porous rock.

After brine injection at the highest rate (16,000 cm³/hr), the flow rate was reduced to 100 cm³/hr. At this final rate, the pressure gradient was 0.34 psi/ft, compared to 3.9 psi/ft at the same rate at the start of this part of the experiment (solid versus open triangles at 100 cm³/hr in Fig. 114). Also, the percent of brine flow through the matrix was 6.1%, compared to 82.5% at the same rate at the start of the rate portion of the experiment (solid versus open circles at 100 cm³/hr in Fig. 114). With this information, the average wormhole radius was estimated to increase from 97 μm to 276 μm during this experiment.

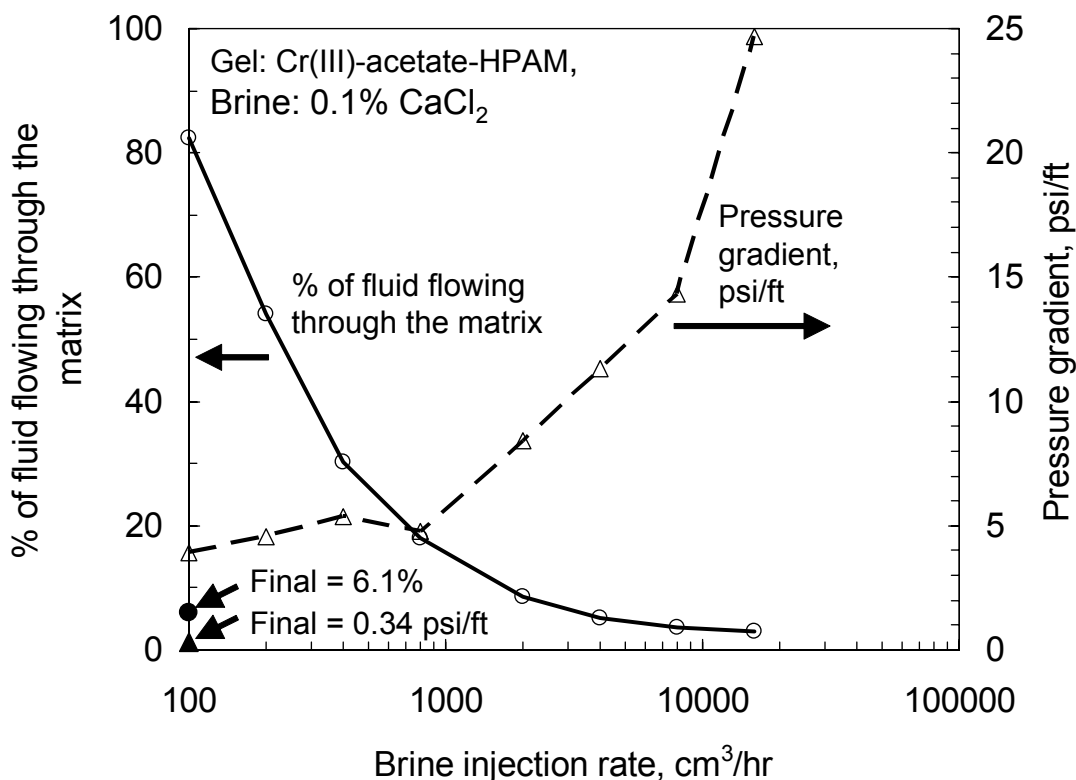


Fig. 114—Higher rates and pressure gradients shift flow away from the matrix.

Injecting Distilled Water Rehydrated Gel Rapidly. Brine Rapidly Dehydrated Gel. The results to this point indicated that injection of brine with 1% NaCl and 0.1% CaCl₂ did not swell or rehydrate gels that were prepared using this same brine. Also, injection of brine with 0.1% CaCl₂ swelled two of the gels, but this was a very gradual process. No swelling was evident for the polyethyleneimine-HPAM gel. Now, we examine what happened when distilled water was injected (after obtaining the data in Figs. 112, 113, and 114).

After re-establishing baselines using brine with 0.1% CaCl₂, distilled water was injected. For all three gels, injection of distilled water had an immediate swelling effect on the gel. For the Cr(III)-acetate-HPAM gel, within a few fracture volumes of the start of distilled water injection,

the fraction of fluid flowing through the matrix jumped from 6.1% to 99.6% (dashed curve in Fig. 115) and the average pressure gradient across the core jumped (in two steps) from 0.34 to 5.9 to 9.1 psi/ft (dashed curve in Fig. 116). Similar behavior was seen for the other two gels (Figs. 117-120). In several of these figures, significant intermediate jumps occurred during injection of distilled water. These jumps occurred when the pumps were refilled—suggesting dislodging or rearrangement of gel to restrict or plug the fracture.

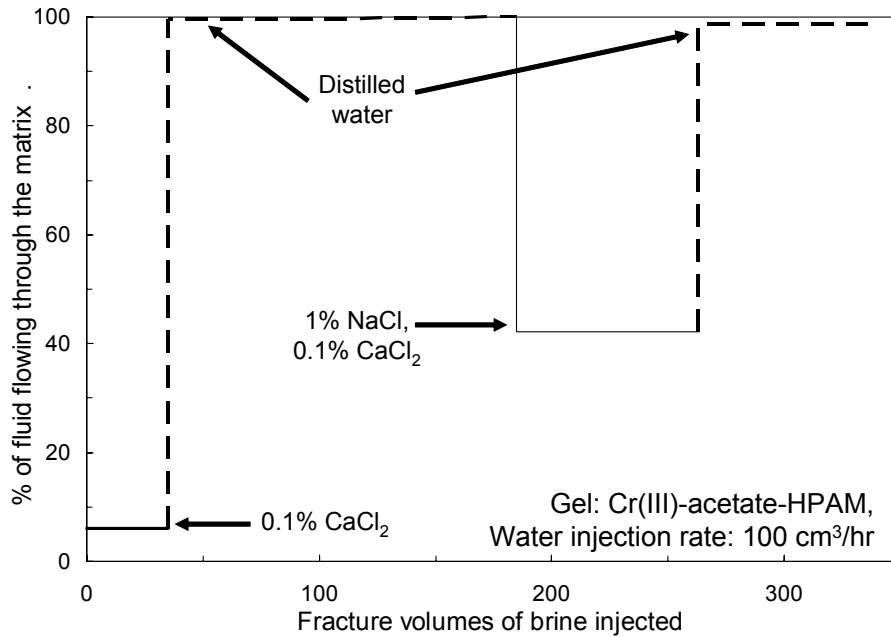


Fig. 115—Distilled water shifted flow to matrix for the Cr(III)-acetate-HPAM gel.

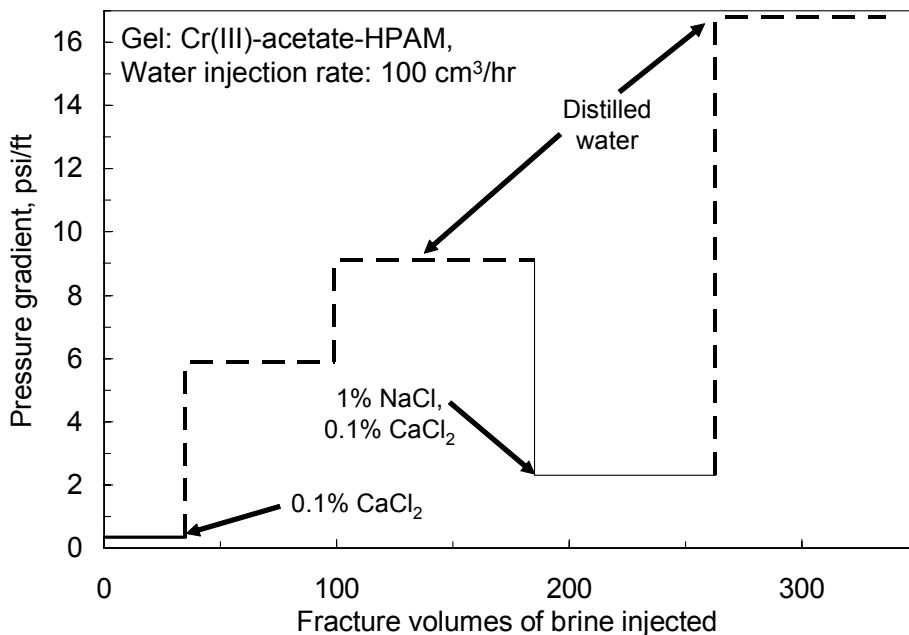


Fig. 116—Distilled water increased dp/dl for the Cr(III)-acetate-HPAM gel.

Injection of brine (containing 1% NaCl and 0.1% CaCl₂ or simply 0.1% CaCl₂) reversed the swelling caused by the distilled water. This finding is evident (in Figs. 115-120) by the sharp reductions in pressure gradient and percent flow through the matrix when brine injection replaced distilled water. Cycling from brine to distilled water showed largely reversible effects.

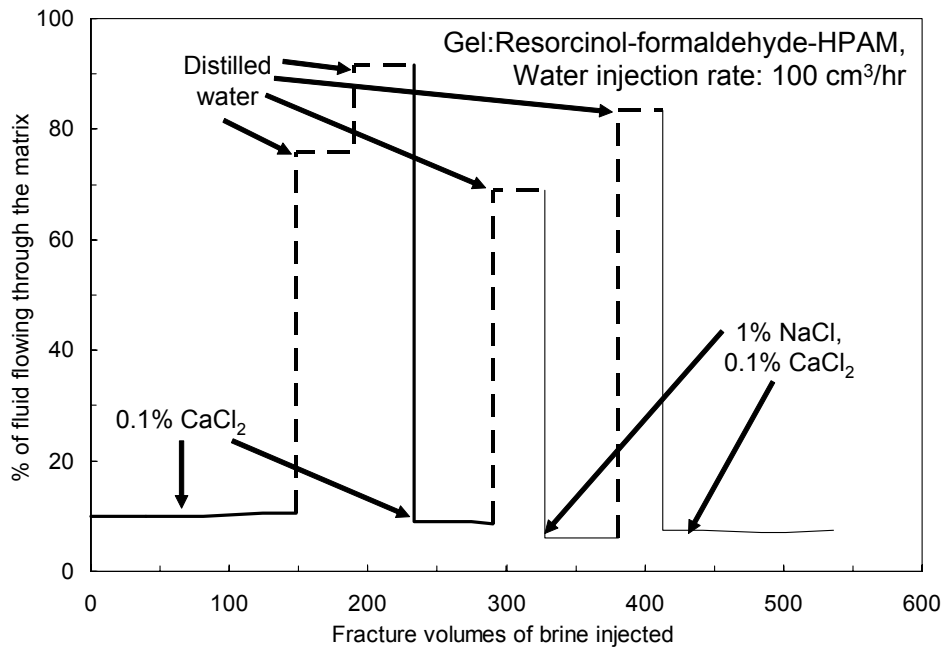


Fig. 117—Distilled water shifted flow to matrix for the resorcinol-formaldehyde-HPAM gel.

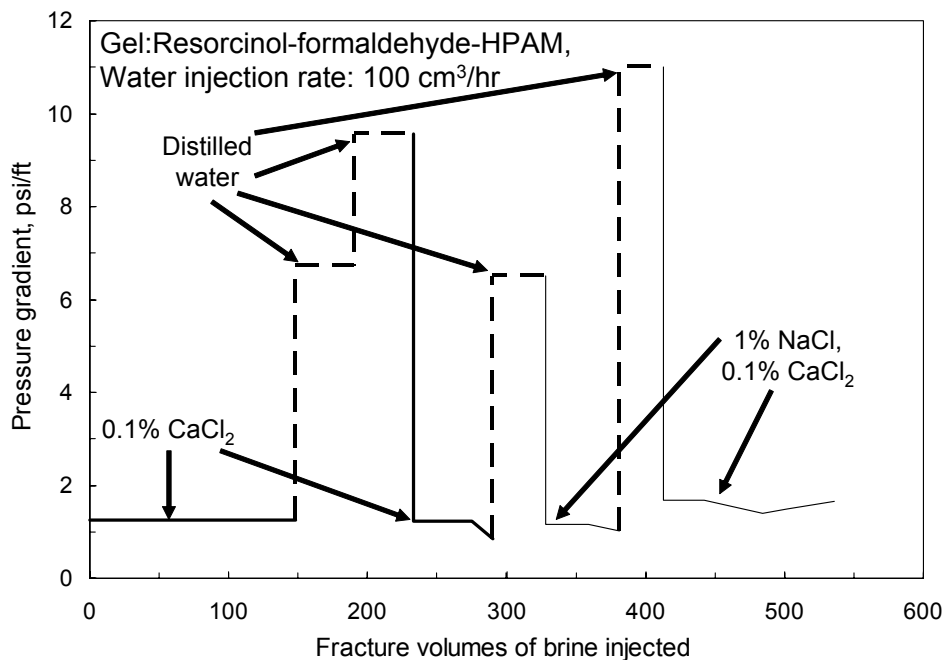


Fig. 118—Distilled water increased dp/dl for the resorcinol-formaldehyde-HPAM gel.

For the polyethyleneimine-HPAM gel, injection of distilled water had noticeable effects on the flow distribution and the pressure gradient, but these effects were much less dramatic than for the other two gels. Perhaps this occurred because the polyethyleneimine-HPAM gel experienced much greater damage during the first brine injection after gel placement.

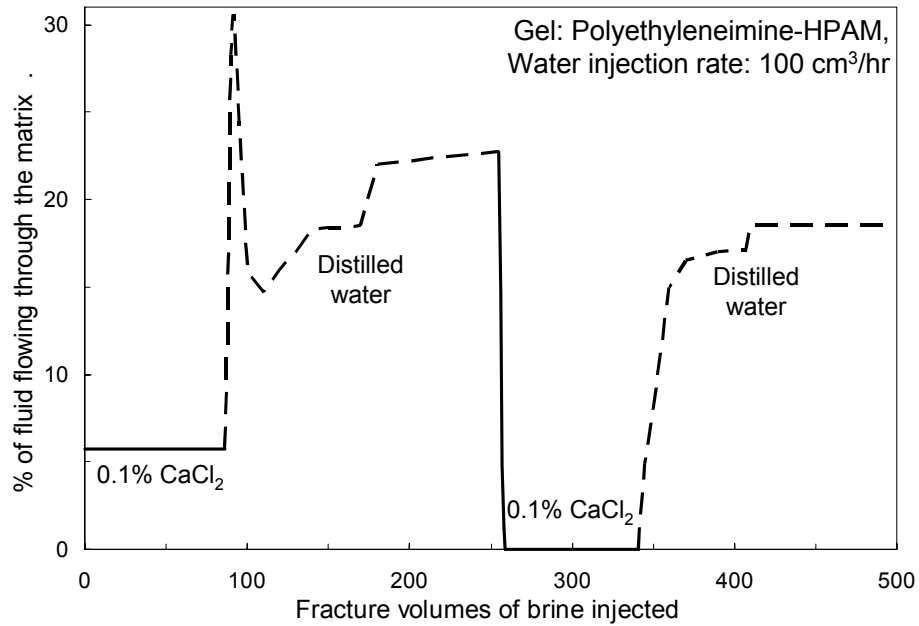


Fig. 119—Distilled water shifted flow to matrix for the polyethyleneimine-HPAM gel.

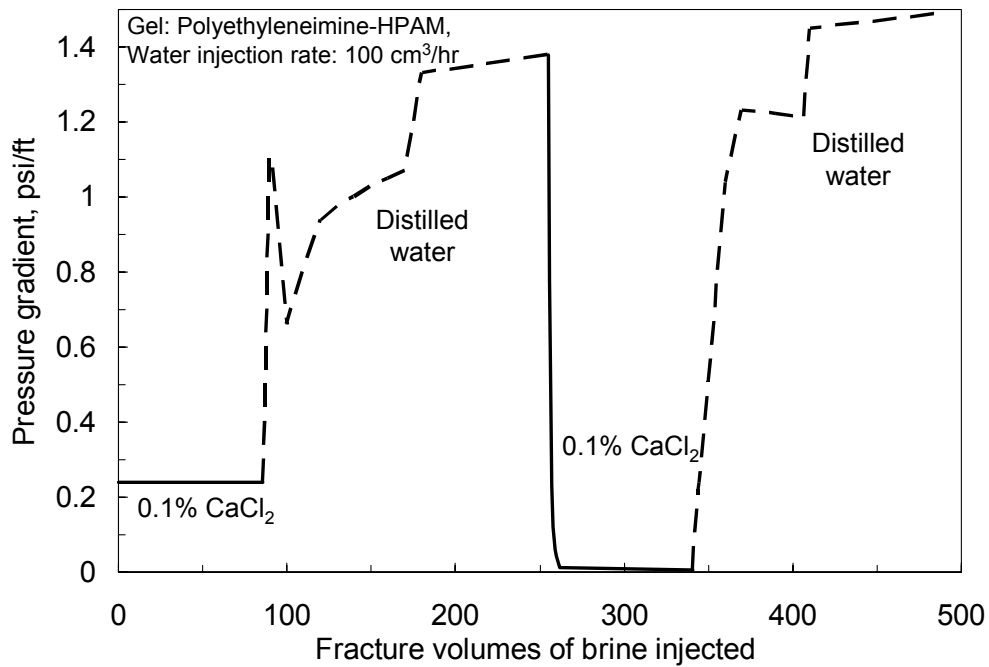


Fig. 120—Distilled water increased dp/dl for the polyethyleneimine-HPAM gel.

Cr(III)-Acetate-HPAM Gel Using HPAM with 30% Degree of Hydrolysis. In the above experiments, we were somewhat surprised that more dramatic changes were not observed when switching between injection of brine with 1% NaCl and 0.1% CaCl₂ and brine with only 0.1% CaCl₂. The HPAM used in the previous experiments (Ciba Alcoflood 935) had a degree of hydrolysis between 5% and 10%. We wondered whether greater changes would be seen using HPAM with a higher degree of hydrolysis. Therefore, we performed a set of experiments using SNF 3830 HPAM, which had a 30% degree of hydrolysis.

Using our standard procedures, we prepared a 4-ft long Berea core with a 1-mm-wide fracture running lengthwise down the core's center. The core was initially saturated with brine containing 1% NaCl and 0.1% CaCl₂. All experiments were performed at 41°C. We also prepared a one-day old Cr(III)-acetate-HPAM gel containing 0.5% SNF 3830 HPAM, 0.0417% Cr(III) acetate, 1% NaCl, and 0.1% CaCl₂. We injected 80 fracture volumes of this gel at 2,000 cm³/hr (4,130 ft/d). The average pressure gradient during gel injection was 14.5 psi/ft, which was fairly typical of the pressure gradient observed in 1-mm-wide fractures using gels of the same composition except that the HPAM was Alcoflood 935.³⁵

After gel placement, the core was shut in for one day, followed by injection of 268 fracture volumes of brine (1% NaCl, 0.1% CaCl₂) at a rate of 100 cm³/hr (206 ft/d). Fig. 121 shows pressure gradients during the first 10 fracture volumes of brine injection. Results from the Cr(III)-acetate gel made with Alcoflood 935 are shown for comparison (i.e., data from Fig. 109). As with our other experiments, the pressure gradient rose to a peak (around 0.5 fracture volumes in this case). This peak represents the pressure gradient at which brine first breached the gel. The pressure gradient associated with this peak (5.1 psi/ft) was on the same order as for other experiments. We noted an anomalous pressure behavior from 3 to 10 fracture volumes. However, we place no particular significance to this behavior, other than perhaps that a spurious piece of gel broke off and lodged to temporarily block the brine wormhole.

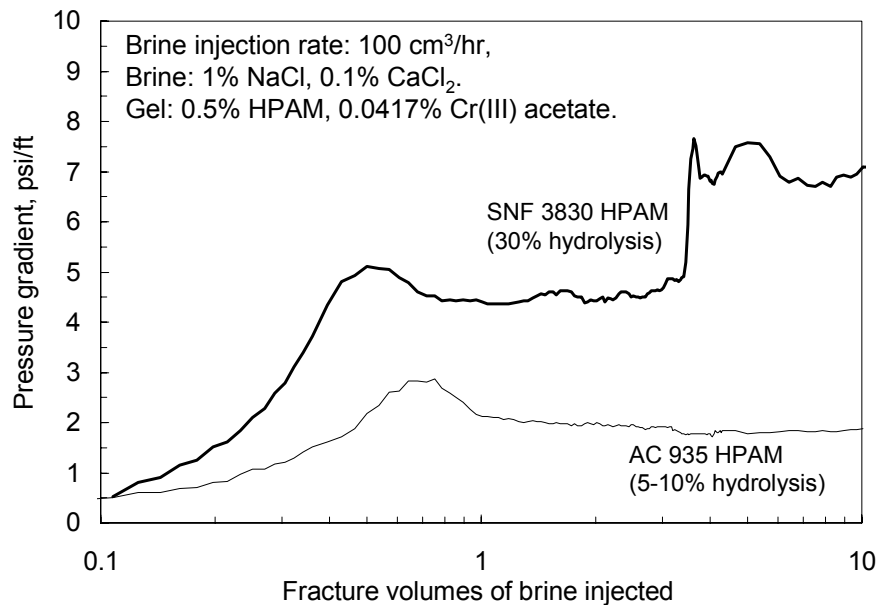


Fig. 121—Breaching pressure gradient versus HPAM degree of hydrolysis.

During the course of injecting over 250 fracture volumes of brine with 1% NaCl and 0.1% CaCl₂, the pressure gradients did not increase significantly for either HPAM gel (Fig. 122).

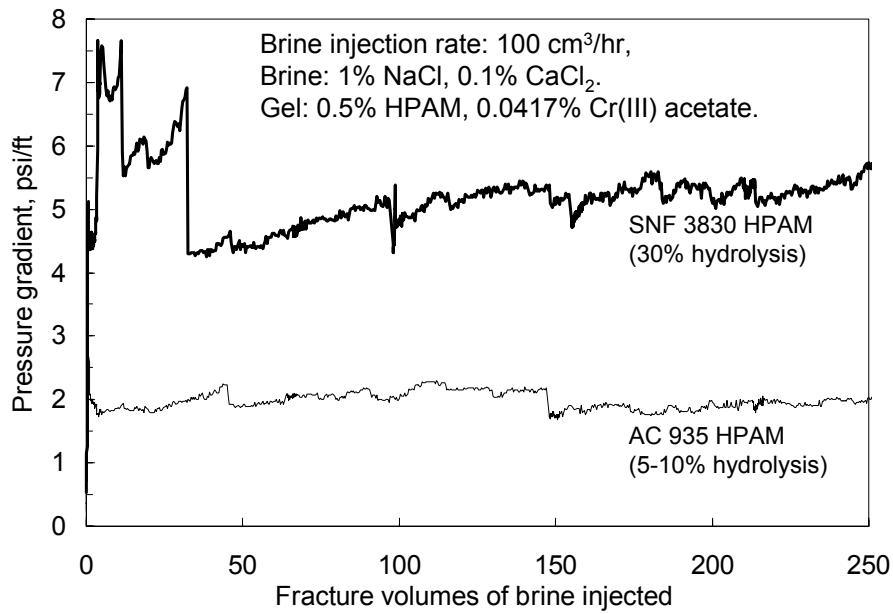


Fig. 122—Stabilized pressure gradients versus degree of hydrolysis: 1% NaCl, 0.1% CaCl₂.

Fig. 123 indicates that the HPAM with 30% degree of hydrolysis provided 100% flow through the matrix for substantially longer than did the HPAM with 5-10% degree of hydrolysis.

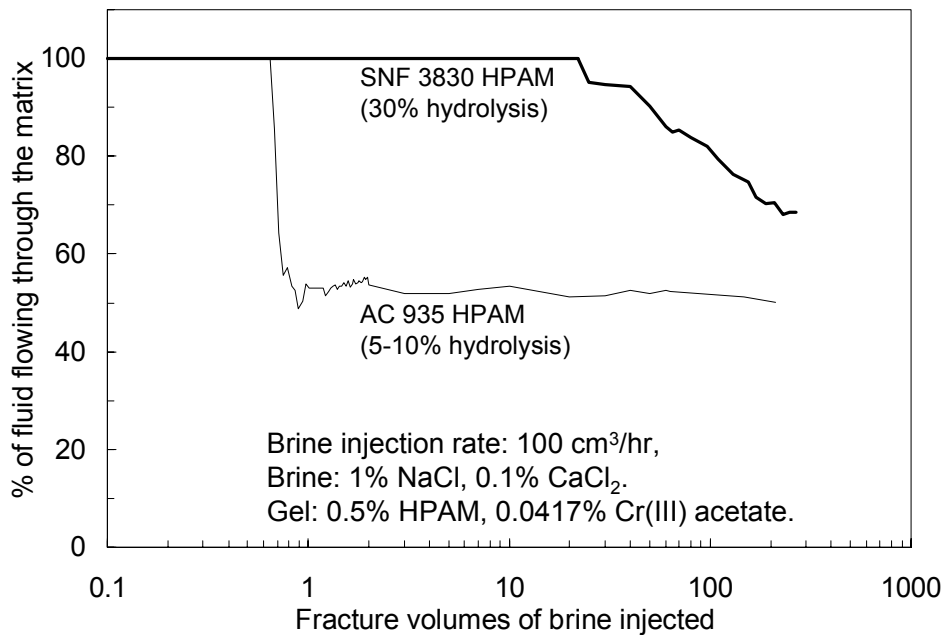


Fig. 123—Percent of flow through matrix versus degree of hydrolysis: 1% NaCl, 0.1% CaCl₂.

After injecting 268 fracture volumes of the brine with 1% NaCl and 0.1% CaCl₂, we injected 307 fracture volumes of brine with 0.1% CaCl₂. Pressure gradients during injection of the less saline brine did not result in pressure gradients that were much greater than those associated with the HPAM with 5-10% degree of hydrolysis (Fig. 124). However, a significant jump was noted in the fraction of brine flowing through matrix when injecting the 0.1% CaCl₂ brine with the 30% hydrolyzed HPAM (Fig. 125). In contrast, the polymer with 5-10% degree of hydrolysis provided a much more gradual increase in fraction of brine flowing through the matrix.

For the gel with the SNF polymer, significant volumes of fluid began to flow through the fracture after 33 fracture volumes. Perhaps this occurrence was related to mobilization or breakdown of a small piece of gel within the fracture.

For the SNF polymer gel, we returned to injecting the original brine (1% NaCl, 0.1% CaCl₂) after the 307 fracture volumes of brine with 0.1% CaCl₂. Interestingly, this switch had relatively little effect on both the pressure gradient and the fraction of fluid flowing through the matrix (dashed curves in Figs. 124 and 125).

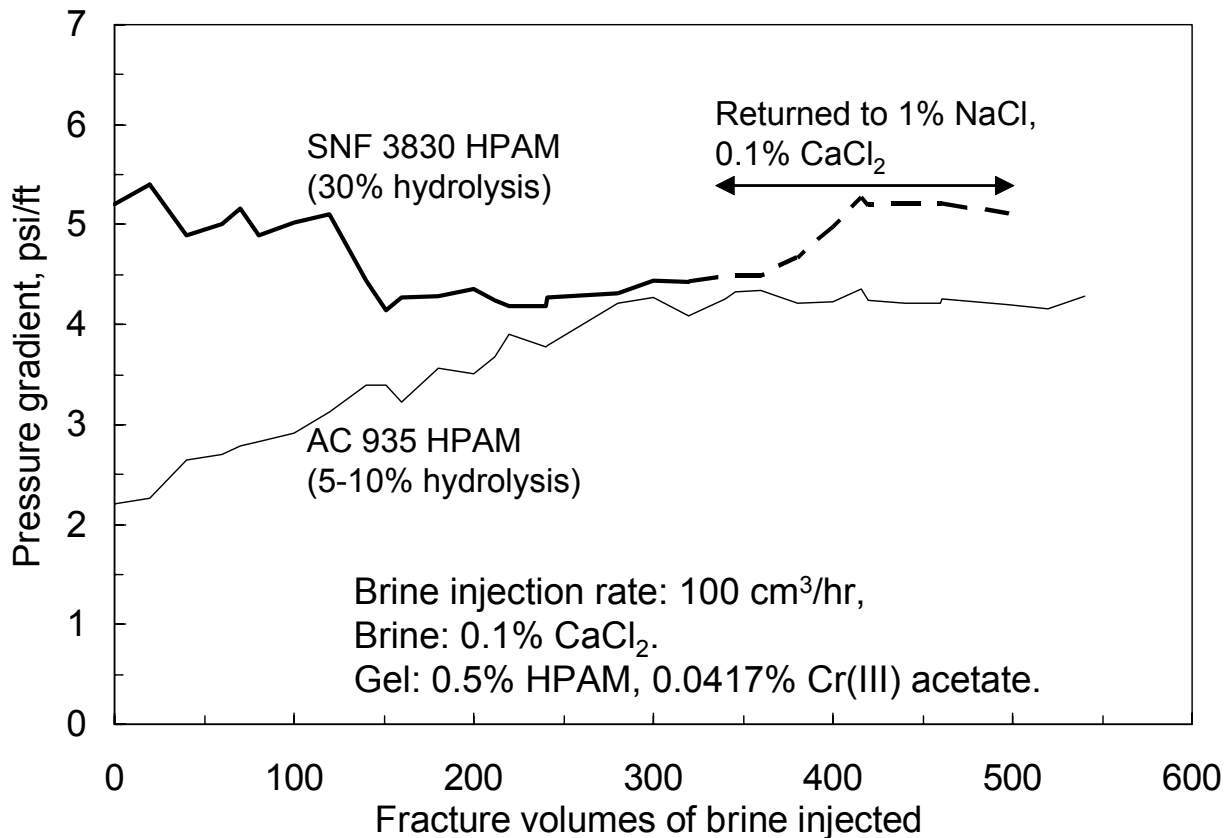


Fig. 124—Pressure gradients versus degree of hydrolysis: 0.1% CaCl₂.

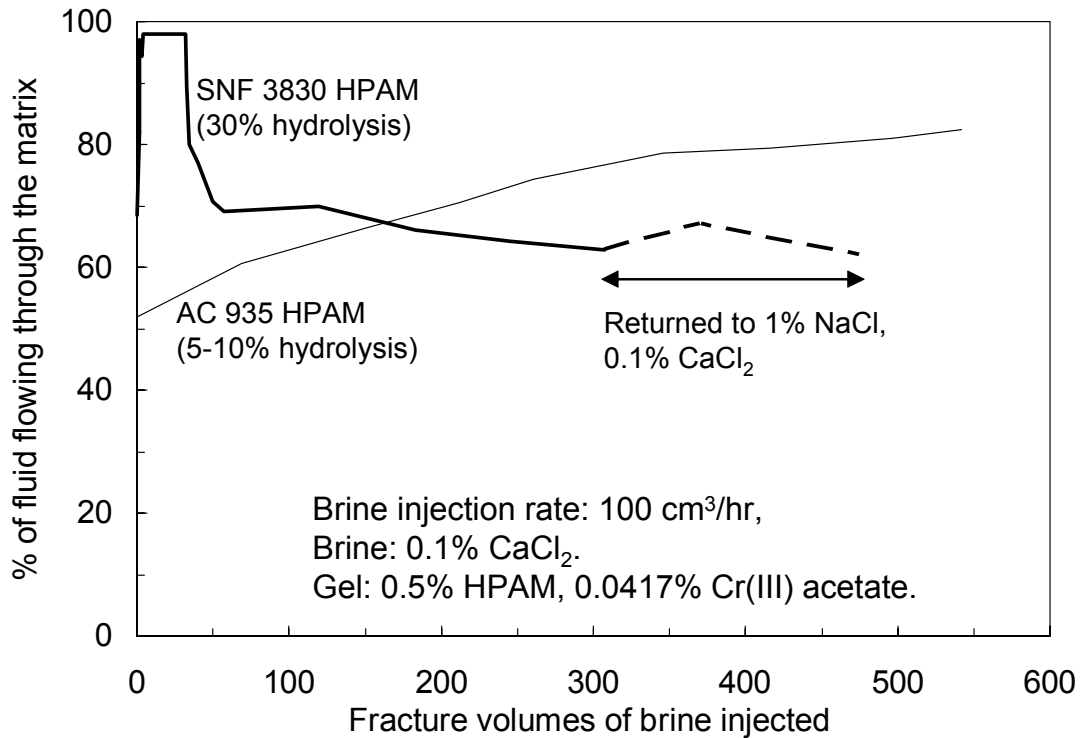


Fig. 125—Percent of flow through matrix versus degree of hydrolysis: 0.1% CaCl_2 .

For the SNF polymer gel, after collecting the data shown in Figs. 124 and 125, we increased the brine injection rate in stages up to $2,000 \text{ cm}^3/\text{hr}$. Then, brine rates were decreased in stages back to $100 \text{ cm}^3/\text{hr}$ (see Fig. 126). As rates were increased from 100 to $2,000 \text{ cm}^3/\text{hr}$, the fraction of brine flowing through the matrix decreased from 62.1% to 9.1% . Thus, higher rates promoted greater channeling through the fracture. However, when rates were decreased back to $100 \text{ cm}^3/\text{hr}$, the fraction of brine flowing through the matrix increased to 44% . Since much of the channeling effect was reversed by reducing the rate, gel in the fracture apparently exhibited a significant degree of deformability.

For comparison, Fig. 114 shows results from rate experiments using gel made with Alcoflood 935 HPAM (5-10% degree of hydrolysis). Of course, Figs. 114 and 126 are not directly comparable because the maximum rate in Fig. 114 was eight times greater than that in Fig. 126. However, in Fig. 114, we noted very little reversibility (in the fraction of fluid flowing through the matrix) when the rate was returned to $100 \text{ cm}^3/\text{hr}$. More work is needed to establish whether the gel diversion properties are strongly influenced by the polymer degree of hydrolysis.

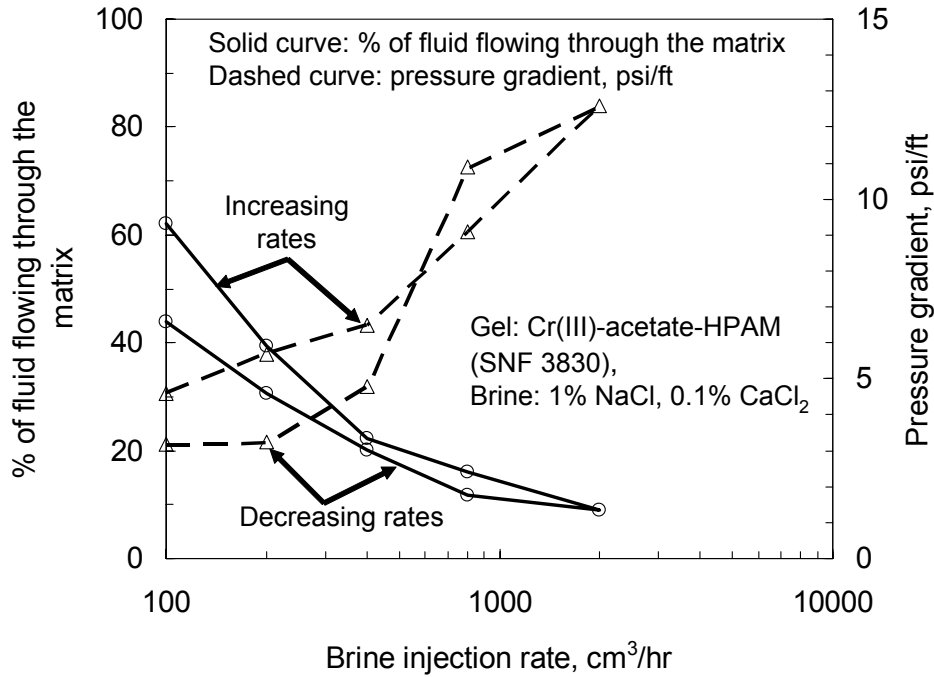


Fig. 126—Effect of rate on gel with SNF 3830 HPAM.

After performing the experiments associated with Fig. 126, we injected large banks of distilled water, brine with 1% NaCl and 0.1% CaCl₂, brine with 0.1% CaCl₂, and finally, distilled water. Pressure gradients are shown in Fig. 127, while the fraction of fluid flowing through the matrix is shown in Fig. 128. Switching injection from brine to distilled water (and *visa versa*) exhibited large fracture-plugging/gel-swelling effects, while switching between brines had little effect. These findings are consistent with those reported earlier for the gels made with Alcoflood 935 (Figs. 115 to 120).

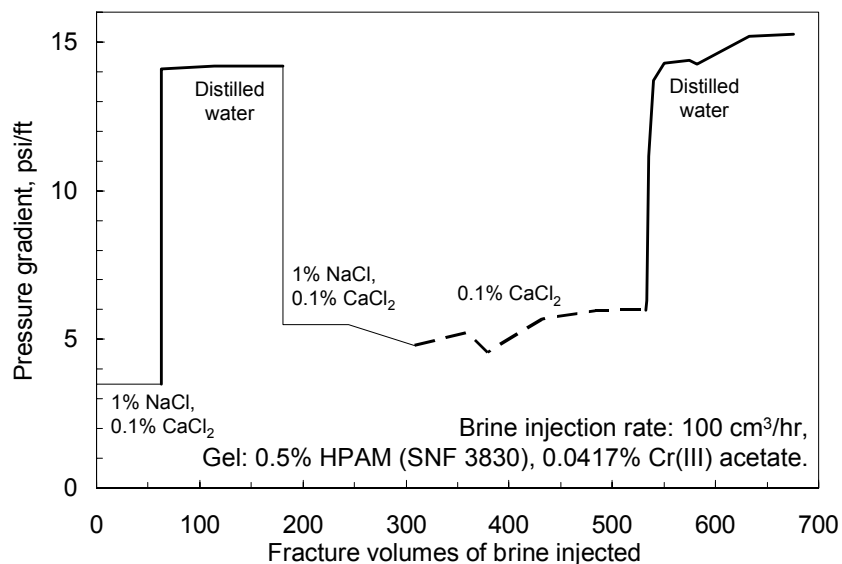


Fig. 127—Pressure gradients for SNF 3830: effect of salinity.

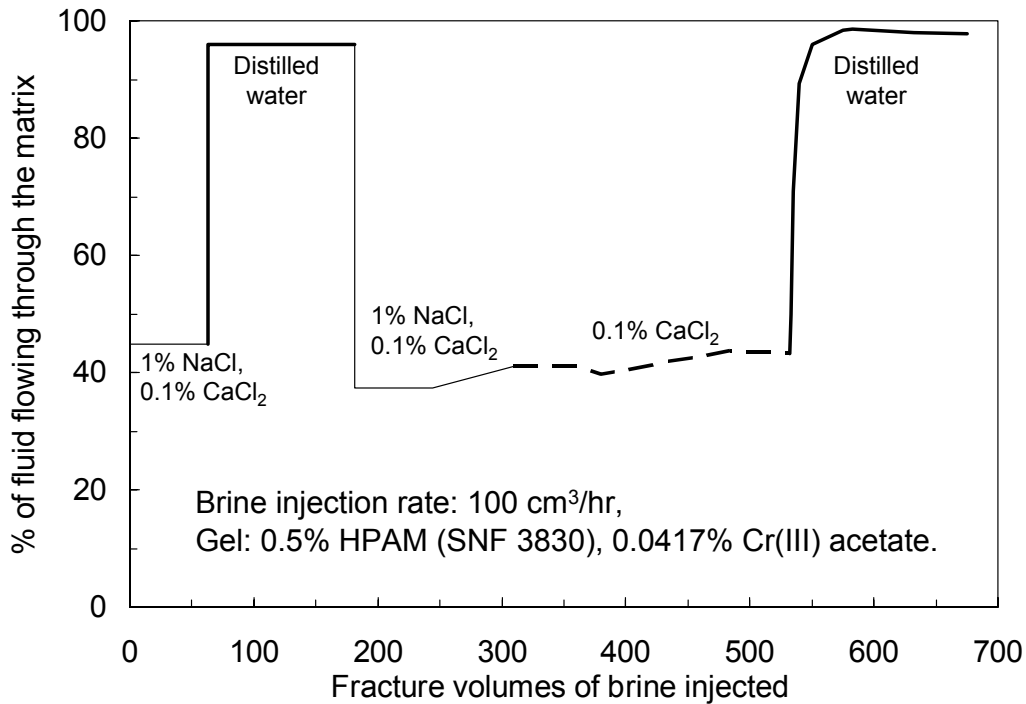


Fig. 128—Percent of flow through matrix for SNF 3830: effect of salinity.

In summary, gel made using HPAM with a 30% degree of hydrolysis showed many similarities in behavior to gel made using HPAM with 5-10% degree of hydrolysis. In particular, similar behavior was observed for (1) the pressure gradient required to extrude the gels through 1-mm-wide fractures, (2) the pressure gradient to breach the gel during first brine flow after gel placement, (3) large changes in fracture-plugging/gel-swelling when switching from brine to distilled water injection, and (4) generally small changes in fracture-plugging/gel-swelling when switching between brines. However, a few observations suggested that gel made using HPAM with a 30% degree of hydrolysis might exhibit better fracture-plugging properties. More work is needed to establish whether the gel diversion properties are strongly influenced by the polymer degree of hydrolysis.

To What Degree Must Flow in a Fracture Be Restricted?

In the previous sections, distilled water effectively swelled the gel, closed the wormholes, and diverted most flow away from the fracture and into the porous rock. Of course, injection of distilled water will be impractical in most field applications. So, how important is it to completely heal fractures? Earlier, for one gel after injection of the brine with 1% NaCl and 0.1% CaCl₂, we calculated that the flow capacity of the 1-mm wide fracture was reduced by a factor of 7,000, even though about half the brine still flowed through the fracture (see the discussion just after Fig. 109). In field applications, is a reduction of flow capacity by a factor of 7,000 enough, or must the fracture be completely plugged?

Laboratory Flow Capacities. For a 3.8-cm high, 1-mm wide fracture in our 700-md Berea cores (with area cross-section of 14.4 cm²), the flow capacity of an open fracture (i.e., before gel placement) was 3,200 times greater than that of the porous rock (i.e., 32,300 darcy-cm² for the fracture versus 10.1 darcy-cm² for the rock). In our lab experiments, one gel reduced the fracture flow capacity by a factor of 7,000—to ~4 darcy-cm²—a value on the order of the pre-gel flow capacity of the porous rock. Considering that some of the injected gel plated on the injection surface of the porous rock and reduced the matrix flow capacity, the post-gel flow capacity of the fracture can easily be expected to exceed the post-gel flow capacity of the porous rock.

Flow Capacities in Field Applications. For field applications where a single vertical fracture intersected a vertical well, and the fracture had the same height as the porous rock, the ratio of fracture flow capacity to flow capacity of the porous rock was given by the following expression:

$$[k_f w_f / r_e] / [k_{matrix} / \ln(r_e / r_w)] \dots\dots\dots (8)$$

Consider radial flow into a vertical well where the wellbore radius (r_w) was 0.5 ft and the external drainage radius (r_e) was 500 ft. In this case, the flow capacity of a 1-mm wide fracture would be only 5.5 times the flow capacity of 700-md rock, 55 times that of 70-md rock, and 550 times that of 7-md rock. Thus, a gel that reduces the flow capacity of the fracture by more than a factor of 1,000 should substantially divert flow away from the fracture and into the porous rock in most reservoirs with 1-mm wide fractures. Complete healing of the fracture (so that no flow occurs through the fracture) may not be necessary. More importantly, the flow capacity of the fracture must be reduced by a large enough factor so that fluids are diverted largely into the porous rock.

Fig. 129 plots Eq. 8 for a range of matrix permeabilities and fracture widths. This figure can provide guidance on how much flow in a fracture must be restricted to divert flow into the porous rock. To be effective, a gel should reduce the flow capacity of the fracture to a level that is comparable to or less than the flow capacity of the matrix. For example, in 10-md rock, gel must reduce the flow capacity of a 2-mm wide fracture by a factor of 3,100 or more to match the flow capacity of the matrix. In contrast, in the same rock, gel must reduce the flow capacity of a 0.5-mm wide fracture by a factor of only 50 to match the matrix flow capacity.

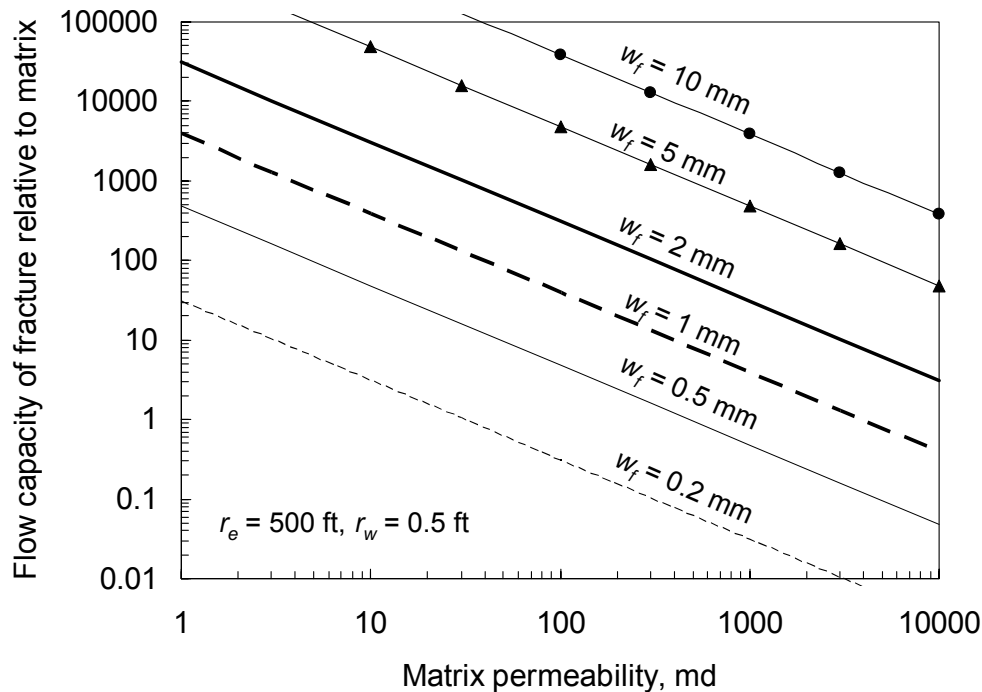


Fig. 129—Flow capacity of fracture relative to matrix: vertical well, vertical fracture.

Summary

Gels dehydrate when extruding through fractures. This concentrated gel is quite immobile and can effectively reduce the flow capacity of fractures. When brine or oil flow is resumed after gel placement, small wormhole paths open through the gel in the fractures when a critical pressure gradient is reached. In many cases (e.g., fractures or fracture-like features in very permeable sand and rock), these wormhole pathways do not restore fracture conductivity enough to be of concern. However, for other cases (e.g., wide fractures in moderate to low permeability rock), plugging of these wormholes may be desirable to divert flow through the porous rock and eliminate channeling through the fractures. We investigated the ability of concentrated gels to rehydrate (swell) during water flow after gel placement. Three gels were examined that contained the same HPAM concentration, but that used different crosslinkers, including Cr(III) acetate, resorcinol formaldehyde, and polyethyleneimine. For all three gels, no gel rehydration or restriction of the wormholes occurred when flooding with large volumes of brine with the same composition as that used to prepare the gels (1% NaCl, 0.1% CaCl₂). Very gradual rehydration and restriction of the wormholes occurred when flooding with large volumes of brine containing 0.1% CaCl₂. Flooding with distilled water caused immediate swelling and restriction of the wormholes and diversion of water away from the fractures and into the porous rock. Switching back to brine injection (1% NaCl and 0.1% CaCl₂, or 0.1% CaCl₂) caused immediate gel dehydration and re-opening of the wormholes. Of course, injection of distilled water is impractical in most cases. Nevertheless, these results provide hope that a swelling mechanism may be exploitable in future developments.

NOMENCLATURE

- C = polymer concentration, %
 F_{rr} = residual resistance factor (permeability before/after gel placement)
 F_{rro} = residual resistance factor for oil
 F_{rrw} = residual resistance factor for water
 h_f = fracture height, ft [m]
 h_{matrix} = height of matrix rock, ft [m]
 k_f = fracture permeability, darcys [μm^2]
 k_{gel} = inherent permeability of gel to water, darcys [μm^2]
 k_{matrix} = rock matrix permeability, darcys [μm^2]
 k_{new} = rock matrix permeability for target reservoir, darcys [μm^2]
 k_o = permeability to oil, darcys [μm^2]
 k_w = permeability to water, darcys [μm^2]
 L_e = external drainage distance, ft [m]
 L_p = distance of polymer or gelant leakoff, ft [m]
 n = number of fractures oriented in the y -direction in the pattern
 Δp = pressure drop, psi [Pa]
 dp/dl = pressure gradient, psi/ft [Pa/m]
 PV = pore volumes of fluid injected
 q = flow rate, BPD [m^3/d]
 q_o = flow rate before polymer or gel placement, BPD [m^3/d]
 R = fracture conductivity ratio defined by Eq. 3 or correlation coefficient
 r_e = external drainage radius, ft [m]
 r_{gel} = radius of gelant penetration, ft [m]
 r_w = wellbore radius, ft [m]
 S_{or} = residual oil saturation
 S_{wr} = residual water saturation
 w_f = fracture width, mm
 w_{fnew} = fracture width for target reservoir, mm
 w_{fref} = fracture width for when $k_{matrix} = 0.1$ darcys, mm
 w_{matrix} = width dimension of the reservoir pattern, ft [m]
 x = abscissa, ft [m]
 y = ordinate, ft [m]

REFERENCES

1. Seright, R.S., Liang, J., and Seldal, M.: "Sizing Gelant Treatments in Hydraulically Fractured Production Wells," *SPE Production & Facilities* (Nov. 1998) 223-229.
2. Seright, R.S., Liang, J., and Sun, H.: "Gel Treatments in Production Wells with Water Coning Problems," *In Situ* (1993) **17**, No.3, 243-272.
3. Seright, R.S. and Lee, R.L.: "Gel Treatments for Reducing Channeling Through Naturally Fractured Reservoirs," *SPE Production & Facilities* (Nov. 1999) 269-276.
4. <http://baervan.nmt.edu/randy/>.
5. O'Brien, W.J., Stratton, J.J., and Lane, R.H.: "Mechanistic Reservoir Modeling Improves Fissure Treatment Gel Design in Horizontal Injectors, Idd El Shargi North Dome Field, Qatar," paper SPE 56743 presented at the SPE Annual Technical Conference and Exhibition, Houston, TX, Oct. 5-8, 1999.
6. Lane, R.H., and Seright, R.S.: "Gel Water Shutoff in Fractured or Faulted Horizontal Wells," paper CIM/SPE 65527 presented at the 2000 SPE/Petroleum Society of CIM International Conference on Horizontal Well Technology held in Calgary, Alberta, Canada, Nov. 6-8.
7. Lane, R.H. and Sanders, G.S.: "Water Shutoff Through Fullbore Placement of Polymer Gel in Faulted and in Hydraulically Fractured Producers of the Prudhoe Bay Field," paper SPE 29475 presented at the 1995 SPE Production Operations Symposium, Oklahoma City, OK, April 2-4.
8. Seright, R.S.: "An Alternative View of Filter Cake Formation in Fractures Inspired by Cr(III)-Acetate-HPAM Gel Extrusion," *SPE Production and Facilities* (Feb. 2003) 65-72.
9. Seright, R.S.: "Conformance Improvement Using Gels," Annual Technical Progress Report (U.S. DOE Report DOE/BC/15316-6), U.S. DOE Contract DE-FC26-01BC15316 (Sept. 2004) 72.
10. Bai, B. *et al.*: "Preformed Particle Gel for Conformance Control: Factors Affecting its Properties and Applications," paper SPE 89389 presented at the 2004 SPE/DOE Symposium on Improved Oil Recovery, Tulsa, OK, April 17-21.
11. Bai, B. *et al.*: "Preformed Particle Gel for Conformance Control: Transport Mechanism Through Porous Media," paper SPE 89468 presented at the 2004 SPE/DOE Symposium on Improved Oil Recovery, Tulsa, OK, April 17-21.
12. Seright, R.S.: "Washout of Cr(III)-Acetate-HPAM Gels from Fractures," paper SPE 80200 presented at the 2003 SPE International Symposium on Oilfield Chemistry, Houston, TX, Feb. 5-7.
13. Seright, R.S.: "Improved Techniques for Fluid Diversion in Oil Recovery Processes," second annual report (DOE/BC/14880-10), Contract No. DE-AC22-92BC14880, U.S. DOE (March 1995) 51-64.
14. Seright, R.S.: "Mechanism for Gel Propagation Through Fractures," paper SPE 55628 presented at the 1999 Rocky Mountain Regional Meeting, Gillette, WY, May 15-18.
15. Liang, J., Sun, H., Seright, R.S.: "Why Do Gels Reduce Water Permeability More Than Oil Permeability?," *SPE Reservoir Engineering* (Nov. 1995) 282-286.
16. Seright, R.S.: "Reduction of Gas and Water Permeabilities Using Gels," *SPE Production & Facilities* (May 1995) 103-108.

17. Zaitoun, A. and Bertin, H.: "Two-Phase Flow Property Modifications by Polymer Adsorption," paper SPE 39631 presented at the 1996 SPE/DOE Improved Oil Recovery Symposium, Tulsa, OK, April 19-22.
18. Al-Sharji, H.H., *et al.*: "Pore-Scale Study of the Flow of Oil and Water through Polymer Gels," paper SPE 56738 presented at the 1999 SPE Annual Technical Conference and Exhibition, Houston, TX, Oct. 3-6.
19. Willhite, G.P., *et al.*: "Mechanisms Causing Disproportionate Permeability in Porous Media Treated With Chromium Acetate/HPAAM Gels," *SPEJ* (March 2002) 100-108.
20. Liang, J., Lee, R.L., and Seright, R.S.: "Placement of Gels in Production Wells," *SPE Production & Facilities* (Nov. 1993) 276-284; *Transactions AIME* **295**.
21. Marin, A., Seright, R., Hernandez, M., Espinoza, M., Mejias, F.: "Connecting Laboratory and Field Results for Gelant Treatments in Naturally Fractured Production Wells," paper SPE 77411 presented at the 2002 SPE Annual Technical Conference and Exhibition, San Antonio, TX, Sept. 29- Oct. 2.
22. Seright, R.S.: "Conformance Improvement Using Gels," first annual technical progress report, Contract No. DE-FC26-01BC15316, U.S. DOE (Sept. 2002) 43-59.
23. Seright, R.S. and Martin, F.D.: "Impact of Gelation pH, Rock Permeability, and Lithology on the Performance of a Monomer-Based Gel," *SPE Reservoir Engineering* (Feb. 1993) 43-50.
24. <http://baervan.nmt.edu/randy/webschool/>.
25. Seright, R.S.: "Effect of Rock Permeability on Gel Performance in Fluid-Diversion Applications," *In Situ* (1993) **17** (4), 363-386.
26. Seright, R.S.: "Impact of Permeability and Lithology on Gel Performance," paper SPE 24190 presented at the 1992 SPE/DOE Symposium on Enhanced Oil Recovery, Tulsa, OK, April 22-24.
27. Rousseau, D., *et al.*: "Rheology and Transport in Porous Media of New Water Shutoff/Conformance Control Microgels," paper SPE 93254 presented at the 2005 SPE International Symposium on Oilfield Chemistry, Houston, TX, Feb. 2-4.
28. Seright, R.S.: "Placement of Gels to Modify Injection Profiles," paper SPE/DOE 17332 presented at the 1988 SPE/DOE Enhanced Oil Recovery Symposium, Tulsa, OK, April 17-20.
29. Vela, S., Peaceman, D.W. and Sandvik, E.I.: "Evaluation of Polymer Flooding in a Layered Reservoir with Crossflow, Retention, and Degradation," *Soc. Pet. Eng. J.* (April 1976) 82-96.
30. Seright, R.S.: "Clean Up of Oil Zones after a Gel Treatment," paper SPE 92772 presented at the 2005 SPE International Symposium on Oilfield Chemistry, Houston, TX, Feb. 2-4.
31. Seright, R.S.: "Using Chemicals to Optimize Conformance Control in Fractured Reservoirs," first annual report (DOE/BC/15110-2), Contract No. DE-AC26-98BC15110, U.S. DOE (Sept. 1999) 24.
32. Seright, R.S., Prodanovic, M., and Lindquist, W.B.: "X-Ray Computed Microtomography Studies of Disproportionate Permeability Reduction," paper SPE 89393 presented at the 2004 SPE/DOE Symposium on Improved Oil Recovery, Tulsa, OK, April 17-21.
33. Seright, R.S., Liang J., Lindquist, W.B., and Dunsmuir, J.H.: "Characterizing Disproportionate Permeability Reduction Using Synchrotron X-Ray Computed Microtomography," *SPE Reservoir Evaluation & Engineering*, **5**(5), (Oct. 2002) 355-364.
34. Seright, R.S.: "Gel Placement in Fractured Systems," *SPE Production & Facilities* (Nov. 1995), 241-248.

35. Seright, R.S.: "Gel Propagation Through Fractures," *SPE Production & Facilities* (Nov. 2001) 225-232.
36. Sydansk, R.D., Al-Dhafeeri, A., Xiong, Y., Schrader, R., and Seright, R.S.: "Characterization of Partially Formed Polymer Gels for Application to Fractured Production Wells for Water-Shutoff Purposes," *SPE Production & Facilities* (Aug. 2005), **20**(3) 240-249.
37. Sydansk, R.D., Al-Dhafeeri, A.M., Xiong, Y., and Seright, R.S.: "Polymer Gels Formulated with a Combination of High- and Low-Molecular-Weight Polymers Provide Improved Performance for Water-Shutoff Treatments of Fractured Production Wells," *SPE Production & Facilities* (Nov. 2004), **19**(4) 229-236.

APPENDIX A: Technology Transfer

Presentations

On October 21, 2005, we presented the Workshop, “Polymer and Polymer-Gel Water Shutoff Treatments: What It Takes to Be Successful and Illustrative Field Applications,” for the PTTC and the University of Wyoming Enhanced Oil Recovery Institute in Denver, CO.

On September 27, 2005, we presented the talk, “Physical Realities for In-Depth Profile Modification,” at the SPE Applied Technology Workshop on Chemical Flooding in Daqing, China.

On February 9-10, 2005, we presented the Workshop, “Polymer and Polymer-Gel Water Shutoff Treatments: What It Takes to Be Successful and Illustrative Field Applications,” at the University of Wyoming Enhanced Oil Recovery Institute in Laramie, WY.

On February 2, 2005, we presented the talk, “Clean Up of Oil Zones after a Gel Treatment,” at the 2005 SPE International Symposium on Oilfield Chemistry in Houston, TX.

On November 8-12, 2004, we presented the course, “Water Shutoff” in Mexico City, Mexico.

On October 20, 2004, we presented the talk, “Throughput Dependence of Oil and Water Permeabilities after Treatment with Gel or Polymer,” at the 3rd International Conference on Oil and Gas Development in Chengdu, China.

On October 19, 2004, we presented the talk, “Challenges for the Development of Improved Mobility Control Methods,” for the China Institute for Organic Chemistry in Chengdu, China.

On October 13-14, 2004, we presented the talk, “Three Approaches for Improving Oil Recovery,” for the Research Institute of Exploration and Development of Daqing Oil Field, PetroChina in Daqing, China.

On August 25, 2004, we presented the PTTC Workshop, “Polymer and Polymer-Gel Water Shutoff Treatments: What It Takes to Be Successful and Illustrative Field Applications”, at the Texas Bureau of Economic Geology facility in Houston, TX.

Web Site

A description of our research group can be found at the following New Mexico PRRC/Tech web site: <http://baervan.nmt.edu/randy>. For those new to water shutoff technology, this site provides an extensive introduction. This introduction details the properties of polymers, gelants, and gels—showing what they can and cannot do. Many myths associated with this technology are dispelled. The introduction also provides guidance on where and how gel treatments should (and should not) be applied. For many different types of water shutoff problems, we discuss relevant field examples, including (1) how to diagnose the problem, (2) what gel properties are needed, (3) how much gel should be injected, (4) how the gel should be placed, and (5) how to assess the effectiveness of the treatment.

The web site also describes a strategy for attacking excess water production problems. Many oil and gas producers realize that identifying the problem is critical before attempting a solution, but most producers have limited resources for diagnosis. The site details which problems should be looked for first, which problems are easy to solve, and which are more difficult.

Important equations for use in designing gel treatments are also included. Spreadsheets that perform these important calculations can be readily downloaded from our web site.

For those with more expertise in water shutoff, the site provides a detailed review of the intricacies of gel placement. It also provides discussion of special topics of current interest. For example, "Clean Up of Oil Zones after a Gel Treatment" is of high interest for those who bull-head gel treatments into production wells. Also, "A New Filter Cake Model" is of interest to those involved with hydraulic fracturing and produced water re-injection, as well as to those who inject large gel volumes during water shutoff applications.

Access is provided to annual reports for our work in water shutoff back to 1990. A search engine is included that covers all our reports and publications. This web site is a valuable resource for anyone who needs to reduce excess salt water production during their oil and gas operations.

Papers and Publications

Seright, R.S., Prodanovic, M., and Lindquist, W.B.: "X-Ray Computed Microtomography Studies of Fluid Partitioning in Drainage and Imbibition Before and After Gel Placement: Disproportionate Permeability Reduction," *SPE Journal* (Dec. 2005).

Prodanovic, M., Lindquist, W.B., and Seright, R.S.: "3D Image-Based Characterization of Fluid Displacement in a Berea Core," 2005, Accepted by *Advances in Water Resources*.

Sydansk, R.D., Al-Dhafeeri, A., Xiong, Y., Schrader, R., and Seright, R.S.: "Characterization of Partially Formed Polymer Gels for Application to Fractured Production Wells for Water-Shutoff Purposes," *SPE Production & Facilities* (Aug. 2005), **20**(3) 240-249.

Seright, R.S.: "Clean Up of Oil Zones after a Gel Treatment," paper SPE 92772 presented at the 2005 SPE International Symposium on Oilfield Chemistry, Houston, TX, Feb. 2-4.

Sydansk, R.D., Al-Dhafeeri, A.M., Xiong, Y., and Seright, R.S.: "Polymer Gels Formulated with a Combination of High- and Low-Molecular-Weight Polymers Provide Improved Performance for Water-Shutoff Treatments of Fractured Production Wells," *SPE Production & Facilities* (Nov. 2004), **19**(4) 229-236.

Seright, R.S.: "Throughput Dependence of Oil and Water Permeabilities after Treatment with Gel or Polymer," 3rd International Conference on Oil and Gas Development, Chengdu, China, Oct. 20-21, 2004.